Finite subset spaces of graphs and surfaces

by

Christopher Paul Tuffley

B.Sc. (Hons) (University of Canterbury) 1996
M.Sc. (University of Canterbury) 1997

A dissertation submitted in partial satisfaction of the
requirements for the degree of
Doctor of Philosophy

in

Mathematics

in the

GRADUATE DIVISION
of the
UNIVERSITY of CALIFORNIA at BERKELEY

Committee in charge:

Professor Robion C. Kirby, Chair
Professor John R. Stallings
Professor Robert G. Littlejohn

Spring 2003

Finite subset spaces of graphs and surfaces

Abstract

Finite subset spaces of graphs and surfaces

by

Christopher Paul Tuffley
Doctor of Philosophy in Mathematics

University of California at Berkeley

Professor Robion C. Kirby, Chair

The kth finite subset space of a topological space X is the space $\exp_k X$ of non-empty subsets of X of size at most k, topologised as a quotient of X^k. The construction is a homotopy functor, and may be thought of as a union over $1 \leq j \leq k$ of configuration spaces of unordered j–tuples of distinct points in X.

We study finite subset spaces in the context of the circle, graphs, surfaces, and maps between these spaces. We show that $\exp_k S^1$ has the homotopy type of an odd dimensional sphere of dimension k or $k-1$, that the inclusion map $\exp_{2\ell-1} S^1 \simeq S^{2\ell-1} \hookrightarrow \exp_{2\ell} S^1 \simeq S^{2\ell-1}$ has degree two, and that $\exp_k S^1 \setminus \exp_{k-2} S^1$ has the homotopy type of a $(k-1,k)$–torus knot complement. These results generalise known facts that $\exp_2 S^1$ is a Möbius strip with boundary $\exp_1 S^1$, and that $\exp_3 S^1$ is the three-sphere with $\exp_1 S^1$ forming a trefoil knot inside it.

We build cell structures for the finite subset spaces of a connected graph Γ and use these to calculate $H_*(\exp_k \Gamma)$ and give recipes for the maps induced on homology by a map of graphs $\phi\colon \Gamma \to \Gamma'$. These recipes take the form of a ring structure on the cellular chain groups with respect to which chain maps $(\exp_k \phi)_\sharp$ are ring homomorphisms. The results apply to punctured surfaces also, by homotopy equivalence, and we use them to prove a structure theorem for the induced action of the braid group B_n, acting as the mapping class group of a punctured disc.

We show that the finite subset spaces of a connected finite 2–complex admit "lexicographic cell structures" based on the lexicographic order on I^2, and use these to calculate the rational homology of $\exp_k S^2$ and the top integral homology groups of $\exp_k \Sigma$ for each k and closed surface Σ. In addition, we use the Mayer-Vietoris sequence and the ring structure of $H^*(\mathrm{Sym}^k \Sigma)$ to completely calculate the cohomology groups of $\exp_3 \Sigma$ for Σ closed and orientable.

Finally, we use the homology of $\exp_k \Gamma$ to prove two vanishing theorems for the homotopy and homology groups of the finite subset spaces of a connected cell complex.

Acknowledgments

I would like to thank my advisor, Rob Kirby. He has always been helpful and supportive, and happy to talk when I stuck my head in his door unannounced. He was willing to be temporarily distracted by talk of climbing in the early years, when I tried to shift the conversation away from the mathematics I hadn't done; but he would never let me get away with it entirely, and provided a needed nudge from time to time. He encouraged me to believe in finite subset spaces when I doubted them.

I owe a debt of gratitude to Jacob Mostovoy. His two page arXiv posting caught my eye in late 1999 and gave me something to think about; those thoughts eventually grew into this work. Later he gave me helpful comments on the work in Chapter 5, in response to an arXiv post of my own.

Chuck Livingston has been another source of helpful conversations and ideas.

The Earle C. Anthony Fund and the Julia Robinson Endowment paid my nonresident tuition for the academic year 2002–2003, and in my last semester I was supported by a Raymond H. Sciobereti Scholarship from the department. This was a great help, giving old discarded ideas a chance to take on new life and blossom into Chapter 5 and the first half of Chapter 4.

Finally I would like to thank my family, and my three local families: three generations of housemates at the Berkeley Way house, the Mathcamp staff, and my hiking and climbing partners from Chaos. A special thanks goes to my most frequent companions in the mountains, and especially those who saved my neck on occasions when gravity and the like had ideas all their own.

Chris the Graduate Student
15th May 2003

Contents

List of Figures iv

List of Symbols v

1 Introduction 1

1.1 Configuration spaces . . . 1
1.2 Finite subset spaces: definitions and properties . . . 2
1.3 Overview . . . 4
1.4 The name and notation . . . 5

2 The circle 6

2.1 Introduction . . . 6
2.1.1 Known and new results on $\exp_k S^1$ . . . 6
2.1.2 Notation and terminology . . . 8
2.2 The homotopy type of finite subset spaces of the circle . . . 9
2.2.1 Introduction . . . 9
2.2.2 The homeomorphism type of $\exp_2 S^1$ . . . 9
2.2.3 The homeomorphism types of $\exp_3 S^1$ and $\exp_3 S^1 \setminus \exp_1 S^1$ . . . 9
2.2.4 The homotopy type of $\exp_k S^1$ . . . 12
2.3 The complement of the codimension two stratum . . . 15
2.3.1 A new model for $\exp_k S^1$ . . . 15
2.3.2 The fundamental group of $\exp_k S^1 \setminus \exp_{k-2} S^1$ . . . 17
2.3.3 The homotopy type of $\exp_k S^1 \setminus \exp_{k-2} S^1$ . . . 19
2.4 The degree of an induced map . . . 21
2.5 Cut and paste proof of Theorems 2.1 and 2.2 . . . 23

3 Graphs and punctured surfaces 27

3.1 Introduction . . . 27
3.1.1 Summary of results . . . 27
3.1.2 Outline of the chapter . . . 29
3.1.3 Notation and terminology . . . 29
3.2 The homology of finite subset spaces of graphs . . . 30
3.2.1 Introduction . . . 30
3.2.2 Cell structures for $\exp_k \Gamma_n$ and $\exp_k(\Gamma_n, v)$ . . . 31

3.2.3 Direct proof of the exactness of $\mathcal{C}_{\geq 1}$ 34
3.2.4 The homology groups of $\exp_k(\Gamma_n, v)$ and $\exp_k\Gamma_n$ 35
3.2.5 A basis for $H_k(\exp_k\Gamma_n)$ 37
3.2.6 Generating functions for $b_k(\exp_k\Gamma_n)$ 38
3.3 The calculation of induced maps 38
3.3.1 Introduction 38
3.3.2 The chain ring 39
3.3.3 Calculating induced maps 42
3.3.4 Examples 43
3.4 The action of the braid group 45
3.4.1 Introduction 45
3.4.2 Proof of the structure theorem 45
3.4.3 The action of B_3 on $H_3(\exp_3\Gamma_3)$ 48

4 Closed surfaces **49**
4.1 Introduction 49
4.1.1 Summary of main results 49
4.2 Lexicographic cell structures 51
4.2.1 Conventions 51
4.2.2 Existence of lexicographic cell structures 52
4.2.3 The boundary maps 55
4.2.4 Higher dimensions 58
4.3 The two-sphere 59
4.3.1 Introduction 59
4.3.2 The chain complexes 59
4.3.3 Small values of k 61
4.3.4 The general case 66
4.4 Higher genus surfaces 70
4.5 A homotopy model for the third finite subset space 72
4.5.1 The model 72
4.5.2 Symmetric products of surfaces 72
4.5.3 The proof of homotopy equivalence 73
4.6 The calculation of $H^*(\exp_3\Sigma)$ 74
4.6.1 Introduction 74
4.6.2 The rings $H^*(\Sigma^k)$ and $H^*(\mathrm{Sym}^k\Sigma)$ 74
4.6.3 The cohomology calculation 75

5 An application to cell complexes **79**
5.1 Introduction 79
5.2 Proof of the vanishing theorems 79
5.3 Discussion 81

Bibliography **84**

A Table of Betti numbers of finite subset spaces of graphs **87**

List of Figures

2.1 The space $\exp_2 S^1$ is a Möbius strip . . . 9
2.2 A Möbius strip showing $\exp_1(S^1, 1)$ . . . 10
2.3 Simplicial decomposition of $\exp_3 S^1$ . . . 10
2.4 A cell complex homotopy equivalent to a $(k-1, k)$–torus knot complement 15
2.5 The new model for $\exp_k S^1$ in the case $k = 2$ . . . 16
2.6 Movies of the generators of $\pi_1(\exp_4 S^1 \setminus \exp_2 S^1)$ . . . 18
2.7 The movie of a null-homotopy in $\exp_k S^1 \setminus \exp_{k-3} S^1$ . . . 19
2.8 Degree calculation of an induced map $\exp_k f\colon\ \exp_k S^1 \to \exp_k S^1$ . . . 22
2.9 A regular neighbourhood of the dual 1–skeleton of $\exp_3 S^1$ . . . 23
2.10 Heegaard diagrams of $\exp_3 S^1$ . . . 24
2.11 Perturbing $\exp_1 S^1 \subseteq \exp_3 S^1$ to lie on the Heegaard surface . . . 25
2.12 Heegaard diagram of $\exp_3 S^1$ showing a push-off of $\exp_1 S^1$ . . . 26

3.1 The graphs Γ_2 and Γ_3 . . . 30
3.2 Relations in $\pi_1(\exp_k \Gamma_n)$ arising from the 2–cells . . . 33
3.3 The 3–cube complex C^3_* . . . 35
3.4 Pascal's other triangle . . . 41
3.5 Generators of the braid group . . . 46

4.1 The crunching map κ . . . 52
4.2 Open cell decomposition of $\exp_3(\operatorname{int} I^2) \setminus \exp_2(\operatorname{int} I^2)$ . . . 53
4.3 Boundary calculations for finite subset spaces of 2–complexes . . . 57
4.4 Cell counts for $\exp_5(S^2, *)$ and $\exp_5 S^2$ . . . 60
4.5 The clipped cube complex . . . 61
4.6 Generators of the four dimensional clipped cube complex . . . 64
4.7 A homotopy model for the third finite subset space of a surface . . . 73

List of Symbols

$\mathsf{1}$, $\mathsf{2}_i$, $\mathsf{3}_i$, $\mathsf{4}_i$	partitions of k, 66
α_i	(Chapter 4) ith generator of $H^1(\Sigma_g)$, 74
$b_i(X)$	ith Betti number of X
B_n	braid group on n strands
B^j	j dimensional ball
β	(Chapter 4) generator of $H^2(\Sigma_g)$, 74
$\mathcal{B}(k,n)$	basis for $H_k(\exp_k\Gamma_n)$, 37
$\partial\sigma$, ∂M	boundary of cell σ or manifold M
$\partial_i(J)$	map on n–tuples $J \mapsto (j_1, \ldots, j_i - 1, \ldots, j_n)$, 30
∂^ν, ∂^λ, ∂^γ, $\partial^\lambda_{\mathbf{Q}}$	boundary maps for finite subset spaces of 2–complexes, 55, 60
$\mathcal{C}_*, \tilde{\mathcal{C}}_*$	cellular chain groups of $\exp\Gamma_n$, 33
$\mathcal{C}^S_*, \mathcal{C}^{[m]}_*(L)$	subcomplexes of $\mathcal{C}_*$ determined by S and by $[m]$ and L, 34
C^m_*	m–cube complex, 34
$\chi(X)$	Euler characteristic of X
$\mathbf{C}$	the complex numbers
$\mathbf{C}P^n$	complex projective n–space
$\mathcal{D}$	branch locus of $\Sigma^3 \to \mathrm{Sym}^3\Sigma$, 72
D_n	n–punctured disc
Δ_j, $\tilde{\Delta}_j$, Δ_J, $\tilde{\Delta}_J$	(Chapter 3 on) domains of cells of $\exp_k\Gamma_n$, 31
e_i, $\bar{e}_i$	edge i of Γ_n, 29, edge i with opposite orientation, 39
$E_3\Sigma$	homotopy model for $\exp_3\Sigma$, 72
ϵ^j	positive generator of $H_j(B^j, \partial B^j)$, 39
η	degree 2 generator of $H^*(\mathrm{Sym}^3\Sigma)$, 75
$\exp_k f$	map on $\exp_k$ induced by f, 2
$\exp X$	full finite subset space of X, 3
$\exp_k X$	kth finite subset space of X, 2
$\exp_k(X, x_0)$	kth based finite subset space of X, 3
$\mathcal{F}_j$	filtration of $H_k(\exp_k\Gamma_n)$, 46
f_i	ith two-cell of 2–complex X, 51
ϕ_i	characteristic map of ith two-cell of X, 51
Γ_n	connected graph with one vertex and n edges, 29
$H_i(X;G)$	ith homology group of X with co-efficients in G
$H^i(X;R)$	ith cohomology group of X with co-efficients in R
$H_i(X), H^i(X)$	integral (co)homology

$\tilde{H}_i$	reduced homology
I	closed interval $[0,1]$
int	interior, 8
$\mathcal{J}(\Lambda)$	edge incidence n–tuple of $\Lambda \in \exp_k\Gamma_n$, 29
κ	crunching map $I^2 \to D^2$, 51
$\ell(S)$	length of partition S, 52
M_f	mapping cylinder of f
μ_i	merging map on partitions $S \mapsto (s_1, \ldots, s_i + s_{i+1}, \ldots, s_\ell)$, 52
$\mathbf{N}$	the natural numbers
P_n	pure braid group on n–strands
$\pi_i(X)$	ith homotopy group of X
$\mathbf{Q}$	the rational numbers
q_k	quotient map $\Sigma^k \to \mathrm{Sym}^k\Sigma$, 72
$\mathbf{R}$	the real numbers
$\mathbf{R}P^n$	real projective n–space
S_k	symmetric group on k letters
S^n	the n-sphere
$\sigma^j, \tilde{\sigma}^j, \sigma_i^j, \tilde{\sigma}_i^j, \sigma^J, \tilde{\sigma}^J$	cells of $\exp_k S^1$, 12, cells of $\exp_k\Gamma_n$, 32
$\mathcal{S}(\Lambda)$	partition associated to $\Lambda \subseteq \mathrm{int}\, I^2$, 53
$\mathrm{supp}\, J$, $\mathrm{supp}_2\, J$	support, mod two support of n–tuple J, 30
$\mathrm{Sym}^k X$	kth symmetric product X^k/S_k, 2
$\mathcal{S}_{\ell,j}$, $\tilde{\mathcal{S}}_{\ell,j}$	chain groups of $\exp_k S^2$, 59
T^2	2–torus $S^1 \times S^1$
$T_x M$	tangent space to M at x
τ_i	ith generator of B_n, 45
$\tilde{\tau}_i^S$, τ_i^S	cells for finite subset spaces of 2–complex X, 53
$\tau_{\mathbf{Q}}^S$	multiple of τ^S, 57
θ	(Chapter 4) degree 2 generator of $H^*(\mathrm{Sym}^2\Sigma)$, 75
v_i	point $(\underbrace{0, \ldots, 0}_{k-i}, \underbrace{1, \ldots, 1}_{i}) \in \mathbf{R}^k$, 12
ξ_i	ith degree 1 generator of $H^*(\mathrm{Sym}^3\Sigma)$, 75
$\mathbf{Z}$	the integers
ζ_i	ith degree 1 generator of $H^*(\mathrm{Sym}^2\Sigma)$, 75
$\sim$	gluing relation, equivalence relation
$\simeq$	homotopy, homotopy equivalence
$\cong$	isomorphism, homeomorphism
$\prec$	lexicographic order, 51
$g \cup h$	composition $Y \times Z \xrightarrow{g \times h} \exp_k X \times \exp_\ell X \xrightarrow{\cup} \exp_{k+\ell} X$, 3
$\cup\{x_0\}$	map $\exp_k X \to \exp_{k+1}(X, x_0) : S \mapsto S \cup \{x_0\}$, 3
$\otimes$, $\oplus$	tensor product, direct sum
$\times$, $\vee$, $\amalg$	cartesian product, wedge product, disjoint union
$f_\sharp$	chain map induced by f
f_*, f^*	push forward by f, pull back by f
$\tilde{\sigma}$	image of chain σ under $\sigma^J \mapsto \tilde{\sigma}^J$, $\tau^S \mapsto \tilde{\tau}^S$, 36, 56

$\bar{\beta}$	permutation induced by braid β, 45
$[\phi]$, $[m]$	equivalence class of ϕ; set $\{i \in \mathbf{Z} \mid 1 \leq i \leq m\}$, 29
$[u_0, \ldots, u_n]$	affine simplex with vertices $u_0, \ldots, u_n$, 8
$[u_0, \ldots, \hat{u}_i, \ldots, u_n]$	affine simplex with vertex u_i omitted, 8
$\begin{bmatrix} n \\ r \end{bmatrix}_{-1}$	(-1)–binomial co-efficient n choose r, 40
$\langle g, \tilde{\sigma}^J \rangle$	degree of g on cell $\tilde{\sigma}^J$, 39
$\langle x_i \mid r_i \rangle$	group generated by $\{x_i\}$ with relations $\{r_i\}$
$\lvert\Lambda\rvert$, $\lvert J\rvert, \lvert J\rvert_2$	cardinality of set Λ; norm, mod two norm of n–tuple J, 29
$f\rvert_A$, $J\rvert_S$	restriction of map f to A; restriction of n–tuple J to S, 30
$\lfloor x \rfloor$, $\lceil x \rceil$	floor and ceiling functions of x
$\binom{n}{r}$	binomial co-efficient n choose r

Chapter 1

Introduction

1.1 Configuration spaces

Finite subset spaces are an example of a *configuration space*: a topological space whose points are collections or *configurations* of points in some underlying space. Useful in physics, where they describe the possible states of a system with several particles, configuration spaces come in various flavours and have long played an important role in topology. Two classical examples, using different configuration space constructions, are Gauss's linking number for pairs of circles in $\mathbf{R}^3$ and Artin's braid group B_n: the linking number $\ell k(L_1, L_2)$ of a pair of circles (L_1, L_2) may be regarded as the degree of the inclusion map of the torus $L_1 \times L_2$ into the space of ordered pairs of distinct points in $\mathbf{R}^3$, and the braid group may be defined as the fundamental group of the space of unordered n-tuples of distinct points in a disc. More recently, configuration spaces played a role in Bigelow's proof [4] that the braid groups have faithful linear representations, and beginning with Bott and Taubes [9] they are being used to understand finite-type knot invariants. This last uses a compactification due to Fulton and MacPherson [15] of the space of ordered n-tuples of distinct points in a manifold, compactified in such a way as to record the manner in which configurations degenerate when points come into coincidence.

Configuration spaces are interesting in their own right, but they are more often studied for the information—such as the linking number—they encode about the underlying space. In some instances the configuration space is arguably the "right" point of view to take. For example, a common definition of the linking number is the signed count of crossings of the first link component over the second. One checks that this is well defined by showing it is invariant under the Reidemeister moves, and with further work it can be seen that $\ell k(L_1, L_2)$ is equal to $\ell k(L_2, L_1)$. This has the value of being extremely elementary, but the configuration space, while requiring more machinery, affords a much better perspective. The space $\mathbf{R}^3 \times \mathbf{R}^3$ less the diagonal $\{(x, x) | x \in \mathbf{R}^3\}$ is homotopic to the two-sphere S^2 via the map

$$(x_1, x_2) \mapsto \frac{x_1 - x_2}{|x_1 - x_2|},$$

and from this viewpoint the signed count of crossings is the sum of local degrees at preimages of the point $(0, 0, 1) \in S^2$. Its invariance under isotopy is immediate and we obtain

$\ell k(L_1, L_2)$ as the degree of an induced map $T^2 \to S^2$. The symmetry $\ell k(L_1, L_2) = \ell k(L_2, L_1)$ is proved just as easily, as switching the order of the components simply reverses the orientation of both the torus and the sphere, introducing a product of two minus signs.

This dissertation studies the space $\exp_k X$ of non-empty finite subsets of X of size at most k. A configuration space in its own right, $\exp_k X$ may also be regarded as the union over $1 \leq j \leq k$ of configuration spaces of unordered j–tuples of distinct points in X, with the topology recognising that configurations of different cardinalities may be considered close. The construction was introduced by Borsuk and Ulam [7] in 1931 as the symmetric product, but it has received very little attention since, to the extent that it was re-introduced independently by Handel [18] in 2000. Moreover, the name symmetric product that Borsuk and Ulam gave it has come to more commonly mean the space $\mathrm{Sym}^k X$ formed by dividing X^k by the natural action of the symmetric group. Although Handel and other authors have established a number of general and homotopy theoretic properties of these spaces of finite subsets, to date little is known about $\exp_k X$ for even familiar X, except in a few special cases. This dissertation seeks to address this, and represents the first systematic study of the finite subset spaces of spaces from the bread and butter of low dimensional topology. Motivated both by their intrinsic interest, and by the hope of laying the groundwork for future applications to questions about the underlying spaces, we study finite subset spaces in the context of the circle, graphs, surfaces, and maps between these spaces.

1.2 Finite subset spaces: definitions and properties

Let X be a topological space and k a positive integer. The *kth finite subset space* of X is the space $\exp_k X$ of non-empty subsets of X of size at most k, topologised as a quotient of X^k via the map

$$(x_1, \ldots, x_k) \mapsto \{x_1\} \cup \cdots \cup \{x_k\}.$$

The construction is functorial: given $f\colon X \to Y$ we obtain a map $\exp_k f\colon \exp_k X \to \exp_k Y$ by sending $S \subseteq X$ to $f(S) \subseteq Y$, and $\exp_k f$ is continuous since it fits into a commutative diagram

$$\begin{array}{ccc} X^k & \xrightarrow{f^k} & Y^k \\ \downarrow & & \downarrow \\ \exp_k X & \xrightarrow{\exp_k f} & \exp_k Y \end{array}$$

in which the vertical arrows are quotient maps. Moreover, if $\{h_t\}$ is a homotopy between f and g then a similar diagram shows that $\{\exp_k h_t\}$ is a homotopy between $\exp_k f$ and $\exp_k g$, so that $\exp_k$ is in fact a homotopy functor.

The first finite subset space is of course simply X, and the second finite subset space co-incides with the second symmetric product $\mathrm{Sym}^2 X$, where $\mathrm{Sym}^k X$ is the space X^k/S_k formed by dividing X^k by the natural action of the symmetric group. However, for $k \geq 3$ we have a proper quotient of the symmetric product as $\exp_k X$ is unable to record multiplicities: both (a, a, b) and (a, b, b) in X^3 map to $\{a, b\}$ in $\exp_3 X$. As a result there are natural inclusion maps

$$\exp_j X \hookrightarrow \exp_k X : S \mapsto S \qquad (1.2.1)$$

whenever $j \leq k$, stratifying $\exp_k X$. We define the full finite subset space $\exp X$ to be the direct limit of this system of inclusions,

$$\exp X = \varinjlim \exp_k X.$$

If X is Hausdorff then the subspace topology on $\exp_j X \subseteq \exp_k X$ co-incides with the quotient topology it receives from X^j [18]. In this case each stratum $\exp_j X \setminus \exp_{j-1} X$ is homeomorphic to the configuration space of sets of j distinct unordered points in X, so that $\exp_k X$ may be regarded as a union over $1 \leq j \leq k$ of these spaces. Moreover $\exp_k X$ is compact whenever X is, in which case it gives a compactification of the corresponding configuration space.

For each k and ℓ the isomorphism $X^k \times X^l \to X^{k+\ell}$ descends to a map

$$\cup \colon \exp_k X \times \exp_\ell X \to \exp_{k+\ell} X$$

sending (S, T) to $S \cup T$. This leads to a form of product on maps $g\colon Y \to \exp_k X$, $h\colon Z \to \exp_\ell X$, and we define $g \cup h\colon Y \times Z \to \exp_{k+\ell} X$ to be the composition

$$Y \times Z \xrightarrow{g \times h} \exp_k X \times \exp_\ell X \xrightarrow{\cup} \exp_{k+\ell} X.$$

Clearly $(f \cup g) \cup h = f \cup (g \cup h)$. Given a point $x_0 \in X$ we obtain as a special case a map

$$\cup\{x_0\}\colon \exp_k X \to \exp_{k+1} X$$

taking $S \subseteq X$ to $S \cup \{x_0\}$. The image of $\cup\{x_0\}$ is the subspace $\exp_{k+1}(X, x_0)$ consisting of the $k+1$ or fewer element subsets of X that contain x_0. In contrast to the symmetric product, where the analogous map plays the role of (1.2.1), the spaces $\exp_k X$ and $\exp_{k+1}(X, x_0)$ are in general topologically different. The map $\cup\{x_0\}$ is one-to-one at the point $\{x_0\} \in \exp_1 X$ and on the top level stratum $\exp_k X \setminus \exp_{k-1} X$, but is two-to-one elsewhere, as S and $S \cup \{x_0\}$ have the same image for $|S| < k$, $x_0 \notin S$. Nevertheless the based finite subset spaces $\exp_k(X, x_0)$ frequently act as a stepping stone in understanding $\exp_k X$, often being topologically simpler.

In their original paper [7] Borsuk and Ulam observe that if X is metric then so is $\exp_k X$, with the Hausdorff metric

$$d(S, T) = \max\Big\{\max_{s \in S} \min_{t \in T} d(s, t), \max_{t \in T} \min_{s \in S} d(s, t)\Big\}.$$

Handel [18] shows that $\exp_k$ is well behaved with respect to several other topological properties: if X is Hausdorff then so is $\exp_k X$, and if in addition X is regular, locally compact, locally contractible, or second countable, then $\exp_k X$ inherits this condition also. Moreover $\exp_k \mathbf{R}^n$ can be embedded in some finite dimensional Euclidean space for each k and n, so if X has an embedding in a finite dimensional Euclidean space so does $\exp_k X$. Handel also shows that for Hausdorff spaces $\exp_k$ is well behaved with respect to taking subspaces: if $A \subseteq X$ then the topology on $\exp_k A$ as a subspace of $\exp_k X$ coincides with the quotient topology from A^k.

We remark that in re-introducing the finite subset space construction Handel defines it only for Hausdorff spaces. Consequently, while this condition appears as a hypothesis in all of his results, in some cases it is simply there so that the definition may be applied. Since we will only be working with Hausdorff spaces ourselves we have not always checked to see where the condition is necessary.

1.3 Overview

The space $\exp_k X$ was introduced by Borsuk and Ulam [7] in 1931 under the name symmetric product, and since then appears to have been studied at irregular intervals, under various notations, and principally from the perspective of general topology. In their original paper Borsuk and Ulam showed that $\exp_k I \cong I^k$ for $k = 1, 2, 3$, but that $\exp_k I$ cannot be embedded in $\mathbf{R}^k$ for $k \geq 4$. In 1957 Molski [28] proved similar results for I^2 and I^n, namely that $\exp_2 I^2 \cong I^4$ but that neither $\exp_k I^2$ nor $\exp_2 I^k$ can be embedded in $\mathbf{R}^{2k}$ for any $k \geq 3$; the last was done by showing that $\exp_2 I^k$ contains a copy of $S^k \times \mathbf{R}P^{k-1}$. In between these papers Bott [8] proved the surprising result that $\exp_3 S^1$ is homeomorphic to the three-sphere, correcting Borsuk's 1949 paper [6], and Shchepin (unpublished) later proved the even more striking result that $\exp_1 S^1$ inside $\exp_3 S^1$ is a trefoil knot. An elegant geometric construction due to Mostovoy [29] in 1999 connects both of these results with known facts about the space of lattices in the plane.

Other authors including Curtis [11], Curtis and To Nhu [12], Handel [18], Illanes [21] and Macías [25] have established general topological and homotopy-theoretic properties of $\exp_k X$ and $\exp X$, and Beilinson and Drinfeld [2, sec. 3.5.1] and Ran [30] have used these spaces in the context of algebraic geometry and mathematical physics. The set $\exp X$ has also been studied extensively under a different topology as the Pixley-Roy hyperspace of finite subsets of X; the two topologies are surveyed in Bell [3]. We mention some results on $\exp_k X$ of a homotopy-theoretic nature. In 1999 Macías showed that for compact connected metric X the Čech cohomology group $\check{H}^1(\exp_k X; \mathbf{Z})$ vanishes for $k \geq 3$, and in 2000 Handel proved that for closed connected n–manifolds, $n \geq 2$, the singular cohomology group $H^i(\exp_k M^n; \mathbf{Z}/2\mathbf{Z})$ is isomorphic to $\mathbf{Z}/2\mathbf{Z}$ for $i = nk$, and 0 for $i > nk$. In addition, Handel showed that the inclusion maps $\exp_k(X, x_0) \hookrightarrow \exp_{2k-1}(X, x_0)$ and $\exp_k X \hookrightarrow \exp_{2k+1} X$ induce the zero map on all homotopy groups for path connected Hausdorff X.

Although these and other properties of $\exp_k$ have been established, prior to the present work it appears that little was known about $\exp_k X$ for specific homotopically nontrivial X and $k \geq 3$, when the construction no longer co-incides with the symmetric product. This dissertation seeks to address this. We begin in Chapter 2 with the circle, showing that Bott's and Shchepin's results may be seen as part of a larger pattern: $\exp_k S^1$ has the homotopy type of an odd dimensional sphere, and $\exp_k S^1 \setminus \exp_{k-2} S^1$ that of a $(k-1, k)$–torus knot complement. We give two simultaneous proofs of Bott's and Shchepin's results, one by cut and paste topology and the other via the classification of Seifert fibred spaces, and calculate the degree of an induced map $\exp_k f \colon \exp_k S^1 \to \exp_k S^1$ in terms of the degree of $f \colon S^1 \to S^1$.

We then study the finite subset spaces of a connected graph Γ in Chapter 3. We use explicit cell structures to calculate the homology of $\exp_k \Gamma$ and find recipes for the maps $(\exp_k \phi)_*$ induced on homology by a map of graphs $\phi \colon \Gamma \to \Gamma'$. These recipes take the form of a ring structure on the cellular chain groups with respect to which chain maps $(\exp_k \phi)_\sharp$ are ring homomorphisms. The results apply to punctured surfaces also, by homotopy equivalence, and as illustration of how much $(\exp_k \phi)_*$ remembers about ϕ we use them to prove a structure theorem for the induced action of the braid group B_n, acting as the mapping class group of a punctured disc.

In Chapter 4 we make the first steps towards an understanding of the finite subset spaces of closed surfaces, studying them using two quite different approaches. We first use ideas and techniques from the previous chapters to show that the finite subset spaces of connected finite 2–complexes admit "lexicographic cell structures" based on the lexicographic ordering of points in I^2. Applying these to the standard cell structures for closed surfaces we calculate the rational homology of the finite subset spaces of S^2 and the top integral homology groups of $\exp_k\Sigma$ for each k and closed surface Σ. Our results refine for $\dim M = 2$ Handel's result on the mod two top cohomology of the finite subset spaces of a closed connected manifold M. We then use quite different methods to calculate the cohomology groups of the third finite subset space of a closed orientable surface. We build a homotopy model for $\exp_3\Sigma$ from $\mathrm{Sym}^3\Sigma$ and the mapping cylinder of $\Sigma^2 \to \mathrm{Sym}^2\Sigma$, and calculate the cohomology using the Mayer-Vietoris sequence and the calculation of $H^*(\mathrm{Sym}^k\Sigma)$ due to Macdonald [24] and Seroul [31, 32].

Finally, in Chapter 5 we use the result of the homology calculation in Chapter 3 to prove two vanishing theorems for the homotopy and homology groups of the finite subset spaces of a connected cell complex X. Namely, we show that the homotopy group $\pi_i(\exp_k X)$ vanishes for $i \leq k-2$, and that the homology group $H_i(\exp_k X)$ vanishes for $i > nk$ if X has finite dimension n. The first result complements Handel's result on the inclusion map $\exp_k X \hookrightarrow \exp_{2k+1} X$, and can be improved to $i \leq k-1$ if X is simply connected.

Chapter 2 is based on *Finite subset spaces of* S^1 [36] published in *Algebraic and Geometric Topology*, and Chapters 3 and 5 are based on preprints arXiv:math.GT/0210315 [35] and arXiv:math.GT/0304086 [37] respectively.

1.4 The name and notation

Various different notations have been used for $\exp_k X$, including $X(k)$, $X^{(k)}$, $\mathcal{F}_k(X)$ and $Sub(X,k)$. Our notation follows that used by Mostovoy [29] and reflects the idea that we are truncating the (suitably interpreted) series

$$\exp X = \emptyset \cup X \cup \frac{X^2}{2!} \cup \frac{X^3}{3!} \cup \cdots$$

at the $X^k/k! = X^k/S_k$ term. The name, however, is our own. There does not seem to be a satisfactory name in use among geometric topologists—indeed, recent authors Mostovoy and Handel do not use any name at all—and while symmetric product has stayed in use among general topologists we prefer to use this for X^k/S_k. We therefore propose the descriptive name "kth finite subset space" used here and in our papers.

Chapter 2

The circle

2.1 Introduction

We begin our investigation of finite subset spaces with the circle. The circle is conveniently described both as the unit circle in the complex plane and as the quotient of the unit interval by its endpoints, and we shall freely use both models. In passing between the two we use the restriction of the covering map $\mathbf{R} \to S^1 : t \mapsto e^{2\pi i t}$.

The work in this chapter has been published as *Finite subset spaces of* S^1 in *Algebraic and Geometric Topology* [36]. The chapter is based on that paper, edited for inclusion. In editing it we have also changed some notation and orientation conventions to conform with those adopted in [35], the arXiv version of Chapter 3.

2.1.1 Known and new results on $\exp_k S^1$

A sequence of pictures, outlined in section 2.2.2, shows that $\exp_2 S^1$ is a Möbius strip with boundary $\exp_1 S^1$. Note in particular that both $\exp_1 S^1$ and $\exp_2 S^1$ have the homotopy type of a circle, and that the inclusion map induces multiplication by two on H_1. The homeomorphism type of $\exp_3 S^1$ is also known and was calculated by Bott, correcting Borsuk's 1949 paper [6]:

Theorem 2.1 (Bott [8]). *The space* $\exp_3 S^1$ *is homeomorphic to the 3-sphere* S^3*.*

Bott proves this using a cut-and-paste argument, first showing that $\exp_3 S^1$ may be obtained from a single 3-simplex by gluing faces in pairs, then using this to find $\pi_1(\exp_3 S^1) \cong \{1\}$. He then divides the simplex into a number of pieces which he re-assembles to form solid tori, which give $\exp_3 S^1$ when glued along their boundary. This exhibits $\exp_3 S^1$ as a simply connected lens space, hence S^3. An explicit homeomorphism is not given, and indeed it is non-obvious, as the following theorem of E. Shchepin illustrates.

Theorem 2.2 (Shchepin, unpublished). *The inclusion* $\exp_1 S^1 \hookrightarrow \exp_3 S^1$ *is a trefoil knot.*

As further illustration, the two-cells in the above simplicial decomposition of S^3 form a Möbius strip and a dunce cap. The first is of course $\exp_2 S^1$ bounding $\exp_1 S^1$, and the second is $\exp_3(S^1, 1)$, the subspace of subsets containing $1 \in S^1$.

Shchepin's proof of Theorem 2.2 is apparently based on a direct calculation of the fundamental group of $\exp_3 S^1 \setminus \exp_1 S^1$. We will give two independent simultaneous proofs of Theorems 2.1 and 2.2, one via cut and paste topology, and the second via the classification of Seifert fibred spaces. The natural action of S^1 on itself gives an action of S^1 on $\exp_k S^1$ for each k, and for $k = 3$ we obtain the following refinement of Bott's and Shchepin's results:

Theorem 2.3. *The space $\exp_3 S^1$ is a Seifert fibred 3–manifold, and as such is oriented fibre preserving diffeomorphic to S^3 with the $(2, -3)$ S^1 action*

$$\lambda \cdot (z_1, z_2) = (\lambda^2 z_1, \lambda^{-3} z_2), \tag{2.1.1}$$

where we regard S^1 and S^3 as sitting in $\mathbf{C}$ and $\mathbf{C}^2$ respectively and give $\exp_3 S^1$ the canonical orientation it inherits from S^1.

We mention also an elegant geometric construction due to Mostovoy [29] showing that both Theorems 2.1 and 2.2 can be deduced from known facts about lattices in the plane. Namely, the space $SL(2, \mathbf{R})/SL(2, \mathbf{Z})$ of plane lattices modulo scaling is diffeomorphic to a trefoil complement (the proof, due to D. Quillen, may be found in [27, page 84] and uses the Weierstrass $\wp$ function associated to the lattice), and this space may be compactified by adding degenerate lattices to obtain S^3. Together with Theorems 2.1 and 2.2 this shows $\exp_3 S^1 \setminus \exp_1 S^1 \cong SL(2, \mathbf{R})/SL(2, \mathbf{Z})$, and Mostovoy's construction fills in the third side of this triangle, associating to each lattice a finite subset of S^1, thought of as $\mathbf{R}P^1$. Each degenerate lattice corresponds to a one element subset, each rectangular lattice a two element subset, and all other lattices correspond to three element subsets. Moreover, his map is equivariant with respect to the natural actions of S^1 on $\exp_3 S^1$ and $PSO(2) \subseteq PSL(2, \mathbf{R})$ on $SL(2, \mathbf{R})/SL(2, \mathbf{Z})$.

The first three of the following new results generalise the theorems and observations above. Proofs appear in subsequent sections. Theorems 2.4, 2.5 and the observation on the map $\exp_{k-1} S^1 \to \exp_k S^1 : \Lambda \mapsto \Lambda \cup \{1\}$ that follows their proofs have also been proved independently by David Handel [17, unpublished work], using essentially the same argument.

Theorem 2.4. *The space $\exp_k S^1$ has the homotopy type of an odd dimensional sphere, of dimension k or $k - 1$ according to whether k is odd or even.*

Since $\exp_{2k-1} S^1 \simeq S^{2k-1} \simeq \exp_{2k} S^1$ we may ask how $\exp_{2k-1} S^1$ sits inside $\exp_{2k} S^1$. The following result falls out of the proof of Theorem 2.4 and shows that the situation is analogous to $\exp_1 S^1$ inside $\exp_2 S^1$:

Theorem 2.5. *The inclusion $\exp_{2k-1} S^1 \hookrightarrow \exp_{2k} S^1$ induces multiplication by two on H_{2k-1}.*

As our last generalisation, $\exp_{k-2} S^1$ inside $\exp_k S^1$ is in some sense a homotopy $S^{\ell-2}$ inside a homotopy S^ℓ, so it is natural to ask if this is embedded in some interesting way too. Analogously to Theorem 2.2 we have:

Theorem 2.6. *The complement of the codimension two stratum $\exp_{k-2} S^1$ in $\exp_k S^1$ has the homotopy type of a $(k - 1, k)$–torus knot complement.*

Finally, a map $f\colon S^1 \to S^1$ induces a map $\exp_k f$ of homotopy spheres, and we calculate its degree in terms of k and the degree of f.

Theorem 2.7. *If $f\colon S^1 \to S^1$ then*

$$\deg \exp_k f = (\deg f)^{\lfloor \frac{k+1}{2} \rfloor} .$$

Remark. It is perhaps worth noting that although $\exp_k S^1$ is a manifold for $k = 1, 2, 3$, it is not a manifold for any $k \geq 4$. Subsets of size k do have k–ball neighbourhoods in $\exp_k S^1$ and this transition may be understood in terms of neighbourhoods of $k-1$ element subsets as follows. Given such a subset Λ of S^1 there are $k-1$ choices for which point to consider "doubled" and split in two to obtain a k element subset. Each such choice leads to a k–dimensional halfspace containing Λ and we obtain a neighbourhood of Λ by gluing these together along their boundaries. The transition thus occurs when $k-1$ increases above two, and we see also that when $k = 2$ points in $\exp_1 S^1$ have halfspace neighbourhoods and thus form the boundary of a 2–manifold.

Later we shall see this more explicitly when we show that $\exp_k S^1$ may be obtained from a single k–simplex by identifying faces. Under the identifications the zeroth and first faces become one face and the remaining $k-1$ faces a second, corresponding to $\exp_{k-1} S^1$.

2.1.2 Notation and terminology

The proofs of our main results make use of arguments involving simplices and simplicial decompositions and we take a moment to fix language. For the most part we follow Hatcher [20, section 2.1], and will use "simplicial decomposition" in the sense of his Δ–complexes. In particular, we will not require that the simplices in our decompositions be determined by their vertices.

Given $k+1$ points $u_0, \ldots, u_k$ in an affine space let

$$[u_0, \ldots, u_k] = \left\{ \textstyle\sum_i t_i u_i \middle| \sum_i t_i = 1 \text{ and } t_i \geq 0 \text{ for all } i \right\},$$

the set of convex combinations of the u_i. We will typically only write this when the points are affinely independent, in which case $[u_0, \ldots, u_k]$ is a k–simplex with (ordered) vertices $u_0, \ldots, u_k$. For $\sigma \in S_{k+1}$ we regard $[u_{\sigma(0)}, \ldots, u_{\sigma(k)}]$ as the same simplex with orientation $\operatorname{sign} \sigma$ times that of $[u_0, \ldots, u_k]$.

The canonical map between two simplices $[u_0, \ldots, u_k]$ and $[v_0, \ldots, v_k]$ is the unique map given by sending u_i to v_i for each i and extending affinely. A hat ˆ over a vertex means it is to be omitted, in other words

$$[u_0, \ldots, \hat{u}_i, \ldots, u_k] = [u_0, \ldots, u_{i-1}, u_{i+1}, \ldots, u_k],$$

and unless indicated otherwise the interior of a simplex $[u_0, \ldots, u_k]$ will always mean the open simplex

$$\operatorname{int}[u_0, \ldots, u_k] = \left\{ \textstyle\sum_i t_i u_i \middle| \sum_i t_i = 1 \text{ and } t_i > 0 \text{ for all } i \right\}$$

regardless of whether this is an open subset of the ambient space.

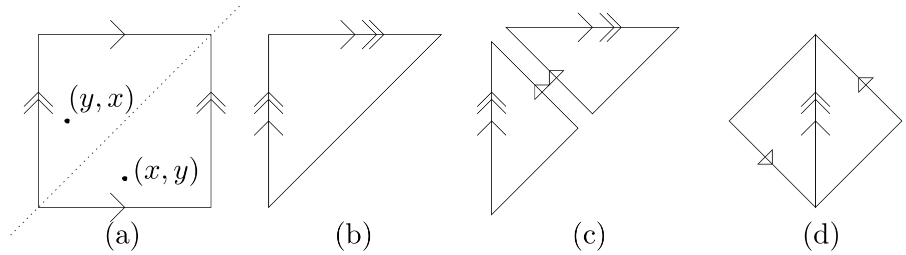

Figure 2.1: The space $\exp_2 S^1$ is a Möbius strip. Fold along the diagonal in (a) to identify (x, y) and (y, x); the result is shown in (b). Cut (c) and re-glue (d) to recognise this as a Möbius strip.

2.2 The homotopy type of finite subset spaces of the circle

2.2.1 Introduction

To prove that $\exp_k S^1$ has the homotopy type of a sphere we will find a cell structure for it and use this to show it has the correct fundamental group and homology. Application of a standard argument that a simply connected homology sphere is a homotopy sphere then yields the result. Before doing so, however, let us look at $\exp_2 S^1$ and $\exp_3 S^1$ in some detail, which will illustrate the situation in higher dimensions.

2.2.2 The homeomorphism type of $\exp_2 S^1$

To see that $\exp_2 S^1$ is a Möbius strip we will use the usual picture of $S^1 \times S^1$ as a square with opposite sides identified. In forming $\exp_2 S^1$ the point (x, y) is identified with (y, x), so the square is folded along the diagonal shown dotted in figure 2.1(a), resulting in the triangle with two edges identified shown in figure 2.1(b). This possible unfamiliar picture may be recognised as a Möbius strip either by cutting and re-gluing as in figures 2.1(c) and (d), or by gluing just the ends of the hypotenuse together to get a punctured projective plane.

A Möbius strip with the edge corresponding to the glued sides of the triangle shown dotted appears in figure 2.2. The diagonal edge forms the boundary circle. Note that the diagonal comes from the diagonal embedding of S^1 in $S^1 \times S^1$, which maps to $\exp_1 S^1 \subseteq \exp_2 S^1$.

We mention also a construction pointed out by Chuck Livingston. There is a natural map from $\exp_2 S^1$ to $\mathbf{R}P^1$ sending each pair of points on S^1 to the line through the origin bisecting the arc between them. The fibre above each point in $\mathbf{R}P^1$ is an interval of length π and the bundle is easily seen to be non-orientable.

2.2.3 The homeomorphism types of $\exp_3 S^1$ and $\exp_3 S^1 \setminus \exp_1 S^1$

Now consider $\exp_3 S^1$. Begin again with $[0, 1]^3 = I^3$ with opposite faces identified. Each $\Lambda \in \exp_3 S^1$ has at least one representative $(x, y, z) \in I^3$ with $0 \leq x \leq y \leq z \leq 1$, so we may restrict our attention to the simplex with vertices $v_0 = (0, 0, 0)$, $v_1 = (0, 0, 1)$, $v_2 = (0, 1, 1)$ and $v_3 = (1, 1, 1)$ shown in figure 2.3(a). Now $(0, x, y) \sim (x, y, 1)$ in $\exp_3 S^1$,

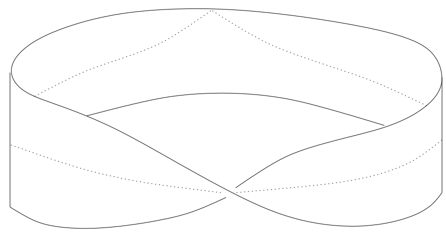

Figure 2.2: A Möbius strip, in which the glued edge-pair of the triangle of figure 2.1(b) corresponding to the subspace $\exp_2(S^1, 1)$ is shown dotted.

so the face $[v_0, v_1, v_2]$ is glued to the face $[v_1, v_2, v_3]$; next $(x, x, y) \sim (x, y, y)$ in $\exp_3 S^1$, so the face $[v_0, v_1, v_3]$ is glued to $[v_0, v_2, v_3]$. This accounts for all the identifications of the simplex arising from $\exp_3 S^1$, and the result, taking account of edge identifications, is shown in figure 2.3(b), viewed from a different angle. There is just one vertex (the set $\{1\}$), two edges and two 2–simplices, one forming a dunce cap and the second a Möbius strip. The dunce cap comes from the two faces $x = 0$ and $z = 1$ and corresponds to the subspace $\exp_3(S^1, 1)$; the Möbius strip comes from the faces $x = y$ and $y = z$ and is of course $\exp_2 S^1 \subseteq \exp_3 S^1$.

From above we have $\chi(\exp_3 S^1) = 1 - 2 + 2 - 1 = 0$; a well known but still magical fact (see [34, p. 122]) then guarantees that the space formed by gluing the faces of the 3–simplex in this fashion is a 3–manifold. Calculating $\pi_1(\exp_3 S^1)$ using figure 2.3(b) we obtain the presentation $\langle a, b | a, a^2 b^{-1} \rangle$, so $\exp_3 S^1$ is in fact a simply connected 3–manifold—and hence almost certainly S^3, especially given its simple construction. Bott [8] completes the proof by showing it has a genus one Heegaard splitting and appealing to the classification of lens spaces. A more informative approach is the proof of Theorem 2.3 given below. In section 2.5 (beginning page 23) we will also show directly that $\exp_3 S^1$ is a 3–sphere (and

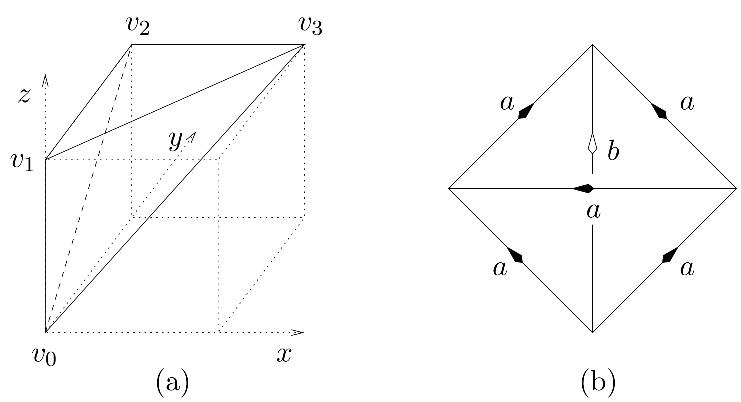

Figure 2.3: Simplicial decomposition of $\exp_3 S^1$. The space $\exp_3 S^1$ may be formed from the simplex $[v_0, v_1, v_2, v_3]$ in (a) by identifying the face $[v_0, v_1, v_2]$ with $[v_1, v_2, v_3]$, and the face $[v_0, v_1, v_3]$ with $[v_0, v_2, v_3]$. This corresponds to the edge and associated face gluings of (b).

that $\exp_1 S^1$ inside it is a trefoil) using the genus two Heegaard splitting obtained from the triangulation above.

Before proving Theorem 2.3 a word is necessary on orientation. Given an orientation of S^1 and a set $\Lambda = \{\lambda, \mu, \nu\}$ of three distinct points in S^1 we may canonically orient

$$T_\Lambda \exp_3 S^1 \cong T_\lambda S^1 \oplus T_\mu S^1 \oplus T_\nu S^1$$

by positively orienting each of the summands and requiring that the cyclic ordering of λ, μ, and ν agree with the orientation of S^1. This extends to an orientation of $\exp_3 S^1$ independent of the orientation on S^1, and we regard this as the canonical orientation of $\exp_3 S^1$. Note that the standard orientation the simplex $0 \le x \le y \le z \le 1$ in figure 2.3 inherits from $\mathbf{R}^3$ co-incides with the canonical orientation of $\exp_3 S^1$.

To orient S^3 we regard it as the boundary of the 4–ball in $\mathbf{C}^2$ with its canonical orientation and use the "outward first" convention for induced orientations on boundaries.

Proof of Theorem 2.3. We have seen that $\exp_3 S^1$ is a closed simply connected 3–manifold and we observe that it is Seifert fibred by the natural action of S^1. There are precisely two exceptional fibres, the orbits of $\{1, -1\}$ and $\{1, e^{\pi i/3}, e^{2\pi i/3}\}$, and these have multiplicities 2 and 3 respectively. Since S^3 with the $(2, -3)$ action of equation (2.1.1) on page 7 shares these properties our aim will be to show that they are enough to completely determine the unoriented fibre type of $\exp_3 S^1$.

To this end let M be a closed simply connected Seifert fibred space with precisely two exceptional fibres, of multiplicities two and three. Simple connectivity of M implies the orbit surface is simply connected also, and therefore S^2. Moreover, the fibres may be consistently oriented. Removing fibred solid torus neighbourhoods of each of the exceptional fibres thus leaves an oriented circle bundle over a twice punctured sphere, which we may write as $S^1 \times I \times S^1$, the base corresponding to the first two factors.

M is completely determined by specifying slopes $\alpha_0/\beta_0, \alpha_1/\beta_1 \in \mathbf{Q}$ along which to glue back in meridional discs to $S^1 \times \{0\} \times S^1$ and $S^1 \times \{1\} \times S^1$. To get the correct multiplicities we must have $\{\beta_0, \beta_1\} = \{2, 3\}$ so without loss of generality let $\beta_0 = 2$, $\beta_1 = 3$. The classification of orientable Seifert fibred spaces (see for example Hatcher's 3–manifold notes [19, p. 25]) tells us that the slopes are only determined mod 1 subject to their sum being fixed (this ambiguity comes from the choice of trivialisation of the circle bundle) so we may further assume $\alpha_0 = 1$ and write $\alpha_1 = \alpha$. We calculate π_1 of the resulting manifold.

The fundamental group of $S^1 \times I \times S^1$ is free abelian, generated by b and f, where b and f are positively oriented generators of π_1 of the base and fibre respectively. Gluing a disc in to $S^1 \times \{0\} \times S^1$ along a line of slope $1/2$ kills $2b + f$ while gluing a disc in to $S^1 \times \{1\} \times S^1$ along a line of slope $\alpha/3$ kills $-3b + \alpha f$, the minus sign coming from the fact that $S^1 \times \{1\} \times S^1$ has orientation $[-b, f]$ (recall that we are using "outward first" to orient boundaries). Thus simple connectivity of M implies

$$\det \begin{bmatrix} 2 & -3 \\ 1 & \alpha \end{bmatrix} = 2\alpha + 3 = \pm 1.$$

Setting the determinant equal to 1 and -1 in turn gives $\alpha = -1$, $\alpha = -2$. Thus there are exactly two possibilities for the oriented fibre type of M; in Hatcher's notation they are

$M(\pm g, b; \alpha_0/\beta_0, \alpha_1/\beta_1) = M(0,0;1/2,-1/3)$ and $M(0,0;1/2,-2/3)$, where $\pm g$ specifies the genus and orientability of the orbit surface and b the number of boundary components.

Reversing the orientation of $M(\pm g, b; \alpha_1/\beta_1, \ldots, \alpha_k/\beta_k)$ simply changes the signs of all the attaching slopes. Thus

$$-M(0,0;1/2,-1/3) \cong M(0,0;-1/2,1/3) \cong M(0,0;1/2,-2/3)$$

and the unoriented fibre type of M is completely determined as claimed. It follows that $\exp_3 S^1$ and S^3 with the $(2,-3)$ action are fibre preserving diffeomorphic, and all that remains is to determine whether orientation is preserved or reversed.

To determine orientations we look at the return map on a disc D transverse to the exceptional fibre of multiplicity three at a point p. The fibre F is oriented by the S^1 action and we orient D such that $T_pF \oplus T_pD$ is positive. In the case of $\exp_3 S^1$ we use the point $p = (1/3, 2/3, 1) \in I^3$ and a small disc containing it in the plane $z = 1$. The vector $(1,1,1)$ forms a positive basis for T_pF so T_pD has orientation $[e_x, e_y]$, and the action of the return map is the 1/3 anti-clockwise twist given by the canonical map from $[v_1, v_2, v_3]$ to $[v_3, v_1, v_2]$. For S^3 we take $p = (0,1)$ and consider the $(2,3)$ action. The tangent space T_pS^3 has orientation $[(0,i),(1,0),(i,0)]$, in which $(0,i)$ forms a positive basis for T_pF, so for a suitable choice of disc D its tangent space at p has positive basis $\{(1,0),(i,0)\}$. The first return is when $\lambda = \omega := e^{2\pi i/3}$ and we see that the derivative of the first return map is multiplication by ω^2 on T_pD. This is a clockwise rotation through $2\pi/3$, so to match orientations with $\exp_3 S^1$ we must reverse the orientation of the orbit through $(0,1)$, giving the $(2,-3)$ S^1 action as claimed. □

2.2.4 The homotopy type of $\exp_k S^1$

Finally we turn our attention to the general case. Proceeding analogously to the two and three dimensional cases we may reduce to the k–simplex $0 \le x_1 \le \cdots \le x_k \le 1$. Working somewhat more formally than above let

$$v_i = (\underbrace{0,\ldots,0}_{k-i},\underbrace{1,\ldots,1}_{i}) \in \mathbf{R}^k$$

for $i = 0, \ldots, k$, and let $\tilde\sigma^k$ be the map of the simplex $[v_0, v_k, \ldots, v_1]$ to $\exp_k S^1$, σ^{k-1} that of the simplex $[v_1, v_k, \ldots, v_2]$. Being a little sloppy with notation we claim:

Lemma 2.1. *The space $\exp_k S^1$ has a simplicial decomposition with one 0-simplex, two i–simplices for each $1 \le i \le k-1$, and one k–simplex, namely, $\tilde\sigma^i$ for $0 \le i \le k$ and σ^i for $1 \le i \le k-1$. The boundary map $\partial_i\colon \mathbf{Z}\tilde\sigma^i \oplus \mathbf{Z}\sigma^i \to \mathbf{Z}\tilde\sigma^{i-1} \oplus \mathbf{Z}\sigma^{i-1}$ has matrix*

$$D_i = \frac{1+(-1)^i}{2}\begin{bmatrix} 1 & 0 \\ -2 & -1 \end{bmatrix}$$

for $2 \le i \le k-1$, is the zero map for $i = 1$ and has matrix $D_k|_{\mathbf{Z}\tilde\sigma^k}$ for $\partial_k\colon \mathbf{Z}\tilde\sigma^k \to \mathbf{Z}\tilde\sigma^{k-1} \oplus \mathbf{Z}\sigma^{k-1}$, $k \ge 2$.

The lemma enables us to calculate the homology of $\exp_k S^1$, obtaining the following.

Corollary 2.1. *The space* $\exp_k S^1$ *has the homology of an odd dimensional sphere, of dimension* k *if* k *is odd and dimension* $k-1$ *if* k *is even. The inclusion map* $\exp_{2k-1}S^1 \hookrightarrow \exp_{2k}S^1$ *induces multiplication by two on* H_{2k-1}.

Note that the notation and vertex ordering used here differ from those in the published version [36] of this chapter, having been changed to conform with the notation and orientation convention adopted in [35], the arXiv version of Chapter 3. As a consequence there is a sign change in the boundary map and the proof of Lemma 2.1 has been rewritten slightly. The vertex ordering is chosen so that the simplices

$$[v_0, v_k, \dots, v_1] = \{(x_1, \dots, x_k) | 0 \leq x_1 \leq \cdots \leq x_k \leq 1\}$$
$$[v_1, v_k, \dots, v_2] = \{(x_1, \dots, x_k) | 0 \leq x_1 \leq \cdots \leq x_k = 1\}$$

have the standard orientations they inherit from $\mathbf{R}^k$ and $\mathbf{R}^{k-1}$ respectively. To see this for $[v_0, v_k, \dots, v_1]$, note that its orientation relative to the standard orientation is given by $\det[(v_k - v_0)^T, \dots, (v_1 - v_0)^T]$, and this is one since the matrix in question is lower triangular with ones on the diagonal. A similar calculation applies to the simplex $[v_1, v_k, \dots, v_2]$.

Proof of Lemma 2.1 and Corollary 2.1. The lemma is proved by induction. Taking $k = 1$ as our base case (although the cases $k = 2$ and 3 are largely established above) this is just the usual cell decomposition of S^1 as $I/\{0, 1\}$, so consider $k \geq 2$. $\tilde{\sigma}^k$ maps $[v_0, v_k, \dots, v_1]$ onto $\exp_k S^1$, taking the interior of the simplex homeomorphically onto its image, so we need only sort out the face gluings. Faces of the form $[v_0, v_k, \dots, \hat{v}_i, \dots, v_1]$ where $1 \leq i \leq k-1$ correspond to $0 \leq x_1 \leq \cdots \leq x_{k-i} = x_{k-i+1} \leq \cdots \leq x_k \leq 1$, giving subsets of S^1 of size $k-1$ or less; therefore $\tilde{\sigma}^k$ restricted to such a simplex factors through $\tilde{\sigma}^{k-1}$. Moreover, the map of simplices factoring this restriction preserves orientation. The simplex $[v_0, v_{k-1}, \dots, v_1]$ is $0 = x_1 \leq \cdots \leq x_k \leq 1$, which is identified with $0 \leq x_1 \leq \cdots \leq x_k = 1$, so $\tilde{\sigma}^k|_{[v_0, v_{k-1}, \dots, v_1]}$ factors through σ^{k-1} via the canonical map $[v_0, v_{k-1}, \dots, v_1] \to [v_1, v_k, \dots, v_2]$. Thus

$$\begin{aligned}
\partial \tilde{\sigma}^k &= \tilde{\sigma}^k|_{[v_k, \dots, v_1]} + \sum_{i=0}^{k-1} (-1)^{i+1} \tilde{\sigma}^k|_{[v_0, v_k, \dots, \hat{v}_{k-i}, \dots, v_1]} \\
&= (-1)^{k-1} \sigma^{k-1} - \sigma^{k-1} + \sum_{i=1}^{k-1} (-1)^{i+1} \tilde{\sigma}^{k-1} \\
&= \frac{1 + (-1)^k}{2} (\tilde{\sigma}^{k-1} - 2\sigma^{k-1}),
\end{aligned}$$

giving the first column of D_k.

Considering now σ^{k-1}, observe that it maps $[v_1, v_k, \dots, v_2]$ onto $\exp_k(S^1, 1)$, taking the interior of this simplex homeomorphically onto its image. A face of $[v_1, v_k, \dots, v_2]$ corresponds to replacing an inequality with an equality in $0 \leq x_1 \leq \cdots \leq x_{k-1} \leq x_k = 1$, and in each case maps onto the $k-1$ or fewer element subsets containing 1. Thus σ^{k-1} factors through σ^{k-2} when restricted to each face. To calculate the boundary note that the map $\cup\{1\} \colon \exp_k S^1 \to \exp_{k+1}(S^1, 1)$ is simplicial, taking both $\tilde{\sigma}^{k-1}$ and σ^{k-1} to σ^{k-1}.

Thus

$$\begin{aligned}\partial\sigma^{k-1} &= \partial(\cup\{1\})_\sharp\tilde{\sigma}^{k-1}\\ &= (\cup\{1\})_\sharp\partial\tilde{\sigma}^{k-1}\\ &= -\frac{1+(-1)^{k-1}}{2}\sigma^{k-2},\end{aligned} \tag{2.2.1}$$

giving the second column of D_{k-1}, the first coming from the inductive hypothesis. This establishes the lemma.

It is now a simple matter to calculate the homology of $\exp_k S^1$. The matrix D_i is zero if i is odd and has determinant -1 if i is even, so the chain maps are alternately zeroes and isomorphisms in the middle dimensions. Thus $H_i(\exp_k S^1) = \{0\}$ for $1 \le i \le k-2$. Clearly $H_0(\exp_k S^1) \cong \mathbf{Z}$, so it remains to determine only H_{k-1} and H_k. When k is odd the top end of the chain complex is

$$0 \longrightarrow \mathbf{Z} \overset{0}{\longrightarrow} \mathbf{Z}\oplus\mathbf{Z} \overset{\cong}{\longrightarrow} \mathbf{Z}\oplus\mathbf{Z} \longrightarrow 0,$$

so H_{k-1} is zero and $H_k(\exp_k S^1) \cong \mathbf{Z}$, generated by $[\tilde{\sigma}^k]$. When k is even we have instead

$$\begin{array}{c}0 \longrightarrow \mathbf{Z} \longrightarrow \mathbf{Z}\oplus\mathbf{Z} \longrightarrow 0,\\ 1 \longmapsto (1,-2)\end{array}$$

making H_k zero and imposing the relation $\tilde{\sigma}^{k-1} = 2\sigma^{k-1}$ on $\ker\partial_{k-1} = C_{k-1}$. Thus for k even we have $H_{k-1}(\exp_k S^1) \cong \mathbf{Z}$, generated by $[\sigma^{k-1}]$. This proves the first statement of the corollary, and for the second simply observe that the generator $[\tilde{\sigma}^{2k-1}]$ of $H_{2k-1}(\exp_{2k-1} S^1)$ is twice $[\sigma^{2k-1}]$, the generator of $H_{2k-1}(\exp_{2k} S^1)$. □

Theorem 2.4 for $k \ge 3$ now follows from Corollary 2.1 and the simple connectivity of $\exp_3 S^1$ by an application of a standard argument.

Corollary 2.2 (Theorem 2.4). $\exp_k S^1$ *has the homotopy type of an odd dimensional sphere of dimension* $d_k = 2\lceil k/2\rceil - 1$.

Proof. We have already seen this for $k = 1, 2$ so we may assume $k \ge 3$. Then the 2–skeleton of $\exp_k S^1$ co-incides with the 2–skeleton of $\exp_3 S^1$, which is simply connected, so $\pi_1(\exp_k S^1) \cong \{1\}$ too. By the Hurewicz theorem $\pi_{d_k}(\exp_k S^1) \cong H_{d_k}(\exp_k S^1) \cong \mathbf{Z}$, so let $\phi\colon S^{d_k} \to \exp_k S^1$ be a generator for $\pi_{d_k}(\exp_k S^1)$. The map ϕ_* is an isomorphism on π_{d_k} and so on H_{d_k} also; since H_0 and H_{d_k} are the only non-vanishing homology groups of both S^{d_k} and $\exp_k S^1$ ϕ_* is an isomorphism on H_n for all n. By the simply connected version of Whitehead's theorem that only requires isomorphisms on homology, ϕ is a homotopy equivalence. □

We close this section with some remarks on the homotopy type of $\exp_k(S^1, 1)$ and $\exp S^1$. Recall that

$$\exp_k(S^1, 1) = \left\{\Lambda \in \exp_k S^1 \middle| 1 \in \Lambda\right\},$$

the subsets of S^1 of size k or less that contain 1. This subspace has a cell structure with one cell σ^i in each dimension less than or equal to $k-1$, and by (2.2.1) the boundary maps

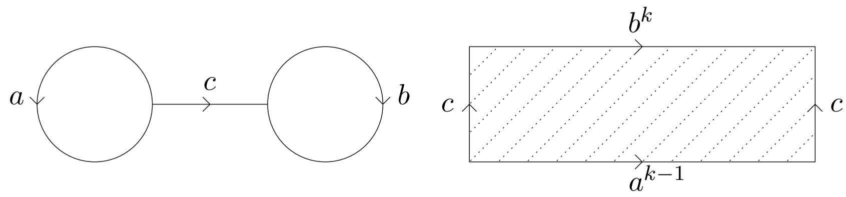

Figure 2.4: A cell complex with the homotopy type of $(k-1,k)$–torus knot complement. There are three 1–cells a, b, c and one 2–cell, attached along $a^{k-1}cb^{-k}c^{-1}$.

are alternately zero and isomorphisms. Thus the reduced homology of $\exp_k(S^1,1)$ is given by

$$\tilde{H}_i(\exp_k(S^1,1)) = \begin{cases} \mathbf{Z} & \text{if } i = k-1 \text{ is odd,} \\ 0 & \text{otherwise,} \end{cases}$$

and moreover $\exp_k(S^1,1)$ is simply connected for $k \geq 3$ since its 2-skeleton is a dunce cap. It follows (by the Whitehead theorem for k odd, and the argument of Corollary 2.2 for k even) that $\exp_k(S^1,1)$ is contractible if k is odd, and homotopy equivalent to S^{k-1} if k is even. The natural map

$$\exp_{k-1}S^1 \to \exp_k(S^1,1) : \Lambda \mapsto \Lambda \cup \{1\}$$

takes $[\tilde{\sigma}^{k-1}]$ to $[\sigma^{k-1}]$ and so has degree one for k even. Note however that this map is not a homeomorphism except when $k=2$ since otherwise $\{\lambda\}$ and $\{\lambda, 1\}$ have the same image.

Lastly, recall that

$$\exp S^1 = \bigcup_{k=1}^{\infty} \exp_k S^1 = \{\Lambda \subseteq S^1 \big| 0 < |\Lambda| < \infty\},$$

topologised as the direct limit of the $\exp_k S^1$, or equivalently, with the CW topology coming from the cell structure consisting of the $\tilde{\sigma}^i, \sigma^i$. The full finite subset space $\exp S^1$ has vanishing reduced homology in all dimensions and is therefore contractible.

2.3 The complement of the codimension two stratum

2.3.1 A new model for $\exp_k S^1$

The strategy for proving Theorem 2.6 is to show that $\exp_k S^1 \backslash \exp_{k-2} S^1$ deformation retracts to a subspace having the cell structure shown in figure 2.4. In order to make calculations easier and the result more transparent we will adopt a slightly different picture of $\exp_k S^1$, using the action of S^1 to model it as a quotient of a $(k-1)$–simplex cross an interval. On the simplex level this action corresponds to the constant vector field equal to $(1,1,\ldots,1)$ everywhere and the orbits are unions of intervals of the form

$$[(0, x_2, \ldots, x_k)\,,\,(y_1, \ldots, y_{k-1}, 1)]\,, \tag{2.3.1}$$

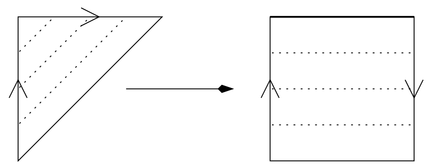

Figure 2.5: The new model in the case $k = 2$. We model $\exp_2 S^1$ as a quotient of a 1–simplex cross an interval by normalising the dotted lines in the triangle on the left (corresponding to subintervals of the S^1 action) to have length one, giving the square on the right. In doing this the top left vertex of the triangle is stretched to become the top edge of the square.

where $y_i = x_i + 1 - x_k$ for each i. The effect of our new model will be to normalise the lengths of these intervals to one. Figure 2.5 depicts this in the case $k = 2$.

Let Δ be the simplex

$$[v_0, \ldots, v_{k-1}] = \{(0, a_1, \ldots, a_{k-1}) | 0 \leq a_1 \leq \cdots \leq a_{k-1} \leq 1\}$$

and consider the map from $\Delta \times I$ to our usual model

$$X = [v_0, \ldots, v_k] = \{(x_1, \ldots, x_k) | 0 \leq x_1 \leq \cdots \leq x_k \leq 1\}$$

given by

$$x_i = \begin{cases} (1 - a_{k-1})t & i = 1, \\ a_{i-1} + (1 - a_{k-1})t & 2 \leq i \leq k. \end{cases}$$

This has inverse

$$\begin{aligned} a_i &= x_{i+1} - x_1 \\ t &= \frac{x_1}{1 - x_k + x_1} \end{aligned}$$

well defined off the codimension two face $[v_1, \ldots, v_{k-1}]$ where $x_1 = 0$ and $x_k = 1$, which has preimage the entire codimension one face $[v_1, \ldots, v_{k-1}] \times I$ due to the intervals (2.3.1) through these points being stretched from length zero to one. We will refer to this as the "fake face" of $\Delta \times I$ and denote the quotient map $\Delta \times I \to X \to \exp_k S^1$ by q.

In forming $\exp_k S^1$ from $\Delta \times I$ the $k - 1$ faces $\{a_1 = 0\} \times I$ and $\{a_i = a_{i+1}\} \times I$, $1 \leq i \leq k - 2$, are all identified according to the maps

$$[v_0, \ldots, \hat{v}_i, \ldots, v_{k-1}] \times I \to [v_0, \ldots, \hat{v}_j, \ldots, v_{k-1}] \times I \qquad (i, j \neq 0) \tag{2.3.2}$$

given by the product of the canonical map with the identity. The face $\{a_{k-1} = 1\} \times I$ is collapsed back down to $\{a_{k-1} = 1\}$ by projection on the first factor, and $\Delta \times \{0\}$ is glued to $\Delta \times \{1\}$ according to $(a, 1) \sim (\phi(a), 0)$, where

$$\phi_i(a) = \begin{cases} 1 - a_{k-1} & i = 1, \\ a_{i-1} + 1 - a_{k-1} & 2 \leq i \leq k. \end{cases}$$

The map ϕ is affine and permutes the vertices $v_0, \ldots, v_{k-1}$ cyclicly according to the permutation $i \mapsto i-1 \pmod{k-1}$ and so is the canonical map $[v_0, \ldots, v_{k-1}] \to [v_{k-1}, v_0, \ldots, v_{k-2}]$. In particular $\exp_k S^1 \setminus \exp_{k-1} S^1$, as the quotient of $(\text{int}\,\Delta) \times I$, is the mapping torus of $\phi|_{\text{int}\,\Delta}$ and has the homeomorphism type of an $\mathbf{R}^{k-1}$ bundle over S^1, with monodromy of order k. The gluing reverses orientation exactly when k is even so the bundle is trivial for k odd and nontrivial for k even.

Although we shall not explicitly do so, there is no loss in generality in regarding Δ as the more symmetrical standard $(k-1)$–simplex

$$\left\{(t_0, t_1, \ldots, t_{k-1}) \in \mathbf{R}^k \middle| \textstyle\sum_i t_i = 1 \text{ and } t_i \geq 0 \text{ for all } i\right\},$$

and what follows may be read with this picture in mind.

2.3.2 The fundamental group of $\exp_k S^1 \setminus \exp_{k-2} S^1$

As a first application of our new model we calculate the fundamental group of $\exp_k S^1 \setminus \exp_{k-2} S^1$. This calculation is in some sense redundant, in that in the following section we will find a 2–complex to which it is homotopy equivalent. However, the proof given below that this space has the correct fundamental group strongly echoes the corresponding calculation for the torus knot complement. In doing so it carries the main insight as to why the two have the same homotopy type, while the proof of this fact, while geometric in nature, is somewhat technical. We therefore include both proofs to further understanding of the result.

We take as our base point the kth roots of unity. Let γ be the path from the kth roots of unity to the $(k-1)$th given by projecting to $\exp_k S^1$ the linear homotopy from $(0, 1/k, \ldots, (k-1)/k)$ to $(0, 0, 1/(k-1), \ldots, (k-2)/(k-1))$. Let α be the loop given by rotating the kth roots of unity anti-clockwise through $2\pi/k$, and β the loop based at $\{\lambda^k = 1\}$ given by taking γ to $\{\lambda^{k-1} = 1\}$, rotating the circle anti-clockwise through $2\pi/(k-1)$, then following γ back to the basepoint. Then:

Theorem 2.8. *$\pi_1(\exp_k S^1 \setminus \exp_{k-2} S^1)$ has presentation $\langle \alpha, \beta | \alpha^k = \beta^{k-1} \rangle$.*

Remark. Another choice of second generator is the loop δ given by "teleporting" a point from $e^{2\pi i/k}$ to $e^{-2\pi i/k}$ as follows. Between time $t = 0$ and $1/2$ move one point from 1 to $e^{2\pi i/k}$, keeping the rest fixed. At time $t = 1/2$ the moving point merges with $e^{2\pi i/k}$ and we may regard it as being at $e^{-2\pi i/k}$ instead; between $t = 1/2$ and 1 move the extra point at $e^{-2\pi i/k}$ back to 1, keeping the rest fixed. Figure 2.6 illustrates that β is homotopic to $\delta\alpha$, and we will use this below to show that the inclusion

$$\exp_k S^1 \setminus \exp_{k-2} S^1 \hookrightarrow \exp_k S^1 \setminus \exp_{k-3} S^1$$

is trivial on π_1.

Proof. The result is an application of the van Kampen theorem. Each of $\exp_k S^1 \setminus \exp_{k-1} S^1$ and $\exp_{k-1} S^1 \setminus \exp_{k-2} S^1$ has the homotopy type of a circle, with fundamental group generated (up to basepoint) by α and β respectively. We show that $\exp_{k-1} S^1 \setminus \exp_{k-2} S^1$ has a neighbourhood N in $\exp_k S^1 \setminus \exp_{k-2} S^1$ that deformation retracts to it and apply the van

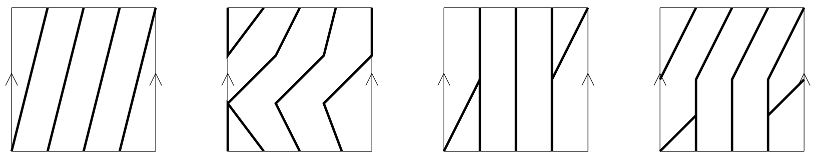

Figure 2.6: Movies of the generators of $\pi_1(\exp_4 S^1 \setminus \exp_2 S^1)$. Each square represents a cylinder $S^1 \times [0,1]$; dark lines show the motion of points. The diagram for β may be isotoped rel boundary (and respecting the fact that each slice $S^1 \times \{t\}$ should meet the curves in either 3 or 4 points) to give the diagram on the right, showing $\beta \simeq \delta\alpha$.

Kampen theorem to the cover consisting of $\exp_k S^1 \setminus \exp_{k-1} S^1$ and N. The intersection N' of these two sets will turn out to have the homotopy type of a circle also, and will lead to the relation $\alpha^k = \beta^{k-1}$.

The preimage of $\exp_k S^1 \setminus \exp_{k-2} S^1$ in $\Delta \times I$ is the product of Δ less all faces of codimension two or more with the interval. Let b be the barycentre of Δ, set

$$\begin{aligned}\Delta_i &= [b, v_{i+1}, \ldots, v_{k-1}, v_0, \ldots, v_{i-1}],\\ \delta_i &= [v_{i+1}, \ldots, v_{k-1}, v_0, \ldots, v_{i-1}],\end{aligned}$$

and note that Δ is the union of the Δ_i and its boundary is the union of the δ_i. Further, ϕ sends Δ_i, δ_i to $\Delta_{i-1}, \delta_{i-1}$ respectively, where subscripts are taken mod $k-1$. Let

$$N = q\left(\bigcup_{i=0}^{k-1} (\operatorname{int}\Delta_i \cup \operatorname{int}\delta_i) \times I\right)$$

and observe that N is a neighbourhood of

$$\exp_{k-1} S^1 \setminus \exp_{k-2} S^1 = q\left(\bigcup_{i=0}^{k-1} \operatorname{int}\delta_i \times I\right)$$

in $\exp_k S^1 \setminus \exp_{k-2} S^1$.

The half open simplex $\operatorname{int}\Delta_i \cup \operatorname{int}\delta_i$ deformation retracts to $\operatorname{int}\delta_i$ and moreover this may be done for each i simultaneously in a way compatible with the action of ϕ. Crossing this with I gives a deformation retraction of

$$\bigcup_{i=0}^{k-1} (\operatorname{int}\Delta_i \cup \operatorname{int}\delta_i) \times I \quad \text{to} \quad \bigcup_{i=0}^{k-1} \operatorname{int}\delta_i \times I$$

that descends to a deformation retraction of N onto $\exp_{k-1} S^1 \setminus \exp_{k-2} S^1$. Thus $\exp_{k-1} S^1 \setminus \exp_{k-2} S^1$ does have a neighbourhood as desired and by the van Kampen theorem

$$\pi_1(\exp_k S^1 \setminus \exp_{k-2} S^1) = \langle\alpha\rangle *_{\pi_1(N')} \langle\beta\rangle,$$

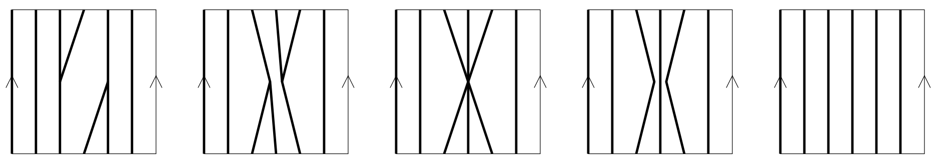

Figure 2.7: The movie of a homotopy from δ to the constant loop in $\exp_k S^1$ less the codimension three stratum. The figures show $k = 6$ but the method clearly generalises. Figure (a) shows δ, where we have cut the circle at -1 for clarity. Planar isotopy gives (b), then we merge the branch points (c) and separate them again (d) so that there are 6 distinct points throughout the path. Planar isotopy leads to the constant loop in (e).

where

$$N' = N \cap (\exp_k S^1 \setminus \exp_{k-1} S^1) = q\Bigg(\bigcup_{i=0}^{k-1} \operatorname{int}\Delta_i \times I\Bigg).$$

Now N' is homeomorphic to $\big(\bigcup_i \operatorname{int}\Delta_i \times I\big)/\,(\Delta_i \times \{1\} \sim \Delta_{i-1} \times \{0\})$, where the gluing relations are given by ϕ. Thus $N' \cong \operatorname{int}\Delta_{k-1} \times S^1$, where we have chosen Δ_{k-1} since $q(\Delta_{k-1} \times \{0\})$ contains the path γ. If $\pi_1(N') = \langle \varepsilon \rangle$ then clearly $\varepsilon = \alpha^k$ in $\pi_1(\exp_k S^1 \setminus \exp_{k-1} S^1)$; it remains to determine the image of ε in $\pi_1(\exp_{k-1} S^1 \setminus \exp_{k-2} S^1)$.

Pushing ε onto $\exp_{k-1} S^1 \setminus \exp_{k-2} S^1$ via the deformation retraction of N we see that upstairs in $\Delta \times I$ ε traverses the length of each $\operatorname{int}\delta_i \times I$ exactly once and positively. For $i = 1, \dots, k-1$ we have $q(\operatorname{int}\delta_i \times I) = \exp_{k-1} S^1 \setminus \exp_{k-2} S^1$ and we pick up a copy of the generator of $\pi_1(\exp_{k-1} S^1 \setminus \exp_{k-2} S^1)$ from each. However, recalling that $\delta_0 \times I$ is the fake face mapping only to $\exp_{k-1}(S^1, 1)$ we see that the contribution from this face is just the constant loop. Thus ε maps to $k-1$ times the generator in $\pi_1(\exp_{k-1} S^1 \setminus \exp_{k-2} S^1)$ and we get the relation $\alpha^k = \beta^{k-1}$ as required. $\square$

Both α and β are null homotopic in $\exp_k S^1$ less the codimension three stratum $\exp_{k-3} S^1$. To see this consider figure 2.7, which shows a movie of a homotopy in $\exp_k S^1 \setminus \exp_{k-3} S^1$ from $\delta = \beta\alpha^{-1}$ to the constant loop. The relation $\alpha^k = \beta^{k-1}$ then gives $\alpha = \beta = 1$.

2.3.3 The homotopy type of $\exp_k S^1 \setminus \exp_{k-2} S^1$

We now turn to the more delicate matter of showing that $\exp_k S^1 \setminus \exp_{k-2} S^1$ deformation retracts to a subspace having a cell structure as in figure 2.4. We will of course construct the deformation retraction upstairs in $\Delta \times I$ and some care will be required to ensure it descends to the quotient.

Let b_i be the barycentre of δ_i. Since affine maps of simplices take barycentres to barycentres the identifications (2.3.2) in section 2.3.1 glue $\{b_i\} \times I$ to $\{b_j\} \times I$ for $i, j \neq 0$ and ϕ glues $[b, b_i] \times \{1\}$ to $[b, b_{i-1}] \times \{0\}$ for each i, while $\{b_0\} \times I$ is of course collapsed to $\{b_0\} \times \{0\}$. Letting B be the star graph $\bigcup_{i=0}^{k-1} [b, b_i]$ it is clear that $q(B \times I)$ may be given a cell structure as in figure 2.4. The fact that $\exp_k S^1 \setminus \exp_{k-2} S^1$ deformation retracts to this subspace is a consequence of the following technical lemma.

Lemma 2.2. *There is a deformation retraction* Φ *from*

$$\operatorname{int}\Delta \cup \bigcup_{i=0}^{k-1} \operatorname{int}\delta_i \quad \text{to} \quad B$$

such that

a. $\Phi_t(\operatorname{int}\delta_i) \subseteq \operatorname{int}\delta_i$ *for all* t *and* $i = 0, \ldots, k-1$*;*

b. Φ_t *commutes with the action of the symmetric group* S_k *on* Δ*, where* $\sigma \in S_k$ *acts by the canonical map* $[v_0, \ldots, v_{k-1}] \to [v_{\sigma(0)}, \ldots, v_{\sigma(k-1)}]$*.*

We will define Φ using the barycentric subdivision of Δ, and first show:

Lemma 2.3. *Let* $\beta_0, \ldots, \beta_n$ *be affinely independent points. Then* $[\beta_0, \ldots, \beta_n] \backslash [\beta_0, \ldots, \beta_{n-2}]$ *deformation retracts to* $[\beta_{n-1}, \beta_n]$ *via a homotopy* Ψ *such that*

$$\Psi_t(\delta \setminus [\beta_0, \ldots, \beta_{n-2}]) \subseteq \delta \setminus [\beta_0, \ldots, \beta_{n-2}] \tag{2.3.3}$$

for all t *and each face* δ *of* $[\beta_0, \ldots, \beta_n]$*.*

Proof. The proof is by induction on n, the case $n = 1$ being trivial. Define a deformation retraction ψ to $[\beta_1, \ldots, \beta_n] \setminus [\beta_1, \ldots, \beta_{n-2}]$ by

$$\psi_t\left(\sum_{i=0}^{n} \lambda_i \beta_i\right) = (1-t)\sum_{i=0}^{n} \lambda_i \beta_i + t \sum_{i=1}^{n} \frac{\lambda_i}{1-\lambda_0}\beta_i \;;$$

this is well defined since λ_0 is never equal to 1, and the co-efficient of at least one of β_{n-1}, β_n is nonzero for all t. Moreover if v is a convex combination of $\beta_{i_0}, \ldots, \beta_{i_\ell}$ then $\psi_t(v)$ is too so the face condition (2.3.3) is satisfied. Applying the induction hypothesis to $[\beta_1, \ldots, \beta_n] \setminus [\beta_1, \ldots, \beta_{n-2}]$ gives the result. □

Proof of Lemma 2.2. A typical simplex in the barycentric subdivision of Δ has the form $[\beta_0, \ldots, \beta_{k-1}]$ where each β_i is the barycentre of an i–dimensional face of Δ containing $\beta_0, \ldots, \beta_{i-1}$. In particular $\beta_{k-1} = b$, β_0 is some vertex v_i and β_{k-2} is b_j for some $j \neq i$. Deleting the codimension two faces of Δ deletes precisely $[\beta_0, \ldots, \beta_{k-3}]$ from $[\beta_0, \ldots, \beta_{k-1}]$ and we define Φ on this simplex using the deformation retraction Ψ given by Lemma 2.3.

Suppose $[\beta_0, \ldots, \beta_{k-1}]$ and $[\beta'_0, \ldots, \beta'_{k-1}]$ share a common face $[\beta_{i_0}, \ldots, \beta_{i_\ell}]$. Then necessarily $\beta_{i_j} = \beta'_{i_j}$ for $j = 1, \ldots, \ell$ and this face is fixed pointwise by the canonical map $[\beta_0, \ldots, \beta_{k-1}] \to [\beta'_0, \ldots, \beta'_{k-1}]$; the face condition (2.3.3) in Lemma 2.3 then shows that Φ is well defined. Condition (a) follows from the face condition (2.3.3) applied to each simplex of the form $[\beta_0, \ldots, \beta_{k-2}]$, and the commutativity of Φ with the action of the symmetric group is a consequence of the fact that any $\sigma \in S_k$ permutes the barycentres of the i–dimensional faces. □

Corollary 2.3 (implies Theorem 2.6). *The space* $\exp_k S^1 \backslash \exp_{k-2} S^1$ *deformation retracts to* $q(B \times I)$*.*

Proof. Crossing Φ with the identity gives a deformation retraction of

$$\left(\operatorname{int}\Delta \cup \bigcup_{i=0}^{k-1} \operatorname{int}\delta_i\right) \times I \quad \text{to} \quad B \times I$$

and we check that this is compatible with the gluings

1. $\phi\colon\ \Delta_i \times \{1\} \to \Delta_{i-1} \times \{0\}$,
2. $[v_0, \ldots, \hat{v}_i, \ldots, v_{k-1}] \times I \to [v_0, \ldots, \hat{v}_j, \ldots, v_{k-1}] \times I$ for $i, j \neq 0$,
3. $\delta_0 \times I \to \delta_0 \times \{0\}$.

Compatibility with (1) follows from commutativity of Φ with S_k; compatibility with (2) uses commutativity with S_k together with condition (a) of Lemma 2.2; and compatibility with (3) comes from constructing the homotopy by crossing Φ with the identity on I. □

2.4 The degree of an induced map

A map $f\colon\ S^1 \to S^1$ induces a map $\exp_k f\colon\ \exp_k S^1 \to \exp_k S^1$ of homotopy spheres, the degree of which depends only on k and the degree of f. We claim (Theorem 2.7) that

$$\deg \exp_k f = (\deg f)^{\left\lfloor \frac{k+1}{2} \right\rfloor}.$$

Proof of Theorem 2.7. We begin by reducing to the case where $k = 2\ell - 1$ is odd, using the commutative diagram

$$\begin{array}{ccc} \exp_{2\ell-1} S^1 & \xrightarrow{\exp_{2\ell-1} f} & \exp_{2\ell-1} S^1 \\ \big\downarrow{\scriptstyle \cup\{1\}} & & \big\downarrow{\scriptstyle \cup\{f(1)\}} \\ \exp_{2\ell} S^1 & \xrightarrow{\exp_{2\ell} f} & \exp_{2\ell} S^1 \end{array}.$$

The vertical arrows are degree one maps by the results of section 2.2.4, so we have

$$\deg \exp_{2\ell} f = \deg \exp_{2\ell-1} f$$

and it suffices to show that $\deg \exp_{2\ell-1} f = (\deg f)^{\ell}$. We do this by considering separately the cases $\deg f > 0$ and $\deg f = -1$; in both cases we assume that f is the map $\lambda \mapsto \lambda^d$ and count the preimages of a generic point with signs.

Suppose that $f(\lambda) = \lambda^d$ with d positive. A generic point Λ of $\exp_k S^1$ will have d^k preimages under $\exp_k f$, corresponding to the d choices for the preimage of each element of Λ. For concreteness let $\lambda_0, \ldots, \lambda_{k-1}$ be the kth roots of unity, cyclicly ordered so that

$$\lambda_r = e^{2\pi i r/k}.$$

Under f each λ_r has d preimages $\lambda_{r,s}$, $s = 0, \ldots, d-1$, which we again cyclicly order so that

$$\lambda_{r,s} = e^{2\pi i(sk+r)/kd}.$$

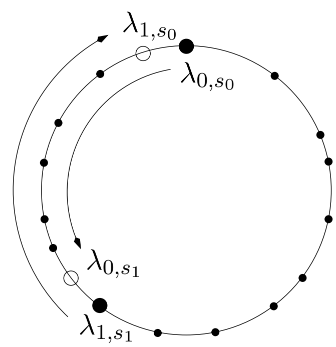

Figure 2.8: The preimages S and $\sigma_{01}(S)$, if different, have opposite signs. We may move from one to the other by hopping a point at λ_{0,s_0} around the circle to λ_{0,s_1}, and then hopping a point at λ_{1,s_1} around the circle to λ_{1,s_0}. If we move both points around the same arc then both move past the same points in between, except that one must pass the other as well. This requires an odd number of transpositions.

Then a preimage of $\{\lambda|\lambda^k = 1\}$ is specified by a k–tuple $(s_0, \ldots, s_{k-1})$ of integers mod d, corresponding to the set

$$\{\lambda_{0,s_0}, \ldots, \lambda_{k-1,s_{k-1}}\},$$

and comes with a positive or negative sign according to whether this set is an even or odd permutation of cyclic order when ordered as written. Note that the sign relative to cyclic ordering makes sense since $k = 2\ell - 1$ is odd.

Our goal is to match the preimages up in cancelling pairs until those that are left are all positive. To this end consider the involution σ_{01} given by $(s_0, \ldots, s_{k-1}) \mapsto (s_1, s_0, s_2, \ldots, s_{k-1})$; we claim that if a preimage S is not fixed by σ_{01} then S and $\sigma_{01}(S)$ have opposite signs. Indeed, if $s_0 \neq s_1$ and we move points from λ_{0,s_0} to λ_{0,s_1} and from λ_{1,s_1} to λ_{1,s_0} around the same arc of the circle then (since there can be no points between λ_{0,s_j} and λ_{1,s_j}) both must pass exactly the same points in between, and in addition one must pass the other (see figure 2.8). This involves an odd number of transpositions so S and $\sigma_{01}(S)$ have opposite signs if $s_0 \neq s_1$.

Applying the same argument in turn to the involutions switching s_{2j} and s_{2j+1}, $1 \leq j \leq \ell - 2$, acting just on those preimages fixed by all previous involutions, we see that we may match up all preimages in cancelling pairs except those for which $s_{2j} = s_{2j+1}$, $0 \leq j \leq \ell - 2$. Since these can all be shuffled to cyclic order by moving points around in pairs they are all positive, and there are d^ℓ of them as there are d choices for each s_{2j}, $j = 0, \ldots, \ell - 1$. This gives $\deg \exp_k f = d^\ell$ as desired.

Now consider $f(\lambda) = \lambda^{-1}$. The sole preimage of the ordered set $\{\lambda_0, \ldots, \lambda_{k-1}\}$ is $\{\lambda_0, \lambda_{k-1}, \ldots, \lambda_1\}$ which may be put in cyclic order using $(k-1)/2 = \ell - 1$ transpositions. We get an additional factor of $(-1)^k$ from the product of the local degrees of f at each λ_j, so

$$\deg \exp_k f = (-1)^{\ell-1} \cdot (-1)^{2\ell-1} = (-1)^{\ell-2} = (\deg f)^\ell$$

as required.

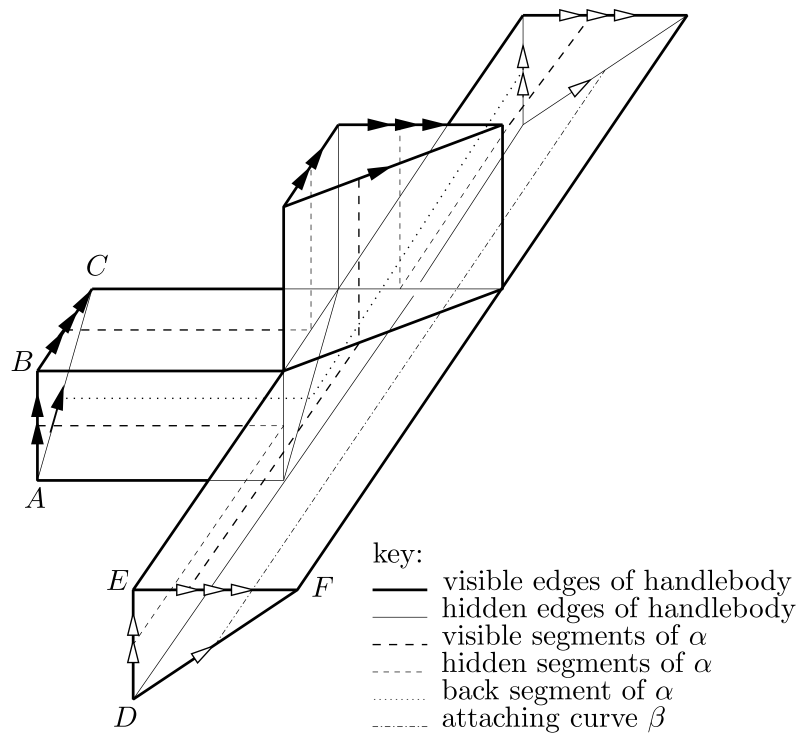

Figure 2.9: A regular neighbourhood of the dual 1–skeleton of the triangulation of $\exp_3 S^1$ in figure 2.3. Glue the triangular faces as indicated to get a genus two solid handlebody H forming half of a Heegaard splitting of $\exp_3 S^1$. The curves α and β bound discs in the second handlebody H'.

If $\deg f = 0$ then clearly $\deg \exp_k f = 0$, so putting the cases $\deg f > 0$ and $\deg f = -1$ together using $\deg(g \circ h) = (\deg g) \cdot (\deg h)$ gives the result. □

2.5 Cut and paste proof of Theorems 2.1 and 2.2

We give a mostly pictorial proof that $\exp_3 S^1$ is S^3 and that $\exp_1 S^1$ inside it is a left-handed trefoil knot.

We found in section 2.2.3 that $\exp_3 S^1$ is a 3–manifold with a triangulation consisting of just one 3–simplex, and in the standard way we obtain a Heegaard splitting by regarding it as the union $H' \cup_\partial H$ of regular neighbourhoods of the 1– and dual 1–skeletons. A regular neighbourhood of the dual 1–skeleton of the 3–simplex of figure 2.3(a) is shown in figure 2.9 and H is the genus two solid handlebody given by gluing the four triangular faces at the end of each "arm" as indicated by the arrows. We keep track of H' by recording loops α and β linking each of the edges, the loops forming the attaching circles for the 2–handles of $\exp_3 S^1$. The loop α linking the edge a of figure 2.3(b) appears in five pieces in figure 2.9, four of which are shown dashed and the fifth dotted, while the loop β linking the edge b appears in just one piece, indicated by the dash-dot-dash-dot line.

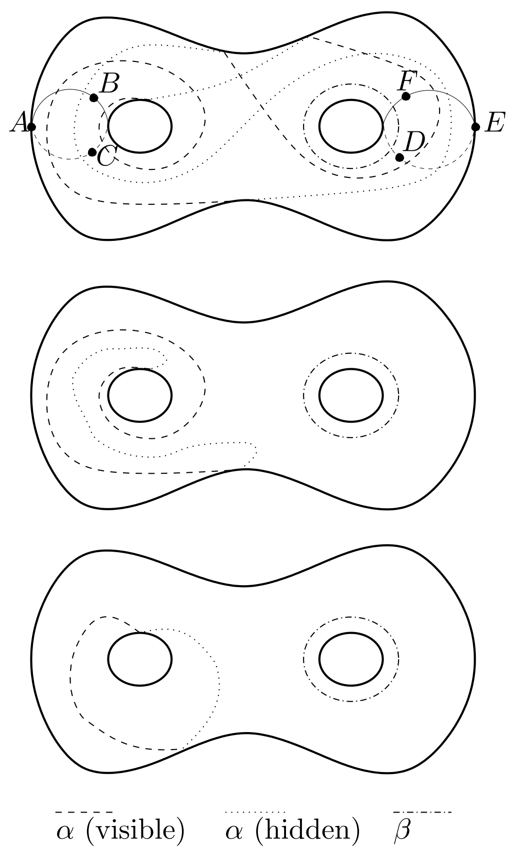

Figure 2.10: Heegaard diagrams of $\exp_3 S^1$. Top: The handlebody H obtained by gluing the triangular faces of figure 2.9. Middle: Attaching curve α after sliding the loops going around the right 1–handle over the cancelling 2–handle. Bottom: After isotopy α forms a $(1,1)$–curve around the left 1–handle, giving a Heegaard diagram of S^3.

Bending the arms and giving the top arm a one-third twist so the arrows match we glue the triangular faces to obtain H, shown in the top diagram in figure 2.10. The curve β is again indicated by a dash-dot-dash-dot pattern and we see immediately that the attached 2–handle cancels the right 1–handle. The curve α linking a, shown dashed when it is on top and dotted when it is underneath, goes geometrically twice over the right 1–handle and we slide each loop over the cancelling 2–handle to get the middle diagram. Further isotopy leads to the bottom diagram in which α appears as a $(1,1)$–curve around the left 1–handle. This may be recognised as a Heegaard diagram for S^3 but we nevertheless apply a Dehn twist to convert it to the standard diagram. Writing the meridian first and giving ∂H the right-hand orientation induced by H the appropriate Dehn twist acts by

$$T = \begin{bmatrix} 1 & -1 \\ 0 & 1 \end{bmatrix}$$

on $H_1(\partial(H \cup_\beta (D^2 \times I)))$.

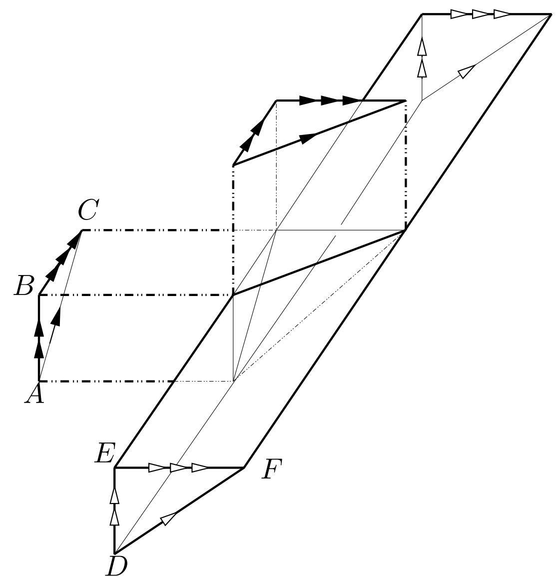

Figure 2.11: Generic orbits of the S^1 action on $\exp_3 S^1$ meet the 3–simplex in three lines parallel to the direction $(1, 1, 1)$. Perturbing them to lie on the Heegaard surface we may obtain the three arcs shown dash-dot-dotted.

We now turn our attention to $\exp_1 S^1 \hookrightarrow \exp_3 S^1$, corresponding to the edge b of figure 2.3(b). We take a push-off of b into the interior of the simplex and perturb it to lie on the Heegaard surface. This is most easily done by recalling that $\exp_1 S^1$ forms a generic (here meaning trivial stabiliser) orbit of the S^1 action on $\exp_3 S^1$, and that generic orbits passing through the interior of the simplex break into three lines parallel to the vector $(1, 1, 1)$. Pushing them onto the Heegaard surface we obtain the arcs shown dash-dot-dotted in figure 2.11. The resulting curve on ∂H appears in figure 2.12, shown dashed when it is on top and dotted underneath, and as might be expected from figure 2.11 it forms a $(1, 3)$–curve around the left 1–handle. The Dehn twist with matrix T that converts the bottom Heegaard diagram of figure 2.10 to the standard diagram takes this curve to a $(-2, 3)$–curve, giving a left-handed trefoil as promised.

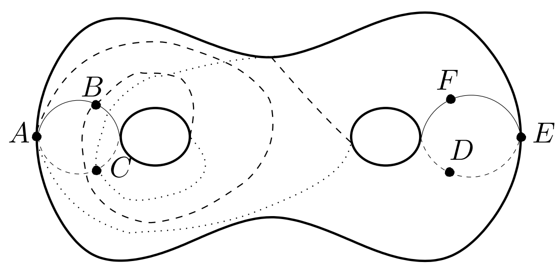

Figure 2.12: The perturbed orbit, shown dashed when on top and dotted when below, after gluing figure 2.11 up to form H. It traces a $(1, 3)$–curve on the left 1–handle and is transformed to a $(-2, 3)$–curve by the Dehn twist.

Chapter 3

Graphs and punctured surfaces

3.1 Introduction

3.1.1 Summary of results

We now extend the techniques from the previous chapter to study the finite subset spaces of a connected graph Γ. Since $\exp_k$ is a homotopy functor we may reduce to the case where Γ has a single vertex, and accordingly define Γ_n to be the graph with one vertex v and n edges $e_1, \ldots, e_n$. Our first result is a complete calculation of the homology of $\exp_k(\Gamma_n, v)$ and $\exp_k\Gamma_n$ for each k and n:

Theorem 3.1. *The reduced homology groups of* $\exp_k(\Gamma_n, v)$ *vanish outside dimension* $k-1$ *and those of* $\exp_k\Gamma_n$ *vanish outside dimensions* $k-1$ *and* k*. The non-vanishing groups are free. The maps*

$$i\colon\ \exp_k(\Gamma_n, v) \hookrightarrow \exp_k\Gamma_n$$

and

$$\cup\{v\}\colon\ \exp_k\Gamma_n \to \exp_{k+1}(\Gamma_n, v)$$

induce isomorphisms on H_{k-1} *and* H_k *respectively while*

$$\exp_k\Gamma_n \hookrightarrow \exp_{k+1}\Gamma_n$$

is twice $(i \circ \cup\{v\})_*$ *on* H_k*. The common rank of*

$$H_k(\exp_k\Gamma_n) \cong H_k(\exp_{k+1}\Gamma_n) \cong H_k(\exp_{k+1}(\Gamma_n, v))$$

is given by

$$\begin{aligned} b_k(\exp_k\Gamma_n) &= \sum_{j=1}^{k}(-1)^{j-k}\binom{n+j-1}{n-1} \\ &= \begin{cases} \sum_{j=1}^{\ell}\binom{n+2j-2}{n-2} & \text{if } k = 2\ell \text{ is even,} \\ n + \sum_{j=1}^{\ell}\binom{n+2j-1}{n-2} & \text{if } k = 2\ell+1 \text{ is odd.} \end{cases} \end{aligned} \tag{3.1.1}$$

A list of Betti numbers $b_k(\exp_k\Gamma_n)$ for $1 \leq k \leq 20$ and $1 \leq n \leq 10$ appears as table A.1 in the appendix on page 88.

In the case of a circle the homology and fundamental group of $\exp_k S^1$ were enough to determine its homotopy type completely. The argument no longer applies to $\exp_k\Gamma_n$, $n \geq 2$, and its applicability for $n = 1$ is perhaps properly regarded as being due to a "small numbers co-incidence", the vanishing of $H_{2\ell}(\exp_{2\ell}\Gamma_1)$. However, the argument does apply to $\exp_k(\Gamma_n, v)$, and for $k \geq 2$ we have the following:

Theorem 3.2. *For $k \geq 2$ the space $\exp_k(\Gamma_n, v)$ has the homotopy type of a wedge of $b_{k-1}(\exp_k(\Gamma_n, v))$ $(k-1)$–spheres.*

Having calculated the homology of $\exp_k\Gamma_n$ we turn our attention to the maps $(\exp_k\phi)_*$ induced by maps $\phi\colon \Gamma_n \to \Gamma_m$. Our main result is to reduce the problem of calculating such maps to one of finding images of chains under maps

$$\exp_1 S^1 \to \exp_1 S^1$$

and

$$\exp_2 S^1 \to \exp_2 \Gamma_2$$

induced by maps $S^1 \to S^1$ and $S^1 \to \Gamma_2$ respectively. The reduction is achieved by defining a ring without unity structure on a subgroup $\tilde{\mathcal{C}}_*$ of the cellular chain complex of $\exp\Gamma_n$. The subgroup carries the top homology of $\exp_k\Gamma_n$ and is preserved by chain maps of the form $(\exp\phi)_\sharp$, and the ring structure is defined in such a way that these chain maps are ring homomorphisms. The ring $\tilde{\mathcal{C}}_* \otimes_{\mathbf{Z}} \mathbf{Q}$ is generated over $\mathbf{Q}$ by cells in dimensions one and two, leaving a mere $2n$ cells whose images must be found directly.

As an application of these results and as an illustration of how much $(\exp_k\phi)_*$ remembers about ϕ we study the action of the braid group B_n on $H_k(\exp_k\Gamma_n)$. The braid group may be regarded as the mapping class group of a punctured disc and as such it acts on the graph Γ_n via homotopy equivalence. We show that, for a suitable choice of basis, the braid group acts by block upper-triangular matrices whose diagonal blocks are representations of B_n that factor through S_n. Consequently, the image of the pure braid group consists of upper-triangular matrices with ones on the diagonal and is therefore nilpotent. The number of blocks depends mildly on k and n but is no more than about $n/2$, and this leads to a bound on the length of the lower central series.

We remark that the main results of this chapter may be used to study the finite subset spaces of a closed surface Σ via Mayer-Vietoris type arguments. This may be done by constructing a cover of $\exp_k\Sigma$ such that each element of the cover and each m–fold intersection is a finite subset space of a punctured surface, as follows. Choose $k+1$ distinct points $p_1, \ldots, p_{k+1}$ in Σ and let $\mathcal{U}_i = \exp_k\big(\Sigma \backslash \{p_i\}\big)$. The $\mathcal{U}_i$ form an open cover of $\exp_k\Sigma$, since each $\Lambda \in \exp_k\Sigma$ must omit at least one of the p_i, and moreover each m–fold intersection has the form

$$\bigcap_{j=1}^{m} \mathcal{U}_{i_j} = \exp_k\big(\Sigma \backslash \{p_{i_1}, \ldots, p_{i_m}\}\big),$$

a finite subset space of a punctured surface as desired. The results of this chapter may then be used to calculate the homology of each intersection and the maps induced by inclusion, leading to a spectral sequence for $H_*(\exp_k\Sigma)$.

We will use this idea in Chapter 5 to prove two vanishing theorems for the homotopy and homology groups of the finite subset spaces of a connected cell complex.

3.1.2 Outline of the chapter

The calculation of the homology of $\exp_k\Gamma_n$ and $\exp_k(\Gamma_n, v)$ is the main topic of section 3.2. We find explicit cell structures for these spaces in section 3.2.2 and use them to calculate their fundamental groups. We then show that the reduced chain complex of $\exp(\Gamma_n, v)$ is exact in section 3.2.3, and use this to prove Theorems 3.1 and 3.2 in section 3.2.4. We give an explicit basis for $H_k(\exp_k\Gamma_n)$ in section 3.2.5 and close with generating functions for the Betti numbers $b_k(\exp_k\Gamma_n)$ in section 3.2.6. A table of Betti numbers for $1 \leq k \leq 20$ and $1 \leq n \leq 10$ appears in Appendix A on page 88.

We then turn to the calculation of induced maps in section 3.3. The ring structure on $\tilde{\mathcal{C}}_*$ is motivated and defined in section 3.3.2 and we show that maps $\phi\colon \Gamma_n \to \Gamma_m$ induce ring homomorphisms in section 3.3.3. As illustration of the ideas we calculate two examples in section 3.3.4, the first giving an alternate proof of Theorem 2.7 and the second relating to the generators of the braid groups. We then state and prove the structure theorem for the braid group action in sections 3.4.1 and 3.4.2, and conclude by looking at the action of B_3 on $H_3(\exp_3\Gamma_3)$ in some detail in section 3.4.3.

3.1.3 Notation and terminology

We take a moment to fix some language and notation that will be used throughout this chapter.

We will work exclusively with graphs having just one vertex, so as above we define Γ_n to be the graph with one vertex v and n edges $e_1, \ldots, e_n$. As usual write I for the interval $[0, 1]$, and for each non-negative integer m let $[m] = \{i \in \mathbf{Z} | 1 \leq i \leq m\}$. We parameterise Γ_n as the quotient of $I \times [n]$ by the subset $\{0, 1\} \times [n]$, sending $\{0, 1\} \times [n]$ to v and $[0, 1] \times \{i\}$ to e_i. This directs each edge, allowing us to order any subset of its interior, and we will use this extensively.

Associated to a finite subset Λ of Γ_n is an n–tuple $\mathcal{J}(\Lambda) = (j_1, \ldots, j_n)$ of non-negative integers $j_i = |\Lambda \cap \operatorname{int} e_i|$. Given an n–tuple $J = (j_1, \ldots, j_n)$ we define its support $\operatorname{supp} J$ to be

$$\operatorname{supp} J = \{i \in [n] \big| j_i \neq 0\}$$

and its norm $|J|$ by

$$|J| = \sum_{i=1}^{n} j_i \,.$$

Note that

$$|\mathcal{J}(\Lambda)| = \begin{cases} |\Lambda| & \text{if } v \notin \Lambda, \\ |\Lambda| - 1 & \text{if } v \in \Lambda. \end{cases}$$

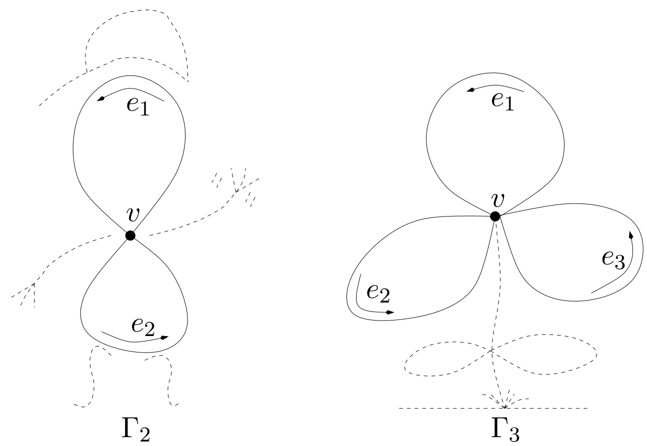

Figure 3.1: The graphs Γ_2 and Γ_3.

In addition we define the mod 2 support and norm by

$$\text{supp}_2(J) = \{i \in [n] \big| j_i \not\equiv 0 \bmod 2\}$$

and

$$|J|_2 = |\text{supp}_2(J)| \,.$$

Bringing two points together in the interior of e_i or moving a point to v decreases $\mathcal{J}(\Lambda)_i$ by one. It will be convenient to have some notation for this, so we define

$$\partial_i(J) = (j_1, \ldots, j_i - 1, \ldots, j_n)$$

provided $j_i \geq 1$. Lastly, for each subset S of $[n]$ and n–tuple J we write $J|_S$ for the $|S|$–tuple obtained by restricting the index set to S.

3.2 The homology of finite subset spaces of graphs

3.2.1 Introduction

Our first step in calculating the homology of a finite subset space of a connected graph Γ is to find explicit cell structures for $\exp_k(\Gamma_n, v)$ and $\exp_k \Gamma_n$. The approach will be similar to that of the previous chapter, and we will make use of the boundary map calculated there.

Our cell structure for $\exp_k(\Gamma_n, v)$ will consist of one j–cell σ^J for each n–tuple J such that $|J| = j \leq k-1$, the interior of σ^J containing those $\Lambda \in \exp_k(\Gamma_n, v)$ such that $\mathcal{J}(\Lambda) = J$. A cell structure for $\exp_k \Gamma_n$ will be obtained by adding additional cells $\tilde{\sigma}^J$ for each J with $|J| = j \leq k$; the interior of $\tilde{\sigma}^J$ will contain those $\Lambda \subseteq \Gamma_n \setminus \{v\}$ such that $\mathcal{J}(\Lambda) = J$. By a "stars and bars" argument there are $\binom{n+j-1}{n-1}$ solutions to

$$j_1 + \cdots + j_n = j$$

in non-negative integers (count the arrangements of j ones and $n-1$ pluses), so that

$$\chi(\exp_k(\Gamma_n, v)) = \sum_{j=0}^{k-1}(-1)^j \binom{n+j-1}{n-1} \tag{3.2.1}$$

and

$$\chi(\exp_k\Gamma_n) = 1 + 2\sum_{j=1}^{k-1}(-1)^j \binom{n+j-1}{n-1} + (-1)^k \binom{n+k-1}{n-1}.$$

A cell structure may be found in a similar way for an arbitrary connected graph Γ, with up to $2^{|V(\Gamma)|}$ j–cells for each $|E(\Gamma)|$–tuple J with $|J| = j$.

In these cell structures $\exp_{k+1}(\Gamma_n, v)$ and $\exp_{k+1}\Gamma_n$ are obtained from $\exp_k(\Gamma_n, v)$ and $\exp_k\Gamma_n$ by adding cells in dimensions k and $k+1$. This has the following consequence for their homotopy groups. The $(k-1)$–skeleta of $\exp_k(\Gamma_n, v)$ and $\exp_\ell(\Gamma_n, v)$ co-incide for $\ell \geq k$, and this means that the map on π_i induced by the inclusion $\exp_k(\Gamma_n, v) \hookrightarrow \exp_\ell(\Gamma_n, v)$ is an isomorphism for $i \leq k-2$. By Handel [18] this map is zero for $\ell = 2k-1$, implying that $\exp_k(\Gamma_n, v)$ (and by a similar argument $\exp_k\Gamma_n$) is $(k-2)$–connected. It follows immediately that the augmented chain complex of $\exp(\Gamma_n, v)$ is exact, and in conjunction with the Euler characteristic (3.2.1) and the boundary maps (3.2.2) and (3.2.3) this is enough to prove Theorem 3.1. We nevertheless show directly that this chain complex is exact in section 3.2.3 in order to find bases for the homology groups in section 3.2.5.

In Chapter 5 we will use the fact that the kth finite subset space of a connected graph is $(k-2)$–connected to show that the same conclusion holds for the kth finite subset space of a connected cell complex.

3.2.2 Cell structures for $\exp_k\Gamma_n$ and $\exp_k(\Gamma_n, v)$

We now proceed more concretely. Following the strategy of Chapter 2, each element $\Lambda \in \exp_j e_i$ has at least one representative $(x_1, \dots, x_j) \in [0,1]^j$ such that $x_1 \leq \cdots \leq x_j$. Define simplices

$$\Delta_j = \{(x_1, \dots, x_{j+1}) | 0 \leq x_1 \leq \cdots \leq x_j \leq x_{j+1} = 1\}$$

for each $j \geq 0$, and

$$\tilde{\Delta}_j = \{(x_1, \dots, x_j) | 0 \leq x_1 \leq \cdots \leq x_j \leq 1\}$$

for each $j \geq 1$. There are surjections $\Delta_j \to \exp_{j+1}(e_i, v)$, $\tilde{\Delta}_j \to \exp_j e_i$, and we let σ_i^j be the composition

$$\Delta_j \to \exp_{j+1}(e_i, v) \hookrightarrow \exp_{j+1}(\Gamma_n, v),$$

$\tilde{\sigma}_i^j$ the composition

$$\tilde{\Delta}_j \to \exp_j e_i \hookrightarrow \exp_j\Gamma_n.$$

As before we give both Δ_j and $\tilde{\Delta}_j$ the standard orientation from $\mathbf{R}^j$.

Next, given an n–tuple J let

$$\Delta_J = \Delta_{j_1} \times \cdots \times \Delta_{j_n},$$
$$\tilde{\Delta}_J = \tilde{\Delta}_{j_1} \times \cdots \times \tilde{\Delta}_{j_n},$$

omitting any empty factor $\tilde{\Delta}_0$ from this last product. Finally let

$$\sigma^J = \sigma_1^{j_1} \cup \cdots \cup \sigma_n^{j_n} \colon \ \Delta_J \to \exp_{|J|+1}(\Gamma_n, v),$$
$$\tilde{\sigma}^J = \tilde{\sigma}_1^{j_1} \cup \cdots \cup \tilde{\sigma}_n^{j_n} \colon \ \tilde{\Delta}_J \to \exp_{|J|}\Gamma_n,$$

again omitting any factor with $j_i = 0$ from $\tilde{\sigma}^J$. Each of $\sigma^J\big|_{\operatorname{int}\Delta_J}$, $\tilde{\sigma}^J\big|_{\operatorname{int}\tilde{\Delta}_J}$ is a homeomorphism of an open $|J|$–ball onto its image, and we claim:

Lemma 3.1. *The spaces $\exp_k(\Gamma_n, v)$ and $\exp_k\Gamma_n$ have cell structures consisting respectively of $\{\sigma^J \big| |J| \leq k-1\}$ and of $\{\sigma^J \big| |J| \leq k-1\} \cup \{\tilde{\sigma}^J \big| 1 \leq |J| \leq k\}$. The boundary maps are given by*

$$\partial\sigma^J = -\sum_{i \in \operatorname{supp} J} \frac{1+(-1)^{j_i}}{2} (-1)^{\left|J|_{[i-1]}\right|} \sigma^{\partial_i(J)} \tag{3.2.2}$$

and

$$\partial\tilde{\sigma}^J = \sum_{i \in \operatorname{supp} J} \frac{1+(-1)^{j_i}}{2} (-1)^{\left|J|_{[i-1]}\right|} \left(\tilde{\sigma}^{\partial_i(J)} - 2\sigma^{\partial_i(J)}\right). \tag{3.2.3}$$

Notice that the behaviour of a cell under the boundary map depends only on the support and parity pattern of J. This fact will be of importance in understanding the chain complexes in section 3.2.3.

Proof. Each element $\Lambda \in \exp_k\Gamma_n$ lies in the interior of the image of precisely one cell σ^J or $\tilde{\sigma}^J$, namely $\sigma^{\mathcal{J}(\Lambda)}$ if $v \in \Lambda$ and $\tilde{\sigma}^{\mathcal{J}(\Lambda)}$ if $v \notin \Lambda$. The image of σ^J is contained in $\exp_{|J|+1}(\Gamma_n, v)$ and that of $\tilde{\sigma}^J$ in $\exp_{|J|}\Gamma_n$, so we may set the j–skeleton of $\exp_k(\Gamma_n, v)$ equal to $\exp_{j+1}(\Gamma_n, v)$ and the j–skeleton of $\exp_k\Gamma_n$ equal to $\exp_j\Gamma_n \cup \exp_{j+1}(\Gamma_n, v)$ for $j < k$ and $\exp_k\Gamma_n$ for $j = k$. The boundary of $\tilde{\Delta}_j$ is found by replacing one or more inequalities in $0 \leq x_1 \leq \cdots \leq x_j \leq 1$ with equalities, resulting in fewer points in the interior of e_i; thus the image of the boundary of $\tilde{\Delta}_J$ under $\tilde{\sigma}^J$ is contained in $\exp_{|J|-1}\Gamma_n \cup \exp_{|J|}(\Gamma_n, v)$. Similarly, σ^J maps the boundary of Δ_J into $\exp_{|J|}(\Gamma_n, v)$. So the boundary of a j–cell is contained in the $(j-1)$–skeleton, and the σ^J, $\tilde{\sigma}^J$ form cell structures as claimed.

To calculate the boundary map we use Lemma 2.1, which in the present context says

$$\partial\sigma_i^j = -\frac{1+(-1)^j}{2}\sigma_i^{j-1},$$
$$\partial\tilde{\sigma}_i^j = \frac{1+(-1)^j}{2}(\tilde{\sigma}_i^{j-1} - 2\sigma_i^{j-1}), \tag{3.2.4}$$

together with the relation $\partial(\sigma \times \tau) = (\partial\sigma) \times \tau + (-1)^{\dim\sigma}\sigma \times (\partial\tau)$. Calculating the boundary of $\tilde{\sigma}_1^{j_1} \times \cdots \times \tilde{\sigma}_1^{j_n}$ and then applying $\cup_*$ it follows that

$$\partial\tilde{\sigma}^J = \sum_{i \in \operatorname{supp} J} (-1)^{\left|J|_{[i-1]}\right|} \tilde{\sigma}_1^{j_1} \cup \cdots \cup \partial\tilde{\sigma}_i^{j_i} \cup \cdots \cup \tilde{\sigma}_n^{j_n}.$$

Substituting (3.2.4) and observing that $\tilde{\sigma}_1^{j_1} \cup \cdots \cup \sigma_i^{j_1} \cup \cdots \cup \tilde{\sigma}_n^{j_n} = \sigma^J$ gives (3.2.3), and (3.2.2) follows by a similar argument or by using $\partial\sigma^J = \partial(\cup\{v\})_\sharp\tilde{\sigma}^J$. $\square$

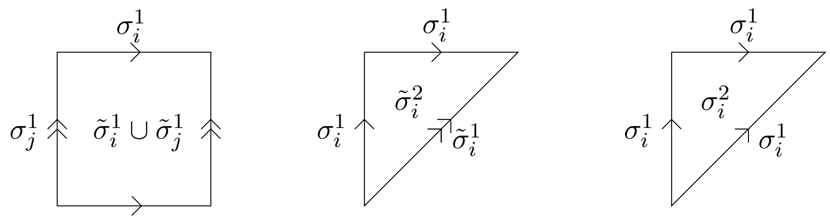

(a) (b) (c)

Figure 3.2: Relations in $\pi_1(\exp_k\Gamma_n)$ arising from the 2–cells. The boundary of a cell is found by moving a point in the interior of an edge to v, or bringing two points in the interior into co-incidence. The first gives an untilded cell and the second a cell of the same kind as the interior. In (a) we see a torus killing the commutator of $[\sigma_i^1]$ and $[\sigma_j^1]$; in (b) a Möbius strip with fundamental group generated by $[\sigma_i^1]$ and boundary $[\tilde{\sigma}_i^1]$; and in (c) a dunce cap killing $[\sigma_i^1]$.

Let $\mathcal{C}_*$ be the free abelian group generated by the σ^J, $0 \leq |J| < \infty$, and $\tilde{\mathcal{C}}_*$ the free abelian group generated by the $\tilde{\sigma}^J$, $1 \leq |J| < \infty$, each graded by degree. Then

$$H_*(\exp_k(\Gamma_n, v)) = H_*(\mathcal{C}_{\leq k-1})$$

and

$$H_*(\exp_k\Gamma_n) = H_*(\mathcal{C}_{\leq k-1} \oplus \tilde{\mathcal{C}}_{\leq k}).$$

As discussed at the end of section 3.2.1 we know a priori that $(\mathcal{C}_*, \partial)$ is exact except at $\mathcal{C}_0$. We nevertheless give a direct proof of this in section 3.2.3, with a view to constructing explicit bases for the homology groups in section 3.2.5 after calculating their ranks in section 3.2.4. Before doing so however we use Lemma 3.1 to calculate the fundamental groups of $\exp_k\Gamma_n$ and $\exp_k(\Gamma_n, v)$ directly for each k and n.

Theorem 3.3. *The fundamental group of* $\exp_k\Gamma_n$ *is*

1. *free of rank* n *if* $k = 1$*;*
2. *free abelian of rank* n*, containing* $i_*\pi_1(\exp_1\Gamma_n)$ *as a subgroup of index* 2^n*, if* $k = 2$*; and*
3. *trivial if* $k \geq 3$.

The fundamental group of $\exp_k(\Gamma_n, v)$ *is free of rank* n *if* $k = 2$ *and trivial otherwise.*

Proof. In the unbased case $\exp_k\Gamma_n$ the result is obvious for $k = 1$ so consider $k = 2$. The group $\pi_1(\exp_2\Gamma_n)$ is generated by $[\sigma_i^1]$, $[\tilde{\sigma}_i^1]$, $1 \leq i \leq n$, with relations arising from the $\tilde{\sigma}_i^2$ and $\tilde{\sigma}_i^1 \cup \tilde{\sigma}_j^1$, $i \neq j$. The image of $\tilde{\sigma}_i^1 \cup \tilde{\sigma}_j^1$ is a torus with meridian $[\sigma_i^1]$ and longitude $[\sigma_j^1]$, while the image of $\tilde{\sigma}_i^2$ is a Möbius strip that imposes the relation $[\tilde{\sigma}_i^1] = [\sigma_i^1]^2$ (see figures 3.2(a) and (b)). It follows that $\pi_1(\exp_2\Gamma_n)$ is free abelian with generators $[\sigma_i^1]$, $1 \leq i \leq n$, and that $i_*\pi_1(\exp_1\Gamma_n) = \langle[\tilde{\sigma}_1^1], \ldots, [\tilde{\sigma}_n^1]\rangle$ has index 2^n. When $k \geq 3$ there are no new generators and additional relations $[\sigma_i^1] = 1$ from each σ_i^2 (see figure 3.2(c)), so that $\pi_1(\exp_k\Gamma_n) = \{1\}$.

In the based case $\exp_1(\Gamma_n, v) = \{\{v\}\}$, the map $\cup\{v\}\colon \exp_1\Gamma_n \to \exp_2(\Gamma_n, v)$ is a homeomorphism, and for $k \geq 3$ the relations $[\sigma_i^1] = 1$ from the σ_i^2 apply as above. □

3.2.3 Direct proof of the exactness of $\mathcal{C}_{\geq 1}$

We show directly that $\mathcal{C}_*$ is exact at each $\ell > 0$ by expressing it as a sum of finite subcomplexes and showing that each summand is exact. This decomposition will be used to construct explicit bases for the homology in section 3.2.5.

As a first reduction, for each subset S of $[n]$ let $\mathcal{C}_*^S$ be the free abelian group generated by $\{\sigma^J | \operatorname{supp} J = S\}$. Since $\partial\sigma^J$ is a linear combination of the cells $\sigma^{\partial_i(J)}$ with $i \in \operatorname{supp} J$ and $j_i \equiv 0 \bmod 2$, each $\mathcal{C}_*^S$ is a subcomplex and we have

$$\mathcal{C}_* = \bigoplus_{S \subseteq [n]} \mathcal{C}_*^S\,.$$

Note that $\mathcal{C}_*^\emptyset = \mathcal{C}_0$. Clearly $\mathcal{C}_*^S \cong \mathcal{C}_*^T$ if $|S| = |T|$ so we will show $\mathcal{C}_*^{[m]}$ is exact for each $m > 0$.

We claim that $\mathcal{C}_*^{[m]}$ may be regarded as a sum of many copies of a single finite complex, the m–cube complex. For each m–tuple L with all entries odd let $\mathcal{C}_*^{[m]}(L)$ be the subgroup of $\mathcal{C}_*^{[m]}$ generated by $\left\{\sigma^J \middle| j_i - \ell_i \in \{0,1\}\right\}$. Again the fact that $\partial\sigma^J$ is a linear combination of $\{\sigma^{\partial_i(J)} | i \in \operatorname{supp} J, j_i \equiv 0 \bmod 2\}$ implies $\mathcal{C}_*^{[m]}(L)$ is a subcomplex, and moreover that

$$\mathcal{C}_*^{[m]} = \bigoplus_{L : |L|_2 = m} \mathcal{C}_*^{[m]}(L).$$

Further each $\mathcal{C}_*^{[m]}(L)$ can be seen to be isomorphic to $\mathcal{C}_*^{[m]}((1,\ldots,1))$ with its grading shifted by $|L| - m$ on translating each m–tuple by $(\ell_1 - 1, \ldots, \ell_m - 1)$. We call this common isomorphism class of complex the m–cube complex C_*^m, and, replacing J with the set of indices of its even entries, will take the free abelian group generated by the power set of $[m]$, graded by cardinality and with boundary map

$$\partial S = \sum_{i \in S} (-1)^{|[i-1] \setminus S|} S \setminus \{i\}$$

to be its canonical representative; for aesthetic purposes we are dropping the minus sign outside the sum. The name m-cube complex comes from the fact that the lattice of subsets of $[m]$ forms an m–dimensional cube, and that ∂S is a signed sum of the neighbours of S of smaller degree. See figure 3.3 for the case $m = 3$.

Let

$$\mathsf{V}_j = \{S \subseteq [m] \big| |s| = j \text{ and } 1 \in S\}.$$

The exactness of $\mathcal{C}_*^{[m]}$ follows from the first statement of the following lemma; the second statement will be used in section 3.2.5 to construct explicit bases for $H_*(\exp_k\Gamma_n)$.

Lemma 3.2. *The m–cube complex C_*^m is exact. The homology of the truncated complex $\mathsf{C}_{\leq j}^m$ is free of rank $\binom{m-1}{j}$ in dimension j, with basis $\{\partial S | S \in \mathsf{V}_{j+1}\}$, and zero otherwise.*

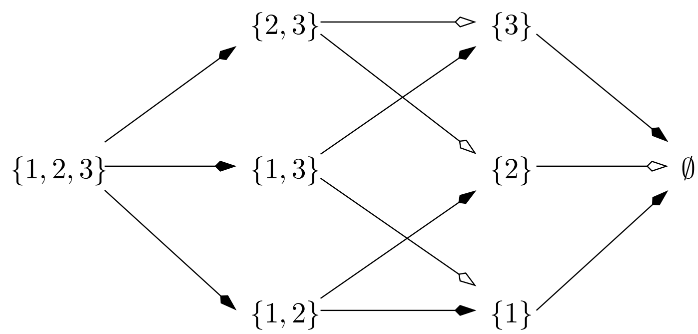

Figure 3.3: The 3–cube complex C^3_*. The lattice of subsets of $\{1,2,3\}$ forms a 3–dimensional cube and ∂S is a signed sum of the neighbours of S of smaller cardinality. In the diagram positive terms are indicated by solid arrowheads, negative terms by empty arrowheads.

Proof. We claim that $\mathsf{V}_j \cup \partial \mathsf{V}_{j+1}$ forms a basis for C^m_j, from which the lemma follows. Since $\mathsf{V}_j \cup \partial \mathsf{V}_{j+1}$ has at most $\binom{m-1}{j-1} + \binom{m-1}{j} = \binom{m}{j} = \operatorname{rank} \mathsf{C}^m_j$ elements we simply check that $\mathsf{V}_j \cup \partial \mathsf{V}_{j+1}$ spans C^m_j. It suffices to show that $S \in \operatorname{span} \mathsf{V}_j \cup \partial \mathsf{V}_{j+1}$ for each subset S of size j not containing 1; this follows from

$$\partial(S \cup \{1\}) = S - \sum_{i \in S} (-1)^{|[i-1] \setminus S|} S \cup \{1\} \setminus \{i\}$$

if $1 \notin S$. □

3.2.4 The homology groups of $\exp_k(\Gamma_n, v)$ and $\exp_k \Gamma_n$

We calculate the homology groups of $\exp_k(\Gamma_n, v)$ and $\exp_k \Gamma_n$ using the exactness of $\mathcal{C}_{\geq 1}$, the Euler characteristic (3.2.1), and the boundary maps (3.2.2) and (3.2.3). Explicit bases are found in section 3.2.5 using the decomposition of $\mathcal{C}_*$ into subcomplexes.

Proof of Theorem 3.1. Since $\exp_k(\Gamma_n, v)$ is path connected and $H_*(\exp_k(\Gamma_n, v))$ is equal to $H_*(\mathcal{C}_{\leq k-1})$, the reduced homology vanishes except perhaps in dimension $k-1$, by the exactness of $\mathcal{C}_{\geq 1}$. Moreover H_{k-1} is equal to $\ker \partial_{k-1}$ and is therefore free; its rank may be found using $\chi(\exp_k(\Gamma_n, v)) = b_0 + (-1)^{k-1} b_{k-1}$ and equation (3.2.1), yielding

$$b_{k-1}(\exp_k(\Gamma_n, v)) = \sum_{j=1}^{k-1} (-1)^{k-j-1} \binom{n+j-1}{n-1}.$$

This may be expressed as a sum of purely positive terms by grouping the summands in pairs, starting with the largest, and using $\binom{p}{q} - \binom{p-1}{q} = \binom{p-1}{q-1}$. Doing this for $b_k(\exp_{k+1}(\Gamma_n, v))$ gives the expression in equation (3.1.1).

Now consider $H_*(\exp_k \Gamma_n) = H_*(\mathcal{C}_{\leq k-1} \oplus \mathcal{C}_{\leq k})$. Write C_j for the jth chain group of $\mathcal{C}_{\leq k-1} \oplus \tilde{\mathcal{C}}_{\leq k}$, $\mathcal{Z}_j$ for the j–cycles in $\mathcal{C}_j$ and Z_j for the j–cycles in C_j. Extending $\sigma^J \mapsto \tilde{\sigma}^J$

linearly to a group isomorphism from $\mathcal{C}_j$ to $\tilde{\mathcal{C}}_j$ for each $j \geq 1$, the boundary maps (3.2.2) and (3.2.3) give

$$\partial\tilde{c} = 2\partial c - \widetilde{\partial c}$$

for each chain $c \in \mathcal{C}_{\geq 1}$. It follows that $Z_j = \mathcal{Z}_j \oplus \tilde{\mathcal{Z}}_j$ for $1 \leq j \leq k-1$ and that $H_k(\exp_k\Gamma_n) = Z_k$ is equal to $\tilde{\mathcal{Z}}_k$. Moreover

$$\partial C_k = \{2z - \tilde{z} | z \in \mathcal{Z}_{k-1}\}$$

by the exactness of $\mathcal{C}_*$ at $\mathcal{C}_{k-1}$, so that $H_{k-1}(\exp_k\Gamma_n) = \mathcal{Z}_{k-1}$. We show that the remaining reduced homology groups vanish.

Let $z = z_1 \oplus \tilde{z}_2 \in Z_j$ for some $1 \leq j \leq k-2$. By the exactness of $\mathcal{C}_{\geq 1}$ there are $w_1, w_2 \in \mathcal{C}_{j+1}$ such that

$$\begin{aligned}\partial w_1 &= z_1 + 2z_2,\\ \partial w_2 &= z_2.\end{aligned}$$

Since $j \leq k-2$ we have $w_1 - \tilde{w}_2 \in C_{j+1}$, and

$$\begin{aligned}\partial(w_1 - \tilde{w}_2) &= \partial w_1 - \partial\tilde{w}_2\\ &= z_1 + 2z_2 - 2\partial w_2 + \widetilde{\partial w_2}\\ &= z_1 + \tilde{z}_2,\end{aligned}$$

so that C_* is exact at C_j as claimed.

It remains to determine the maps induced by

$$\begin{aligned}i\colon\ \exp_k(\Gamma_n, v) &\hookrightarrow \exp_k\Gamma_n,\\ \cup\{v\}\colon\ \exp_k\Gamma_n &\to \exp_{k+1}(\Gamma_n, v)\end{aligned}$$

and

$$\exp_k\Gamma_n \hookrightarrow \exp_{k+1}\Gamma_n$$

on homology. In each case there is only one dimension in which the induced map is not trivially zero. We have $H_{k-1}(\exp_k(\Gamma_n, v)) = \mathcal{Z}_{k-1} = H_{k-1}(\exp_k\Gamma_n)$, so that i_* is an isomorphism on H_{k-1}, and adding v to each element of $\exp_k\Gamma_n$ sends $\tilde{z}$ to z for each $z \in \mathcal{Z}_k$, inducing an isomorphism on H_k. Lastly, $\exp_k\Gamma_n \hookrightarrow \exp_{k+1}\Gamma_n$ sends $[\tilde{z}]$ to $[\tilde{z}] = 2[z] = 2(i \circ \cup\{v\})_*[\tilde{z}]$ for each $z \in \mathcal{Z}_k$, inducing two times $(i \circ \cup\{v\})_*$ as claimed. □

The homology and fundamental group of $\exp_k(\Gamma_n, v)$ are enough to determine its homotopy type completely. When $k = 1$ it is a single point $\{\{v\}\}$, and when $k \geq 2$ we have:

Corollary 3.1 (Theorem 3.2). *For $k \geq 2$ the space $\exp_k(\Gamma_n, v)$ has the homotopy type of a wedge of $b_{k-1}(\exp_k(\Gamma_n, v))$ $(k-1)$–spheres.*

Proof. Since $\exp_2(\Gamma_n, v)$ is homeomorphic to Γ_n we may assume $k \geq 3$. But then $\exp_k(\Gamma_n, v)$ is a simply connected Moore space $M(\mathbf{Z}^{b_{k-1}}, k-1)$ and the result follows from the Hurewicz and Whitehead theorems. □

3.2.5 A basis for $H_k(\exp_k \Gamma_n)$

We use the decomposition of $\mathcal{C}_*$ as a sum of subcomplexes to give an explicit basis for $H_k(\exp_k \Gamma_n)$.

Theorem 3.4. *The set*

$$\mathcal{B}(k,n) = \left\{ \widetilde{\partial\sigma^J} \middle| |J| = k+1 \text{ and } j_i \equiv 0 \bmod 2 \text{ for } i = \min(\operatorname{supp} J) \right\}$$

is a basis for $H_k(\exp_k \Gamma_n)$.

Proof. It suffices to find a basis for $\mathcal{Z}_k$ and map it across to $\tilde{\mathcal{Z}}_k$. Extending notation in obvious ways we have

$$\begin{aligned} \mathcal{Z}_k &= \bigoplus_{S \subseteq [n]} \mathcal{Z}_k^S \\ &= \bigoplus_{S \subseteq [n]} \bigoplus_{\substack{L:\operatorname{supp} L = S, \\ |L|_2 = |S|}} \mathcal{Z}_k^S(L). \end{aligned}$$

Each $\mathcal{Z}_k^S(L)$ in this sum is isomorphic to $\mathsf{Z}_j^{|S|}$ for some j, and tracing back through this isomorphism we see that V_{j+1} is carried up to sign to

$$\mathcal{V}_{k+1}^S(L) = \{\sigma^J \big| |J| = k+1, j_i - \ell_i \in \{0,1\}, j_i \equiv 0 \bmod 2 \text{ for } i = \min(\operatorname{supp} J)\}.$$

By Lemma 3.2 $\{\partial\sigma | \sigma \in \mathcal{V}_{k+1}^S(L)\}$ is a basis for $\mathcal{Z}_k^S(L)$, and taking the union over S and L completes the proof. □

As an exercise in counting we check that $\mathcal{B}(k,n)$ has the right cardinality. This is equivalent to showing that the number $s(k,n)$ of non-negative integer solutions to

$$j_1 + \cdots + j_n = k$$

in which the first non-zero summand is odd is given by equation (3.1.1). We do this by induction on k, inducting separately over the even and odd integers.

In the base cases $k = 1$ and 2 there are clearly n and $\binom{n}{2}$ solutions respectively. It therefore suffices to show that $s(k,n) - s(k-2,n) = \binom{n+k-2}{n-2}$. Adding two to the first non-zero summand gives an injection from solutions with $k = \ell - 2$ to solutions with $k = \ell$, hitting all solutions except those for which the first non-zero summand is one. If $j_{n-i} = 1$ is the first non-zero summand then what is left is an unconstrained non-negative integer solution to

$$j_{n-i+1} + \cdots + j_n = \ell - 1,$$

of which there are $\binom{\ell+i-2}{\ell-1}$, so that

$$s(k,n) - s(k-2,n) = \sum_{i=1}^{n-1} \binom{k+i-2}{k-1}.$$

This is a sum down a diagonal of Pascal's triangle and as such is easily seen to equal $\binom{k+n-2}{k} = \binom{k+n-2}{n-2}$.

3.2.6 Generating functions for $b_k(\exp_k \Gamma_n)$

We conclude this section by giving generating functions for the Betti numbers $b_k(\exp_k \Gamma_n)$.

Theorem 3.5. *The Betti number $b_k(\exp_k \Gamma_n)$ is the co-efficient of x^k in*

$$\frac{1-(1-x)^n}{(1+x)(1-x)^n}. \tag{3.2.5}$$

Proof. The co-efficient of x^j in

$$\frac{1}{(1-x)^n} = (1 + x + x^2 + x^3 + \cdots)^n$$

is the number of non-negative solutions to $j_1 + \cdots + j_n = j$, in other words $\binom{n+j-1}{n-1}$. Multiplication by $(1+x)^{-1} = 1 - x + x^2 - x^3 + \cdots$ has the effect of taking alternating sums of co-efficients, so we subtract 1 first to remove the unwanted degree zero term from $(1-x)^{-n}$, arriving at (3.2.5). $\square$

3.3 The calculation of induced maps

3.3.1 Introduction

Given a pointed map $\phi\colon (\Gamma_n, v) \to (\Gamma_m, v)$ there are induced maps

$$(\exp_k \phi)_*\colon\ H_{k-1}(\exp_k(\Gamma_n, v)) \to H_{k-1}(\exp_k(\Gamma_m, v))$$

and

$$(\exp_k \phi)_*\colon\ H_p(\exp_k \Gamma_n) \to H_p(\exp_k \Gamma_m)$$

for $p = k-1, k$. In view of the commutative diagrams

$$\begin{array}{ccc} \exp_k(\Gamma_n, v) & \xrightarrow{\exp_k \phi} & \exp_k(\Gamma_m, v) \\ {\scriptstyle i}\downarrow & & \downarrow{\scriptstyle i} \\ \exp_k \Gamma_n & \xrightarrow{\exp_k \phi} & \exp_k \Gamma_m \end{array}$$

and

$$\begin{array}{ccc} \exp_{k-1} \Gamma_n & \xrightarrow{\exp_{k-1} \phi} & \exp_{k-1} \Gamma_m \\ \downarrow{\scriptstyle \cup\{v\}} & & \downarrow{\scriptstyle \cup\{v\}} \\ \exp_k(\Gamma_n, v) & \xrightarrow{\exp_k \phi} & \exp_k(\Gamma_m, v) \end{array}$$

and the isomorphisms induced by i and $\cup\{v\}$ on H_{k-1} and H_k respectively it suffices to understand just one of these, and we will focus our attention on $H_k(\exp_k \Gamma_n) \to H_k(\exp_k \Gamma_m)$. The purpose of this section is to reduce the problem of calculating this map to the problem of finding the images of the basic cells $\tilde{\sigma}_i^1, \tilde{\sigma}_i^2$ under the chain map $(\exp_k \phi)_\sharp$. The reduction will be done by defining a multiplication on $\tilde{\mathcal{C}}_*$, giving it the structure of a ring without unity generated by the $\tilde{\sigma}_i^j$. The multiplication will be defined in such a way that the cellular chain map $(\exp\phi)_\sharp|_{\tilde{\mathcal{C}}_*}$ is a ring homomorphism, reducing calculating $(\exp_k\phi)_*$ to calculations in the chain ring once the $(\exp_k\phi)_\sharp\tilde{\sigma}_i^j$ are found. The reduction to just the cells $\tilde{\sigma}_i^1, \tilde{\sigma}_i^2$ is achieved by working over the rationals, as $\tilde{\mathcal{C}}_* \otimes_{\mathbf{Z}} \mathbf{Q}$ will be generated over $\mathbf{Q}$ by just these $2n$ cells.

In what follows we will assume that ϕ is smooth, in the sense that ϕ is smooth on the open set $\phi^{-1}(\Gamma_m \setminus \{v\})$. This ensures that $\exp_j\phi$ is smooth off the preimage of the $(j-1)$–skeleton $(\exp_j\Gamma_n)^{j-1} = \exp_{j-1}\Gamma_n \cup \exp_j(\Gamma_n, v)$, allowing us to use smooth techniques on the manifold $\exp_j\Gamma_n \setminus (\exp_j\Gamma_n)^{j-1}$. Smoothness of ϕ may be ensured by homotoping it to a standard form defined as follows. The restriction of ϕ to each edge e_i is an element of $\pi_1(\Gamma_m, v)$, and as such is equivalent to a reduced word w_i in the $\{e_a\} \cup \{\bar{e}_a\}$. We consider ϕ to be in standard form if $\phi|_{e_i}$ traverses each letter of w_i at constant speed.

3.3.2 The chain ring

We observe that the operation $(g, h) \mapsto g \cup h$ suggests a natural way of multiplying cells and we study it with an eye to applying the results to maps of the form $(\exp_k\phi) \circ \tilde{\sigma}^J$.

A map of pairs $g\colon (B^j, \partial B^j) \to \big(\exp_j\Gamma_n, (\exp_j\Gamma_n)^{j-1}\big)$ induces a map

$$g_*\colon H_j(B^j, \partial B^j) \to H_j(\exp_j\Gamma_n, (\exp_j\Gamma_n)^{j-1}),$$

and the homology group on the right is canonically isomorphic to the cellular chain group $\tilde{\mathcal{C}}_j$. Writing ϵ^j for the positive generator of $H_j(B^j, \partial B^j)$, if g is smooth on the open set $g^{-1}(\exp_j\Gamma_n \setminus (\exp_j\Gamma_n)^{j-1})$ then this map is given by

$$g_*\epsilon^j = \sum_{|J|=j} \langle g, \tilde{\sigma}^J\rangle \tilde{\sigma}^J,$$

in which $\langle g, \tilde{\sigma}^J\rangle$ is the signed sum of preimages of a generic point in the interior of $\tilde{\sigma}^J$. If h is a second map of pairs $(B^\ell, \partial B^\ell) \to \big(\exp_\ell\Gamma_n, (\exp_\ell\Gamma_n)^{\ell-1}\big)$ then $g \cup h$ is a map of pairs

$$(B^{j+\ell}, \partial B^{j+\ell}) \to \big(\exp_{j+\ell}\Gamma_n, (\exp_{j+\ell}\Gamma_n)^{j+\ell-1}\big)$$

also. The following lemma shows that $\cup$ behaves as might be hoped on the chain level.

Lemma 3.3. *Given maps of pairs $g\colon (B^j, \partial B^j) \to (\exp_j\Gamma_n, (\exp_j\Gamma_n)^{j-1})$, $h\colon (B^\ell, \partial B^\ell) \to (\exp_\ell\Gamma_n, (\exp_\ell\Gamma_n)^{\ell-1})$, each smooth off the preimage of the codimension one skeleton, we have*

$$(g \cup h)_* = \sum_{|J|=j, |L|=\ell} \langle g, \tilde{\sigma}^J\rangle \langle h, \tilde{\sigma}^L\rangle (\tilde{\sigma}^J \cup \tilde{\sigma}^L)_*. \tag{3.3.1}$$

Proof. Fix an n–tuple M such that $|M| = j + \ell$ and let Λ be a generic point in the interior of $\tilde{\sigma}^M$. It suffices to check that $g \times h$ and $\sum_{J,L} \langle g, \tilde{\sigma}^J\rangle \langle h, \tilde{\sigma}^L\rangle \tilde{\sigma}^J \times \tilde{\sigma}^L$ have the same signed sum of preimages at each point $(\Lambda', \Lambda'') \in \exp_{|J|}\Gamma_n \times \exp_{|L|}\Gamma_n$ such that $\Lambda' \cup \Lambda'' = \Lambda$; note that for cardinality reasons (Λ', Λ'') forms a partition of Λ. For $g \times h$ this signed sum is given by

$$\begin{aligned}\langle g \times h, \tilde{\sigma}^{\mathcal{J}(\Lambda')} \times \tilde{\sigma}^{\mathcal{J}(\Lambda'')}\rangle &= \sum_{p \in g^{-1}(\Lambda')} \sum_{q \in h^{-1}(\Lambda'')} \operatorname{sign}(\det D(g \times h)(p,q)) \\ &= \sum_{p \in g^{-1}(\Lambda')} \sum_{q \in h^{-1}(\Lambda'')} \operatorname{sign}\big(\det Dg(p)\big) \operatorname{sign}\big(\det Dh(q)\big) \\ &= \Bigg[\sum_{g^{-1}(\Lambda')} \operatorname{sign}(\det Dg(p))\Bigg]\Bigg[\sum_{h^{-1}(\Lambda'')} \operatorname{sign}(\det Dh(q))\Bigg] \\ &= \langle g, \tilde{\sigma}^{\mathcal{J}(\Lambda')}\rangle \langle h, \tilde{\sigma}^{\mathcal{J}(\Lambda'')}\rangle.\end{aligned}$$

The lemma follows from the fact that $\langle \tilde{\sigma}^J \times \tilde{\sigma}^L, \tilde{\sigma}^{\mathcal{J}(\Lambda')} \times \tilde{\sigma}^{\mathcal{J}(\Lambda'')}\rangle$ is zero unless $J = \mathcal{J}(\Lambda')$ and $L = \mathcal{J}(\Lambda'')$, in which case it is one. □

Since $(\tilde{\sigma}^J \cup \tilde{\sigma}^L)_* \epsilon^{j+\ell}$ is a multiple of $\tilde{\sigma}^{J+L}$ the next step is to understand the pairings $\langle \tilde{\sigma}^J \cup \tilde{\sigma}^L, \tilde{\sigma}^{J+L}\rangle$. Interchanging adjacent factors $\tilde{\sigma}_a^r$ and $\tilde{\sigma}_b^s$ in the product $\tilde{\sigma}^J \cup \tilde{\sigma}^L$ simply introduces a sign $(-1)^{rs}$, so we may gather basic cells from the same edge together and consider pairings of the form

$$\langle (\tilde{\sigma}_1^{j_1} \cup \tilde{\sigma}_1^{\ell_1}) \cup \cdots \cup (\tilde{\sigma}_n^{j_n} \cup \tilde{\sigma}_n^{\ell_n}), \tilde{\sigma}^{J+L}\rangle = \prod_{i=1}^{n} \langle \tilde{\sigma}_i^{j_i} \cup \tilde{\sigma}_i^{\ell_i}, \tilde{\sigma}_i^{j_i+\ell_i}\rangle.$$

The quantity $\langle \tilde{\sigma}_a^r \cup \tilde{\sigma}_a^s, \tilde{\sigma}_a^{r+s}\rangle$ is equal to $\left[\begin{smallmatrix} r+s \\ r \end{smallmatrix}\right]_{-1}$, the q–binomial co-efficient $\left[\begin{smallmatrix} r+s \\ r \end{smallmatrix}\right]$ specialised to $q = -1$. The correspondence can be seen as follows. Take $r+s$ objects, numbered from 1 to $r+s$ and laid out in order, and paint r of them blue and the rest red. Shuffle them so that the blue ones are at the front in ascending order, followed by the red ones in ascending order, giving an element of the symmetric group S_{r+s}. Then $\left[\begin{smallmatrix} r+s \\ r \end{smallmatrix}\right]_{-1}$ is the number of ways of choosing r objects from $r+s$ in this way, counted with the sign of the associated permutation, and is equal to $\langle \tilde{\sigma}_a^r \cup \tilde{\sigma}_a^s, \tilde{\sigma}_a^{r+s}\rangle$: the blue and red points represent the elements of a generic point in $\exp_{r+s} e_a$ coming from $\tilde{\sigma}_a^r$ and $\tilde{\sigma}_a^s$ respectively, and the derivative at this preimage is the matrix of the associated permutation.

The calculation of $\left[\begin{smallmatrix} r+s \\ r \end{smallmatrix}\right]_{-1}$ is the subject of the following lemma. The result, which we might call "Pascal's other triangle"—being a much less popular model than the one we know and love—appears in figure 3.4. For further information on q–binomial co-efficients and related topics see for example Stanley [33], Kac and Cheung [22], and Baez [1, weeks 183–188].

Lemma 3.4. *The value of the signed binomial co-efficient* $\left[\begin{smallmatrix} m \\ r \end{smallmatrix}\right]_{-1}$ *is given by*

$$\begin{bmatrix} m \\ r \end{bmatrix}_{-1} = \frac{1 + (-1)^{r(m-r)}}{2} \binom{\lfloor m/2 \rfloor}{\lfloor r/2 \rfloor}. \tag{3.3.2}$$

$$\begin{array}{ccccccccccccccccccc}
&&&&&&&&&1&&&&&&&&&\\
&&&&&&&&1&&1&&&&&&&&\\
&&&&&&&1&&0&&1&&&&&&&\\
&&&&&&1&&1&&1&&1&&&&&&\\
&&&&&1&&0&&2&&0&&1&&&&&\\
&&&&1&&1&&2&&2&&1&&1&&&&\\
&&&1&&0&&3&&0&&3&&0&&1&&&\\
&&1&&1&&3&&3&&3&&3&&1&&1&&\\
&1&&0&&4&&0&&6&&0&&4&&0&&1&\\
1&&1&&4&&4&&6&&6&&4&&4&&1&&1
\end{array}$$

Figure 3.4: The first ten rows of Pascal's other triangle, enough so that the pattern is clear. Each row of Pascal's triangle appears twice; on the first occurrence zeros are inserted between each entry, and on the second each entry appears twice.

Proof. The q–binomial co-efficient $\left[\begin{smallmatrix} m \\ r \end{smallmatrix}\right]$ satisfies $\left[\begin{smallmatrix} m \\ 0 \end{smallmatrix}\right] = \left[\begin{smallmatrix} m \\ m \end{smallmatrix}\right] = 1$ and

$$\begin{bmatrix} m \\ r \end{bmatrix} = \begin{bmatrix} m-1 \\ r-1 \end{bmatrix} + q^r \begin{bmatrix} m-1 \\ r \end{bmatrix},$$

both easily seen for $q = -1$ from the definition above: the recurrence relation is proved analogously to the familiar one for Pascal's triangle, the sign $(-1)^r$ arising from shuffling the first object into place if it is red instead of blue. The equality (3.3.2) is then readily proved by induction on m, by considering in turn the four possibilities for the parities of m and r. □

We remark that the equality $\left[\begin{smallmatrix} r+s \\ r \end{smallmatrix}\right] = \left[\begin{smallmatrix} r+s \\ s \end{smallmatrix}\right]$ can be seen for $q = -1$ from the fact that $\lfloor r/2 \rfloor + \lfloor s/2 \rfloor = \lfloor (r+s)/2 \rfloor$ unless both r and s are odd, in which case the co-efficient $\left[\begin{smallmatrix} r+s \\ r \end{smallmatrix}\right]_{-1}$ vanishes. Additionally $\left[\begin{smallmatrix} r+s \\ r \end{smallmatrix}\right]_{-1} \left[\begin{smallmatrix} r+s+t \\ r+s \end{smallmatrix}\right]_{-1}$ and $\left[\begin{smallmatrix} r+s+t \\ r \end{smallmatrix}\right]_{-1} \left[\begin{smallmatrix} s+t \\ s \end{smallmatrix}\right]_{-1}$ are both equal to

$$\frac{\lfloor (r+s+t)/2 \rfloor!}{\lfloor r/2 \rfloor! \lfloor s/2 \rfloor! \lfloor t/2 \rfloor!}$$

if no more than two of r, s, t are odd, and zero otherwise.

We now define the chain ring of $\exp \Gamma_n$ to be the ring without unity generated over $\mathbf{Z}$ by the set $\{\tilde{\sigma}_i^j \,|\, 1 \leq i \leq n, j \geq 1\}$, with relations

$$\begin{aligned} \tilde{\sigma}_a^j \tilde{\sigma}_b^\ell &= (-1)^{j\ell} \tilde{\sigma}_b^\ell \tilde{\sigma}_a^j \\ \tilde{\sigma}_a^j \tilde{\sigma}_a^\ell &= \left[\begin{smallmatrix} j+\ell \\ j \end{smallmatrix}\right]_{-1} \tilde{\sigma}_a^{j+\ell} \end{aligned}$$

for all $1 \leq a, b \leq n$ and $j, \ell \geq 1$. This definition is again a specialisation to $q = -1$ of a construction that applies more generally, and is chosen so that the conclusion (3.3.1) of

Lemma 3.3 may be rewritten as

$$(g \cup h)_* \epsilon^{j+\ell} = (g_* \epsilon^j)(h_* \epsilon^\ell), \tag{3.3.3}$$

in which the multiplication on the right hand side takes place in the chain ring. The lack of an identity could be easily remedied but we have chosen not to so that all elements of the ring are chains. We shall denote the chain ring simply by $\tilde{\mathcal{C}}_*$, or $\tilde{\mathcal{C}}_*(\Gamma_n)$ in case of ambiguity.

3.3.3 Calculating induced maps

We now have all the machinery required to state and prove our main result on the calculation of $(\exp_k \phi)_*$, namely that the cellular chain map $(\exp\phi)_\sharp|_{\tilde{\mathcal{C}}_*}$ is a ring homomorphism. This reduces the calculation of the chain map to the calculation of the images of the basic cells $\tilde{\sigma}_i^j$, each an exercise in counting points with signs, and multiplication and addition in the chain ring.

Theorem 3.6. *If* $\phi\colon (\Gamma_n, v) \to (\Gamma_m, v)$ *is smooth on* $\phi^{-1}(\Gamma_m \setminus \{v\})$ *then the cellular chain map* $(\exp\phi)_\sharp\colon \tilde{\mathcal{C}}_*(\Gamma_n) \to \tilde{\mathcal{C}}_*(\Gamma_m)$ *is a ring homomorphism.*

Proof. If ϕ is smooth off $\phi^{-1}(v)$ then as noted on page 39 the map $\exp_j \phi = \exp\phi|_{\exp_j \Gamma_n}$ is smooth off the codimension one skeleton for each j, so we may use Lemma 3.3. Thus

$$\begin{aligned}
(\exp\phi)_\sharp(\tilde{\sigma}^J \tilde{\sigma}^L) &= (\exp_{j+\ell}\phi)_*((\tilde{\sigma}^J \cup \tilde{\sigma}^L)_* \epsilon^{j+\ell}) && \text{since } \tilde{\sigma}^J \tilde{\sigma}^L = (\tilde{\sigma}^J \cup \tilde{\sigma}^L)_* \epsilon^{j+\ell} \\
&= \big((\exp_{j+\ell}\phi) \circ (\tilde{\sigma}^J \cup \tilde{\sigma}^L)\big)_* \epsilon^{j+\ell} \\
&= \big(((\exp_j \phi) \circ \tilde{\sigma}^J) \cup ((\exp_\ell \phi) \circ \tilde{\sigma}^L)\big)_* \epsilon^{j+\ell} \\
&= \big(((\exp_j \phi) \circ \tilde{\sigma}^J)_* \epsilon^j\big)\big(((\exp_\ell \phi) \circ \tilde{\sigma}^L)_* \epsilon^\ell\big) && \text{by (3.3.3)} \\
&= \big((\exp_j \phi)_* \tilde{\sigma}^J_* \epsilon^j\big)\big((\exp_\ell \phi)_* \tilde{\sigma}^L_* \epsilon^\ell\big) \\
&= \big((\exp\phi)_\sharp \tilde{\sigma}^J\big)\big((\exp\phi)_\sharp \tilde{\sigma}^L\big),
\end{aligned}$$

from which the result follows. ☐

As an immediate consequence we have

$$(\exp\phi)_\sharp \tilde{\sigma}^J = \prod_{i=1}^{n} (\exp_k \phi)_\sharp \tilde{\sigma}_i^{j_i},$$

so that $(\exp\phi)_\sharp \tilde{\sigma}^J$ may be found knowing just the images of the basic cells $\tilde{\sigma}_i^j$ as claimed. To reduce the number of cells $\tilde{\sigma}$ for which $(\exp\phi)_\sharp \tilde{\sigma}$ must be calculated directly even further, observe that

$$\tilde{\sigma}_i^j = \begin{cases} \frac{1}{\ell!}\left(\tilde{\sigma}_i^2\right)^\ell & \text{if } j = 2\ell, \\ \frac{1}{\ell!}\tilde{\sigma}_i^1\left(\tilde{\sigma}_i^2\right)^\ell & \text{if } j = 2\ell+1, \end{cases} \tag{3.3.4}$$

so that $\tilde{\mathcal{C}}_* \otimes_{\mathbf{Z}} \mathbf{Q}$ is generated over $\mathbf{Q}$ by the set $\{\tilde{\sigma}_i^j \,|\, 1 \le i \le n, j = 1, 2\}$, subject only to the relations that the $\tilde{\sigma}_i^1$ anti-commute with each other and the $\tilde{\sigma}_i^2$ commute with everything.

In essence this reduces calculating $(\exp\phi)_\sharp$ to understanding the behaviour of chains under maps

$$\exp_1 S^1 \to \exp_1 S^1$$

and

$$\exp_2 S^1 \to \exp_2 \Gamma_2$$

induced by maps $S^1 \to S^1$ and $S^1 \to \Gamma_2$ respectively. These are both simple exercises in counting points with signs and we give the answers, which are easily checked. Let w be a reduced word in $\{e_1, e_2, \bar{e}_1, \bar{e}_2\}$, and let ϕ from $S^1 = \Gamma_1$ to Γ_2 send e_1 to w. Then $\langle(\exp\phi)\circ\tilde{\sigma}_1^1, \tilde{\sigma}_i^1\rangle$ and $\langle(\exp\phi)\circ\tilde{\sigma}_1^2, \tilde{\sigma}_i^2\rangle$ are both given by the winding number of w around e_i, and $\langle(\exp\phi)\circ\tilde{\sigma}_1^2, \tilde{\sigma}^{(1,1)}\rangle$ is the number of pairs of letters (a_1, a_2) in w, $a_i \in \{e_i, \bar{e}_i\}$, counted with the product of a minus one for each bar and a further minus one if a_2 occurs before a_1.

3.3.4 Examples

As an illustration of the ideas in this section we calculate two examples. The first reproduces the degree calculation of section 2.4, and the second will be useful in understanding the action of the braid group.

Let $\phi\colon S^1 \to S^1$ be a degree d map. By Theorem 2.4 or 3.1 we have

$$H_k(\exp_k S^1) \cong \begin{cases} 0 & k \text{ even,} \\ \mathbf{Z} & k \text{ odd,} \end{cases}$$

so the only map of interest is $(\exp_{2\ell-1}\phi)_*$ on $H_{2\ell-1}$. The group $H_{2\ell-1}(\exp_{2\ell-1}S^1)$ is generated by $\tilde{\sigma}_1^{2\ell-1}$, and by (3.3.4) and the discussion at the end of section 3.3.3 we have

$$\begin{aligned}(\exp_{2\ell-1}\phi)_\sharp\tilde{\sigma}_1^{2\ell-1} &= \frac{1}{(\ell-1)!}(\exp_{2\ell-1}\phi)_\sharp\left(\tilde{\sigma}_1^1\left(\tilde{\sigma}_1^2\right)^{\ell-1}\right) \\ &= \frac{1}{(\ell-1)!}(d\tilde{\sigma}_1^1)(d\tilde{\sigma}_1^2)^{\ell-1} \\ &= \frac{d^\ell}{(\ell-1)!}\tilde{\sigma}_1^1\left(\tilde{\sigma}_1^2\right)^{\ell-1} \\ &= d^\ell\tilde{\sigma}_1^{2\ell-1}.\end{aligned}$$

Thus $\exp_{2\ell-1}\phi$ is a degree d^ℓ map, as found in Theorem 2.7.

For the second example consider the map $\tau\colon \Gamma_2 \to \Gamma_2$ sending e_1 to e_2 and e_2 to $e_2e_1\bar{e}_2$. We shall compare this with the map $\bar{\tau}$ that simply switches e_1 and e_2. These two maps are homotopic through a homotopy that drags v around e_2, so we expect the same induced map once we pass to homology, but an understanding of the chain maps will be useful in section 3.4 when we study the action of the braid group. Clearly $(\exp\bar{\tau})_\sharp$ simply interchanges $\tilde{\sigma}_1^j$ and $\tilde{\sigma}_2^j$, and likewise $(\exp\tau)_\sharp\tilde{\sigma}_1^j = \tilde{\sigma}_2^j$ for each j. The only difficulty therefore is in finding $(\exp\tau)_\sharp\tilde\sigma_2^j$, and we shall do this in two ways, first by calculating it directly and then by working over $\mathbf{Q}$ using (3.3.4).

To calculate $(\exp\tau)_\sharp\tilde\sigma_2^j$ directly let $p=(x_1,\dots,x_\ell,y_1,\dots,y_m)$ be a generic point in $\Delta_\ell\times\Delta_m$, $\ell+m=j$, $m\geq 1$. Preimages of p come in pairs that differ only in whether the preimage of y_i comes from the letter e_2 or $\bar e_2$ of w. In the first case the $(\ell+1)$th row of the derivative has a 3 in the first column and zeros elsewhere, and in the second it has a -3 in the last column and zeros elsewhere. Thus each pair contributes $(-1)^\ell+(-1)^m$ times the sign of the corresponding preimage in $\tilde\sigma_2^{j-1}$ of $(x_1,\dots,x_\ell,y_2,\dots,y_m)\in\Delta_\ell\times\Delta_{m-1}$, and consequently

$$\langle(\exp\tau)\circ\tilde\sigma_2^j,\tilde\sigma^{(\ell,m)}\rangle=\big((-1)^\ell+(-1)^m\big)\langle(\exp\tau)\circ\tilde\sigma_2^{j-1},\tilde\sigma^{(\ell,m-1)}\rangle.$$

This recurrence relation is easily solved to give

$$\langle(\exp\tau)\circ\tilde\sigma_2^j,\tilde\sigma^{(\ell,m)}\rangle=\begin{cases}1 & \text{if } m=0,\\ -2 & \text{if } \ell \text{ odd, } m=1,\\ 0 & \text{otherwise,}\end{cases}$$

so that

$$(\exp\tau)_\sharp\tilde\sigma_2^j=\begin{cases}\tilde\sigma_1^j & \text{if } j \text{ is odd,}\\ \tilde\sigma_1^j-2\tilde\sigma^{(j-1,1)} & \text{if } j>0 \text{ is even.}\end{cases}\tag{3.3.5}$$

To find $(\exp\tau)_\sharp\tilde\sigma_2^j$ using (3.3.4) we first need $(\exp\tau)_\sharp\tilde\sigma_2^1=\tilde\sigma_1^1$ and $(\exp\tau)_\sharp\tilde\sigma_2^2=\tilde\sigma_1^2-2\tilde\sigma_1^1\tilde\sigma_2^1$, each easily found directly. Then

$$(\exp\tau)_\sharp\tilde\sigma_2^{2\ell}=\frac{1}{\ell!}(\tilde\sigma_1^2-2\tilde\sigma_1^1\tilde\sigma_2^1)^\ell.$$

The cell $\tilde\sigma_1^2$ commutes with everything, so the binomial theorem applies, but $\tilde\sigma_1^1$ and $\tilde\sigma_2^1$ square to zero, so only two terms are nonzero. We get

$$\begin{aligned}(\exp\tau)_\sharp\tilde\sigma_2^{2\ell}&=\frac{1}{\ell!}\left(\tilde\sigma_1^2\right)^\ell-\frac{2}{\ell!}\ell\tilde\sigma_1^1\tilde\sigma_2^1\left(\tilde\sigma_1^2\right)^{\ell-1}\\&=\tilde\sigma_1^{2\ell}-2\tilde\sigma_1^{2\ell-1}\tilde\sigma_2^1,\end{aligned}$$

the even case of (3.3.5). Multiplying by $(\exp\tau)_\sharp\tilde\sigma_2^1=\tilde\sigma_1^1$ kills the second term and we get the odd case also.

To complete the calculation of $(\exp\tau)_\sharp$ we find the image of the cells $\tilde\sigma^{(\ell,m)}$. If $m=2p+1$ is odd we have simply

$$(\exp\tau)_\sharp\tilde\sigma^{(\ell,2p+1)}=\tilde\sigma_2^\ell\tilde\sigma_1^{2p+1}=(\exp\bar\tau)_\sharp\tilde\sigma^{(\ell,2p+1)},$$

while if $m=2p>0$ is even we get

$$\begin{aligned}(\exp\tau)_\sharp\tilde\sigma^{(\ell,2p)}&=\tilde\sigma_2^\ell\left(\tilde\sigma_1^{2p}-2\tilde\sigma_1^{2p-1}\tilde\sigma_2^1\right)\\&=\tilde\sigma_2^\ell\tilde\sigma_1^{2p}-2(-1)^\ell{\textstyle\left[{\ell+1\atop 1}\right]_{-1}}\tilde\sigma_1^{2p-1}\tilde\sigma_2^{\ell+1}\\&=\begin{cases}\tilde\sigma_2^\ell\tilde\sigma_1^{2p} & \text{if } \ell \text{ is odd,}\\ \tilde\sigma_2^\ell\tilde\sigma_1^{2p}-2\tilde\sigma^{(2p-1,\ell+1)} & \text{if } \ell \text{ is even.}\end{cases}\end{aligned}$$

Thus

$$(\exp\tau)_\sharp\tilde\sigma^{(\ell,m)} = \begin{cases}(\exp\bar\tau)_\sharp\tilde\sigma^{(\ell,m)} - 2\tilde\sigma^{(m-1,\ell+1)} & \ell, m \text{ both even, } m>0,\\ (\exp\bar\tau)_\sharp\tilde\sigma^{(\ell,m)} & \text{otherwise.}\end{cases} \tag{3.3.6}$$

Since elements of homology are linear combinations of cells each having at least one odd index we have $(\exp\tau)_* = (\exp\bar\tau)_*$ as expected.

3.4 The action of the braid group

3.4.1 Introduction

The braid group on n strands B_n may be defined as the mapping class group of an n–punctured disc D_n, or more precisely as the group of homeomorphisms of D_n that fix ∂D_n pointwise, modulo those isotopic to the identity rel ∂D_n. As such it acts on $H_k(\exp_k D_n)$, and since $D_n \simeq \Gamma_n$ we may regard this as an action on $H_k(\exp_k\Gamma_n)$. We prove the following structure theorem for this action.

Theorem 3.7. *The image of the pure braid group P_n under the action of B_n on $H_k(\exp_k\Gamma_n)$ is nilpotent of class at most* $\min\{(k-1)/2, \lfloor(n-1)/2\rfloor\}$ *if k is odd, or* $\min\{(k-2)/2, \lfloor(n-2)/2\rfloor\}$ *if k is even.*

For the above and other definitions of the braid group see Birman [5].

Recall that the pure braid group P_n is the kernel of the map $B_n \to S_n$ sending each braid β to the induced permutation $\bar\beta$ of the punctures. Consider the subgroup of P_n consisting of braids whose first $n-1$ strands form the trivial braid. The nth strand of such a braid may be regarded as an element of $\pi_1(D_{n-1})$, and doing so gives an isomorphism from this subgroup to the free group F_{n-1}. This shows that P_n is not nilpotent for $n \geq 3$. The group P_2 inside B_2 is isomorphic to $2\mathbf{Z}$ inside $\mathbf{Z}$, and is therefore nilpotent of class 1; however the bound for $n=2$ in Theorem 3.7 is zero, implying P_2 acts trivially, and in fact this follows from the second example of section 3.3.4. Thus we have in particular that the action of B_n on $H_k(\exp_k\Gamma_n)$ is unfaithful for all k and $n \geq 2$.

There is an obvious action of S_n on $H_k(\exp_k\Gamma_n)$, induced by permuting the edges of Γ_n. The theorem will be proved by relating the action of each braid β to that of $\bar\beta$. Note that there is again nothing lost by considering only the action on $H_k(\exp_k\Gamma_n)$, because of the isomorphisms induced by i and $\cup\{v\}$. For brevity, in what follows we shall simply write H_k for $H_k(\exp_k\Gamma_n)$.

3.4.2 Proof of the structure theorem

We fix a representation of D_n and a homotopy equivalence $\Gamma_n \to D_n$, the embedding shown in figure 3.5(a). B_n is generated by the "half Dehn twists" $\tau_1, \ldots, \tau_{n-1}$, where τ_i interchanges the ith and $(i+1)$th punctures with an anti-clockwise twist. The effect of τ_i on the embedded graph is shown in figure 3.5(b), and we see that it induces the map

$$e_a \mapsto \begin{cases} e_{i+1} & \text{if } a = i,\\ e_{i+1}e_i\bar e_{i+1} & \text{if } a = i+1,\\ e_a & \text{if } a \neq i, i+1,\end{cases}$$

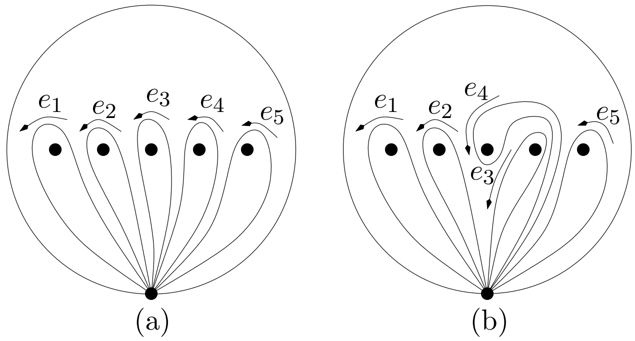

Figure 3.5: The punctured disc D_n and the generators τ_i for $n = 5$ and $i = 3$. We embed Γ_5 in D_5 as shown in (a); the effect of τ_3 on the embedding is shown in (b).

on Γ_n. We will call this map τ_i also, and our goal is to understand the $(\exp \tau_i)_*$ well enough to show that the pure braid group acts by upper-triangular matrices.

To this end we define a filtration of H_k. Each homology class has precisely one representative in $\tilde{\mathcal{C}}_k$, since there are no boundaries, so we may regard H_k as a subspace of $\tilde{\mathcal{C}}_k$ and work unambiguously on the level of chains. Let

$$\mathcal{F}_j = \left\{ \textstyle\sum_J c_J \tilde{\sigma}^J \in H_k \middle| c_J = 0 \text{ if } |J|_2 < n - j \right\},$$

so that $\mathcal{F}_j$ is the subspace spanned by cells having no more than j even indices. Clearly $\{0\} \subseteq \mathcal{F}_0 \subseteq \mathcal{F}_1 \subseteq \cdots \subseteq \mathcal{F}_n = H_k$, so the $\mathcal{F}_j$ form a filtration. Moreover $\mathcal{F}_j$ has $\mathcal{F}_j \cap \mathcal{B}(k, n)$ as a basis: each element of $\mathcal{B}(k, n)$ has the form

$$\widetilde{\partial\sigma^J} = \sum_{i : j_i > 0 \text{ even}} c_i \tilde{\sigma}^{\partial_i(J)}$$

for some J with $|J| = k + 1$, and the mod 2 norm of every term in this sum is $|J|_2 + 1$.

We now describe when $\mathcal{F}_i = \mathcal{F}_j$ for $i \neq j$, as the indexing has been chosen to be uniform and meaningful at the expense of certain a priori isomorphisms among the $\mathcal{F}_j$, arising from the parity and size of k. Since $|J| = k$ for each k–cell $\tilde{\sigma}^J$ we have in particular $|J|_2 \equiv k \bmod 2$. Thus $\mathcal{F}_{j+1} = \mathcal{F}_j$ if $n - j$ and k have the same parity. Next, $|J|_2 \leq |J| = k$, so $\mathcal{F}_j = \{0\}$ if $n - j > k$, or in other words if $j < n - k$. Lastly, no cell for which $|J|_2 = 0$ is a summand of an element of H_k (recall that $\mathcal{C}_*$ is exact, and that such a cell sits at the top of an m–cube complex and so is not part of any boundary), so that either $\mathcal{F}_{n-2}$ or $\mathcal{F}_{n-1}$ is all of H_k, depending on the parity of k. To see that these are the only circumstances in which $\mathcal{F}_i$ and $\mathcal{F}_j$ can coincide suppose that $i < j \leq n - 1$, $n - i$ and $n - j$ have the same parity as k, $n - j \leq k$, and let

$$J = (\underbrace{0, \ldots, 0}_{j}, \underbrace{1, \ldots, 1}_{n-j-1}, k + j + 1 - n).$$

Every non-zero index of J is odd so $\tilde{\sigma}^J$ is a cycle. It has $j > i$ even indices and is therefore non-trivial in the quotient $\mathcal{F}_j / \mathcal{F}_i$.

The significance of the filtration is given by the following lemma, which is the main step in proving the structure theorem for the action.

Lemma 3.5. *Each $\mathcal{F}_j$ is an invariant subspace for the action of B_n on H_k. Moreover, the action on $\mathcal{F}_j/\mathcal{F}_{j-1}$ factors through the symmetric group S_n.*

Proof. The lemma is proved by relating the action of B_n to that of S_n induced by permuting the edges of Γ_n. Much of the work has been done already in section 3.3.4, since τ_i and $\bar{\tau}_i$ act as the maps τ and $\bar{\tau}$ considered there on $e_i \cup e_{i+1}$, and as the identity on the remaining edges.

For each n–tuple J let

$$\delta_i(J) = (j_1, \ldots, j_i + 1, \ldots, j_n)$$

so that

$$\partial_i \circ \delta_{i+1} \circ \bar{\tau}_i(J) = (j_1, \ldots, j_{i-1}, j_{i+1} - 1, j_i + 1, j_{i+2}, \ldots, j_n).$$

By (3.3.6) we may write

$$(\exp \tau_i)_\sharp \tilde{\sigma}^J = \begin{cases} (\exp \bar{\tau}_i)_\sharp \tilde{\sigma}^J - 2\tilde{\sigma}^{\partial_i \circ \delta_{i+1} \circ \bar{\tau}_i(J)} & j_i, j_{i+1} \text{ both even, } j_{i+1} > 0, \\ (\exp \bar{\tau}_i)_\sharp \tilde{\sigma}^J & \text{otherwise.} \end{cases} \tag{3.4.1}$$

If j_i and j_{i+1} are both even then

$$|\partial_i \circ \delta_{i+1} \circ \bar{\tau}_i(J)|_2 = |J|_2 + 2$$

and it follows that

$$(\exp \tau_i)_* c \in (\exp \bar{\tau}_i)_* c + \mathcal{F}_{j-1}$$

for each $c \in \mathcal{F}_j$ and $i \in [n-1]$. Since the τ_i generate B_n we get

$$(\exp \beta)_* c \in (\exp \bar{\beta})_* c + \mathcal{F}_{j-1}$$

for all braids β and $c \in \mathcal{F}_j$, and the lemma follows immediately. □

Proof of Theorem 3.7. By Lemma 3.5, with respect to a suitable ordering of $\mathcal{B}(k,n)$ the braid group acts by block upper-triangular matrices. The diagonal blocks are the matrices of the action on $\mathcal{F}_j/\mathcal{F}_{j-1}$, and since this factors through S_n we have that the pure braids act by upper-triangular matrices with ones on the diagonal. It follows immediately that the image of P_n is nilpotent.

To bound the length of the lower central series we count the number of nontrivial blocks, as the class of the image is at most one less than this. By the discussion following the definition of $\{\mathcal{F}_j\}$ this is the number of $0 \leq j \leq n-1$ such that $n - j \leq k$ and $n - j \equiv k \bmod 2$; letting $\ell = n - j$ this is the number of $1 \leq \ell \leq \min\{n, k\}$ such that $\ell \equiv k \bmod 2$. There are $\lfloor (m+1)/2 \rfloor$ positive odd integers and $\lfloor m/2 \rfloor$ positive even integers less than or equal to a positive integer m, and the given bounds follow. □

3.4.3 The action of B_3 on $H_3(\exp_3\Gamma_3)$

We study the action of B_3 on $H_3(\exp_3\Gamma_3)$, being the smallest non-trivial example, and show that P_3 acts as a free abelian group of rank two.

For simplicity we will simply write J for the cell $\tilde{\sigma}^J$. From Theorem 3.4 we obtain the basis

$$\begin{aligned} u_1 &= (3,0,0) & w_1 &= (0,1,2) + (0,2,1) \\ u_2 &= (0,3,0) & w_2 &= (1,0,2) + (2,0,1) \\ u_3 &= (0,0,3) & w_3 &= (1,2,0) + (2,1,0) \\ v &= (1,1,1) \end{aligned}$$

for $H_3(\exp_3\Gamma_3)$ (in fact this is the negative of the basis given there). Let U be the span of $\{u_1, u_2, u_3\}$, V the span of $\{v\}$, and W the span of $\{w_1, w_2, w_3\}$. The subspaces U, V and $V \oplus W$ are easily seen to be invariant using equation (3.4.1), and moreover the action on U is simply the permutation representation of S_3. We therefore restrict our attention to $V \oplus W$. The actions on V and $(V \oplus W)/V$ are the sign and permutation representations of S_3 respectively, and with respect to the basis $\{v, w_1, w_2, w_3\}$ we find that

$$(\exp_3\tau_1)_*|_{V\oplus W} = T_1 = \begin{bmatrix} -1 & -2 & 0 & 0 \\ 0 & 0 & 1 & 0 \\ 0 & 1 & 0 & 0 \\ 0 & 0 & 0 & 1 \end{bmatrix},$$

$$(\exp_3\tau_2)_*|_{V\oplus W} = T_2 = \begin{bmatrix} -1 & 0 & -2 & 0 \\ 0 & 1 & 0 & 0 \\ 0 & 0 & 0 & 1 \\ 0 & 0 & 1 & 0 \end{bmatrix}.$$

In each case the inverse is obtained by moving the -2 one place to the right.

A product of T_1, T_2 and their inverses has the form

$$P = \begin{bmatrix} \det \bar{P} & p \\ 0 & \bar{P} \end{bmatrix}$$

where $\bar{P}$ is a permutation matrix and $p = (p_1, p_2, p_3)$ is a vector of even integers. Consider $\Sigma(P) = p_1 + p_2 + p_3$. Multiplying P by $T_i^{\pm 1}$ we see that $\Sigma(T_i^{\pm 1}P) = -\Sigma(P) - 2$, and it follows that $\Sigma(P)$ is zero if $\bar{P}$ is even and -2 if $\bar{P}$ is odd. In particular $\Sigma(P)$ is zero if P is the image of a pure braid.

If $P = QR$ where $\bar{Q} = \bar{R} = I$ then $p = q + r$ and it follows that the pure braid group P_3 acts as a free abelian group of rank at most two. That the rank is in fact two can be verified by calculating T_1^2 and T_2^2 and checking that the corresponding vectors are independent.

Chapter 4

Closed surfaces

4.1 Introduction

In this chapter we make the first steps towards an understanding of the finite subset spaces of a closed surface. We do this in two orthogonal directions. We first use ideas and techniques from the previous chapters to show that finite subset spaces of 2–complexes admit "lexicographic cell structures" based on the lexicographic ordering of I^2. Applying these to the standard cell structures for closed surfaces we completely calculate the rational homology of the finite subset spaces of S^2 and determine the top integral homology groups of $\exp_k\Sigma$ for each k and closed surface Σ. We then use a quite different approach to completely calculate the integral cohomology groups of the third finite subset space of a closed orientable surface. This is the first nontrivial case since the second finite subset space co-incides with the second symmetric product, for which the answer is already known. We build a homotopy model for $\exp_3\Sigma$ out of $\mathrm{Sym}^3\Sigma$ and the mapping cylinder of $\Sigma^2 \to \mathrm{Sym}^2\Sigma$, and calculate the cohomology using the Mayer-Vietoris sequence and the calculation of $H^*(\mathrm{Sym}^k\Sigma)$ due to Macdonald [24] and Seroul [31, 32].

Up to this point all homology and cohomology has been with respect to integer co-efficients, but in this chapter other co-efficient groups and rings will appear. We therefore make explicit the convention implicit in the earlier chapters that where a co-efficient group or ring is not specified integer co-efficients should be assumed.

4.1.1 Summary of main results

We first show that the finite subset spaces of a connected finite 2–complex admit cell structures in section 4.2, and then we use these in section 4.3 to completely calculate the rational homology of $\exp_k(S^2,*)$ and $\exp_k S^2$.

Theorem 4.1. *The space* $\exp_k(S^2,*)$ *has the rational homology of* S^{2k-2}*, and the space* $\exp_k S^2$ *has the rational homology of* $S^{2k} \vee S^{2k-2}$*.*

More careful attention at the top end of the chain complex shows that "rational" cannot be replaced by "integral" in this theorem for $k \geq 4$ in the based case and $k \geq 3$ in the unbased case:

Theorem 4.2. *The top three integral homology groups of* $\exp_k(S^2,*)$ *are* $\mathbf{Z}$ *in dimension* $2k-2$*,* $\{0\}$ *in dimension* $2k-3$*, and* $\mathbf{Z}/(k-2)\mathbf{Z}$ *in dimension* $2k-4$*. The group* H_{2k-4} *is generated by the top homology class of* $\exp_{k-1}(S^2,*) \hookrightarrow \exp_k(S^2,*)$*.*

The top three integral homology groups of $\exp_k S^2$ *are* $\mathbf{Z}$ *in dimension* $2k$*,* $\{0\}$ *in dimension* $2k-1$*, and* $\mathbf{Z} \oplus \mathbf{Z}/(k-1)\mathbf{Z}$ *in dimension* $2k-2$*. The group* H_{2k-2} *is generated by the top classes* $[\exp_{k-1}S^2]$ *of* $\exp_{k-1}S^2$ *and* $[\exp_k(S^2,*)]$ *of* $\exp_k(S^2,*)$*, subject to the relation* $(k-1)\big([\exp_{k-1}S^2] - 2[\exp_k(S^2,*)]\big) = 0$*.*

In addition, we calculate the integral homology completely as far as $k=6$ in the based case and $k=5$ in the unbased case.

We then turn to the finite subset spaces of higher genus surfaces in section 4.4. Again using the cell structures constructed in section 4.2 we prove the following refinement for $n=2$ of Handel's result in [18] that $H^{nk}(\exp_k M^n; \mathbf{Z}/2\mathbf{Z})$ has rank one for a closed connected n–manifold, $n \geq 2$:

Theorem 4.3. *Let* Σ *be a closed surface of genus* g*. Then*

$$H_{2k}(\exp_k \Sigma) = \begin{cases} \mathbf{Z} & \text{if } \Sigma \text{ is orientable,} \\ 0 & \text{if } \Sigma \text{ is non-orientable,} \end{cases}$$

and

$$H_{2k-1}(\exp_k \Sigma) = \begin{cases} \mathbf{Z}^{2g} & \text{if } \Sigma \text{ is orientable,} \\ \mathbf{Z}/2\mathbf{Z} & \text{if } \Sigma \text{ is non-orientable.} \end{cases}$$

Given an orientation on Σ we may canonically orient the manifold $\exp_k\Sigma \backslash \exp_{k-1}\Sigma$ by orienting each tangent space as the direct sum

$$T_\Lambda(\exp_k\Sigma \setminus \exp_{k-1}\Sigma) = \bigoplus_{p\in\Lambda} T_p\Sigma. \tag{4.1.1}$$

Since Σ is even dimensional the order of the summands does not matter and we obtain a consistent orientation on the configuration space $\exp_k\Sigma \setminus \exp_{k-1}\Sigma$. This in turn orients H_{2k}, and Theorem 4.3 then implies that a map between the kth finite subset spaces of two closed oriented surfaces has a well defined degree. In the case where the map is induced by a map between the underlying spaces the degree behaves entirely as we might expect:

Theorem 4.4. *If* $f\colon \Sigma \to \Sigma'$ *is a map between closed oriented surfaces then*

$$\deg \exp_k f = (\deg f)^k.$$

We recall that for the circle we found $\deg \exp_k f = (\deg f)^{\lfloor \frac{k+1}{2} \rfloor}$ due to cancellation among the preimages of a generic point in $\exp_k S^1$. The difference lies in the fact that the circle is odd-dimensional, so that orienting tangent spaces to $\exp_k S^1 \backslash \exp_{k-1} S^1$ as in (4.1.1) requires the additional data of an order on the summands.

As our last result for closed surfaces we construct a homotopy model for the third finite subset space of a closed orientable surface in section 4.5, and use this to completely calculate the integral cohomology of the third finite subset space of a closed orientable surface in section 4.6.

Theorem 4.5. *Let Σ_g be a closed orientable surface of genus g. The cohomology group $H^i(\exp_3\Sigma_g)$ is given by*

		$g = 0$	$g = 1$	$g \geq 2$
i	0	$\mathbf{Z}$	$\mathbf{Z}$	$\mathbf{Z}$
	1	0	0	0
	2	0	$\mathbf{Z}$	$\mathbf{Z}^{\binom{2g}{2}}$
	3	0	$\mathbf{Z}^5$	$\mathbf{Z}^{p(g)}$
	4	$\mathbf{Z}$	$\mathbf{Z}^4$	$\mathbf{Z}^{q(g)} \oplus [\mathbf{Z}/2\mathbf{Z}]^{2g}$
	5	$\mathbf{Z}/2\mathbf{Z}$	$\mathbf{Z}^2 \oplus \mathbf{Z}/2\mathbf{Z}$	$\mathbf{Z}^{2g} \oplus \mathbf{Z}/2\mathbf{Z}$
	6	$\mathbf{Z}$	$\mathbf{Z}$	$\mathbf{Z}$

in which

$$p(g) = \binom{2g}{3} + \binom{2g}{2} + \binom{2g}{1} \qquad \text{and} \qquad q(g) = \binom{2g}{2} + 1$$

for $g \geq 2$. The Euler characteristic is

$$\chi(\exp_3\Sigma) = \frac{-4g^3 + 12g^2 - 17g + 9}{3}.$$

In particular $\chi(\exp_3 S^2) = 3$, $\chi(\exp_3 T^2) = 0$, and $\chi(\exp_3\Sigma_2) = -3$.

4.2 Lexicographic cell structures

We show that the finite subset spaces of connected finite 2-complexes admit cell structures based on the lexicographic ordering of I^2. After establishing some conventions in section 4.2.1 we prove the cell structures exist in section 4.2.2 and calculate the boundary maps in section 4.2.3. We close in section 4.2.4 with a brief discussion on constructing lexicographic cell structures for the finite subset spaces of higher dimensional complexes.

4.2.1 Conventions

In constructing cell structures for the finite subset spaces of a connected finite 2–complex X we will work up to homotopy and assume that X has a single vertex v, as we did with graphs. We identify the 1–skeleton of X with Γ_n for some $n \geq 0$, and denote its 2–cells by $f_1, \ldots, f_m$. Each cell f_i has a characteristic map ϕ_i from the unit disc $D^2 \subseteq \mathbf{C}$ to X and we assume that ϕ_i sends $-1 \in \partial D^2$ to v.

Our cell structures will be obtained by using the lexicographic order on I^2 to choose preferred lifts from $\exp_j(\text{int } f_i)$ to X^j, where the lexicographic order $\prec$ is defined by

$$(x_1, y_1) \prec (x_2, y_2) \qquad \text{if } x_1 < x_2, \text{ or if } x_1 = x_2 \text{ and } y_1 < y_2.$$

We transfer this order to D^2 via a "crunching" map $\kappa\colon I^2 \to D^2$ which sends the three sides $x = 0$, $y = 0$ and $y = 1$ to $-1 \in \partial D^2$ and maps the rest of the square homeomorphically

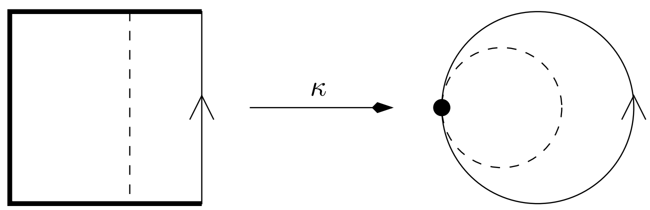

Figure 4.1: The crunching map $\kappa\colon I^2 \to D^2$. The three sides of the square shown in bold map to the dot at -1, the unbolded edge maps to the boundary and the dotted line goes to the dotted circle.

onto the rest of the disc, preserving orientation. The exact form of κ is unimportant, but for the sake of concreteness we let

$$\kappa(x,y) = x(1 - e^{2\pi i y}) - 1.$$

This sends the vertical segment $x = x_0$ to the circle with centre $x_0 - 1$ and radius x_0, as shown in figure 4.1.

As was the case with graphs our cells will be described by vectors of integers arising from ordered partitions. The vectors will contain positive integers only so their lengths will vary and we write $\ell(S) = \ell$ if $S = (s_1, \ldots, s_\ell)$. The boundary of the cell corresponding to S will include cells corresponding to partitions obtained by merging adjacent parts of S, and accordingly we define

$$\mu_i(S) = (s_1, \ldots, s_i + s_{i+1}, \ldots, s_\ell)$$

for $1 \le i \le \ell(S) - 1$. We recall from section 3.2.2 that $\tilde{\Delta}_j$ is the simplex

$$\tilde{\Delta}_j = \{(x_1, \ldots, x_j) | 0 \le x_1 \le \cdots \le x_j \le 1\},$$

and that $\tilde{\Delta}_J = \tilde{\Delta}_{j_1} \times \cdots \times \tilde{\Delta}_{j_n}$, omitting any empty factors $\tilde{\Delta}_0$.

4.2.2 Existence of lexicographic cell structures

The first step in building a cell structure for $\exp_k X$ is to form an open cell decomposition of $\exp_j(\operatorname{int} f_i) \setminus \exp_{j-1}(\operatorname{int} f_i)$, using the fact that each j element subset of $\operatorname{int} I^2$ has a unique lexicographically ordered representative in $(\operatorname{int} I^2)^j$. Figure 4.2 illustrates the idea for $k = 3$. Generically, three points in $\operatorname{int} I^2$ may be ordered by their x co-ordinates, as in the square labeled $(1,1,1)$, and this gives an open 6–ball

$$\operatorname{int}(\tilde{\Delta}_3 \times \tilde{\Delta}_1 \times \tilde{\Delta}_1 \times \tilde{\Delta}_1) = \{0 < x_1 < x_2 < x_3 < 1\} \times \{0 < y_1, y_2, y_3 < 1\}.$$

If two of the x co-ordinates are equal but the third is different there are two possibilities, illustrated by the squares labeled $(2,1)$ and $(1,2)$ and corresponding to the open 5-balls

$$\operatorname{int}(\tilde{\Delta}_2 \times \tilde{\Delta}_2 \times \tilde{\Delta}_1) = \{0 < x_1 = x_2 < x_3 < 1\} \times \{0 < y_1 < y_2 < 1\} \times \{0 < y_3 < 1\},$$
$$\operatorname{int}(\tilde{\Delta}_2 \times \tilde{\Delta}_1 \times \tilde{\Delta}_2) = \{0 < x_1 < x_2 = x_3 < 1\} \times \{0 < y_1 < 1\} \times \{0 < y_2 < y_3 < 1\},$$

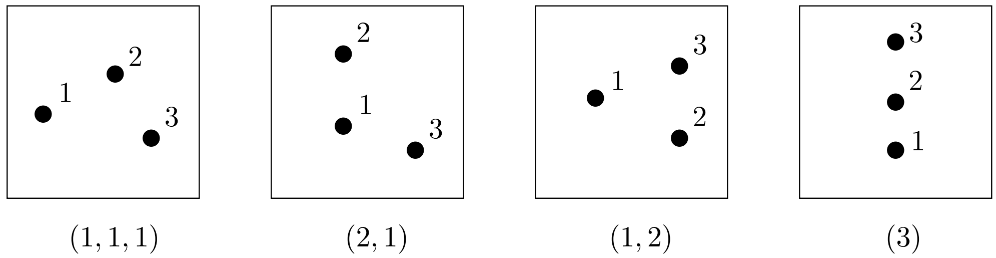

Figure 4.2: Open cell decomposition of $\exp_3(\operatorname{int} I^2) \setminus \exp_2(\operatorname{int} I^2)$. We decompose $\exp_3(\operatorname{int} I^2) \setminus \exp_2(\operatorname{int} I^2)$ as a union of four open cells, corresponding to the four ordered partitions $(1,1,1)$, $(2,1)$, $(1,2)$ and (3) of three as a sum of positive integers.

and when all three x co-ordinates are equal as in the square labeled (3) we have the open 4–ball

$$\operatorname{int}(\tilde{\Delta}_1 \times \tilde{\Delta}_3) = \{0 < x_1 = x_2 = x_3 < 1\} \times \{0 < y_1 < y_2 < y_3 < 1\}.$$

This gives a decomposition of $\exp_3(\operatorname{int} I^2) \setminus \exp_2(\operatorname{int} I^2)$ as a union of four open cells, and more generally we obtain a decomposition of $\exp_j(\operatorname{int} I^2) \setminus \exp_{j-1}(\operatorname{int} I^2)$ as a union of 2^{j-1} open cells, parameterised by the ordered partitions of j as a sum of positive integers. A cell structure for $\exp_k X$ is then obtained by taking products of such cells with the cells $\sigma^J, \tilde{\sigma}^J$ of Γ_n.

Concretely, to each j element subset $\Lambda = \{p_1, \dots, p_j\}$ of $\operatorname{int} I^2$ we associate the ordered partition $\mathcal{S}(\Lambda) = (s_1, \dots, s_\ell)$ of j arising from the equivalence relation $p_i \sim p_j$ if $x_i = x_j$. This gives a partition $\{\Lambda_1, \dots, \Lambda_\ell\}$ of Λ which may be ordered by $\Lambda_a < \Lambda_b$ if $p \in \Lambda_a$, $p' \in \Lambda_b$, and $x < x'$, and we obtain $\mathcal{S}(\Lambda)$ by letting s_i be the size of the ith part. Set

$$\mathcal{E}(S) = \{\Lambda \in \exp_{|S|}(\operatorname{int} I^2) | \mathcal{S}(\Lambda) = S\}$$

for each vector S of positive integers. It is clear that the sets $\mathcal{E}(S)$ with $|S| = j$ form a partition of $\exp_j(\operatorname{int} I^2) \setminus \exp_{j-1}(\operatorname{int} I^2)$, and we claim further that $\mathcal{E}(S)$ is parameterised by the open $(|S| + \ell(S))$–ball $\operatorname{int}(\tilde{\Delta}_S \times \tilde{\Delta}_{\ell(S)})$. To see this, note that if $\{p_1, \dots, p_j\} \in \mathcal{E}(S)$ satisfies $p_1 \prec \cdots \prec p_j$ then $(y_1, \dots, y_j)$ is a point in $\operatorname{int}(\tilde{\Delta}_{s_1} \times \cdots \times \tilde{\Delta}_{s_\ell})$ and the distinct x values $(x_{i_1}, \dots, x_{i_\ell})$ form a point in $\operatorname{int} \tilde{\Delta}_{\ell(S)}$. This leads to a map

$$\operatorname{int}(\tilde{\Delta}_{s_1} \times \cdots \times \tilde{\Delta}_{s_\ell} \times \tilde{\Delta}_\ell) \to (\operatorname{int} I^2)^j \to \exp_j(\operatorname{int} I^2) \tag{4.2.1}$$

hitting precisely $\mathcal{E}(S)$, and this map is injective since each $\Lambda \in \exp_j(\operatorname{int} I^2) \setminus \exp_{j-1}(\operatorname{int} I^2)$ has a unique lexicographically ordered representative in $(\operatorname{int} I^2)^j$.

Having found an open cell decomposition of $\exp_j(\operatorname{int} I^2)$ we now construct cells for $\exp_k X$. The map (4.2.1) extends to a map $\tilde{\Delta}_S \times \tilde{\Delta}_\ell \to \exp_j I^2$ and we let $\tilde{\tau}_i^S$ be the composition

$$\tilde{\Delta}_S \times \tilde{\Delta}_{\ell(S)} \to \exp_{|S|} I^2 \xrightarrow{\exp_{|S|}\kappa} \exp_{|S|} D^2 \xrightarrow{\exp_{|S|}\phi_i} \exp_{|S|} f_i,$$

τ_i^S the composition

$$\tilde{\Delta}_S \times \tilde{\Delta}_{\ell(S)} \xrightarrow{\tilde{\tau}_i^S} \exp_{|S|} X \xrightarrow{\cup\{v\}} \exp_{|S|+1}(f_i, v).$$

Since both $\kappa|_{\mathrm{int}\, I^2}$ and $\phi_i|_{\mathrm{int}\, D^2}$ are homeomorphisms so are $\exp_k(\kappa|_{\mathrm{int}\, I^2})$ and $\exp_k(\phi_i|_{\mathrm{int}\, D^2})$, and it follows that the maps $\tilde{\tau}_i^S$ are injective on the interiors of their balls of definition and give an open cell decomposition of $\exp_j(\mathrm{int}\, f_i)$. Further, τ_i^S is injective on $\mathrm{int}(\tilde{\Delta}_S \times \tilde{\Delta}_{\ell(S)})$ as well, since $\cup\{v\}$ is injective on $\exp_j(\mathrm{int}\, f_i)$. We claim:

Theorem 4.6. *Let X be a connected finite 2–complex with a single vertex v. Then the maps*

$$\left\{\tau_{i_1}^{S_1} \cup \cdots \cup \tau_{i_p}^{S_p} \cup \sigma^J | i_1 < \cdots < i_r \text{ and } |J| + \textstyle\sum_q |S_q| \leq k-1\right\} \tag{4.2.2}$$

are the characteristic maps of a cell structure for $\exp_k(X, v)$, and these maps together with

$$\left\{\tilde{\tau}_{i_1}^{S_1} \cup \cdots \cup \tilde{\tau}_{i_p}^{S_p} \cup \tilde{\sigma}^J | i_1 < \cdots < i_r \text{ and } |J| + \textstyle\sum_q |S_q| \leq k\right\} \tag{4.2.3}$$

are the characteristic maps of a cell structure for $\exp_k X$.

Notice that $\exp_k X$ is obtained from $\exp_{k-1} X$ by adding cells in dimensions $k-1 \leq d \leq 2k$, or $k \leq d \leq 2k$ if X has no edges. By the argument of section 3.2.1 this implies that $\exp_k X$ is $(k-2)$–connected, and $(k-1)$–connected if X is simply connected. We show that this holds more generally for higher dimensional complexes in Chapter 5.

Proof. Each map $\tau_{i_1}^{S_1} \cup \cdots \cup \tau_{i_p}^{S_p} \cup \sigma^J$ in (4.2.2) is a map from a $|J| + \sum_q |S_q| + \sum_q \ell(S_q)$ dimensional ball to $\exp_{(|J|+\sum_q |S_q|+1)}(X, v)$, and since $|J| + \sum_q |S_q| \leq k-1$ the image of each map lies in $\exp_k(X, v)$. Similarly, each map $\tilde{\tau}_{i_1}^{S_1} \cup \cdots \cup \tilde{\tau}_{i_p}^{S_p} \cup \tilde{\sigma}^J$ occurring in (4.2.3) is a map from a ball of dimension $|J| + \sum_q |S_q| + \sum_q \ell(S_q)$ with image lying in $\exp_k X$, and moreover the interior of this ball misses $\exp_k(X, v)$. We show that each map is injective on the interior of its domain, that the open cells partition $\exp_k X$, and that the boundary of each cell lies on open cells of strictly smaller dimension.

To prove injectivity on interiors note that each basic cell $\tilde{\tau}_{i_q}^{S_q}$, $\tilde{\sigma}_i^{j_i}$ is injective on the interior of its domain of definition, and that the images of these cells are disjoint since they lie in disjoint sets $\exp_{|S_q|}(\mathrm{int}\, f_{i_q})$, $\exp_{j_i}(\mathrm{int}\, e_i)$. It follows that the restriction of the cupped map $\tilde{\tau}_{i_1}^{S_1} \cup \cdots \cup \tilde{\tau}_{i_p}^{S_p} \cup \tilde{\sigma}^J$ to the interior of its ball of definition is injective also. Further, as noted above this restriction misses $\exp_k(X, v)$, implying that

$$\tau_{i_1}^{S_1} \cup \cdots \cup \tau_{i_p}^{S_p} \cup \sigma^J = (\cup\{v\}) \circ (\tilde{\tau}_{i_1}^{S_1} \cup \cdots \cup \tilde{\tau}_{i_p}^{S_p} \cup \tilde{\sigma}^J)$$

is injective on the interior of its ball of definition also.

Each $\Lambda \in \exp_k X$ can be written uniquely as

$$\Lambda = (\Lambda \cap \{v\}) \cup \bigcup_{i=1}^{n} (\Lambda \cap (\mathrm{int}\, e_i)) \cup \bigcup_{i=1}^{m} (\Lambda \cap (\mathrm{int}\, f_i))$$

and this data determines a unique open cell from (4.2.2) or (4.2.3) containing Λ. Let $i_1 < \cdots < i_p$ be the indices i such that $\Lambda \cap (\mathrm{int}\, f_i)$ is non-empty, set $S_q = \mathcal{S}(\Lambda \cap (\mathrm{int}\, f_{i_q}))$ and let $j_i = |\Lambda \cap (\mathrm{int}\, e_i)|$. Then the open cell $\tau_{i_1}^{S_1} \cup \cdots \cup \tau_{i_p}^{S_p} \cup \sigma^J$ contains Λ if $v \in \Lambda$, and the open cell $\tilde{\tau}_{i_1}^{S_1} \cup \cdots \cup \tilde{\tau}_{i_p}^{S_p} \cup \tilde{\sigma}^J$ contains Λ if $v \notin \Lambda$. Moreover this is the unique open cell containing Λ: regarding $\tau_{i_1}^{S_1} \cup \cdots \cup \tau_{i_p}^{S_p} \cup \sigma^J$ as $\tilde{\tau}_{i_1}^{S_1} \cup \cdots \cup \tilde{\tau}_{i_p}^{S_p} \cup \tilde{\sigma}^J \cup \{v\}$, the map $\tilde{\tau}_i^S$ can occur as a factor if and only if $\Lambda \cap (\operatorname{int} f_i)$ is non-empty and $S = \mathcal{S}(\Lambda \cap (\operatorname{int} f_i))$, $\tilde{\sigma}^J$ can occur as a factor if and only if $j_i = |\Lambda \cap (\operatorname{int} e_i)|$, and $\{v\}$ can occur as a factor if and only if $v \in \Lambda$. It follows that the open cells (4.2.2) and (4.2.3) partition $\exp_k X$ as claimed.

It remains to check that taking boundaries decreases dimension. It suffices to do this for each factor cell, and since we know the result for $\tilde{\sigma}^J, \sigma^J$ by Lemma 3.1 it will be enough to check the cells τ_i^S, $\tilde{\tau}_i^S$. We do this in section 4.2.3, where we calculate $\partial\tau_i^S$ and $\partial\tilde{\tau}_i^S$. □

4.2.3 The boundary maps

In this section we indicate how to calculate the boundaries of the cells (4.2.2) and (4.2.3), and complete the proof of Theorem 4.6 by showing that taking boundaries decreases dimension. Since

$$\begin{aligned}
\partial(\sigma \cup \tau) &= \partial(\cup \circ (\sigma \times \tau)) \\
&= \cup_* \partial(\sigma \times \tau) \\
&= \cup_* (\partial\sigma \times \tau + (-1)^{\dim \sigma} \sigma \times \partial\tau) \\
&= \partial\sigma \cup \tau + (-1)^{\dim \sigma} \sigma \cup \partial\tau
\end{aligned}$$

we need only calculate the boundary of each basic cell occurring as a factor. As before we calculate $\partial\tilde{\tau}_i^S$ and obtain $\partial\tau_i^S$ as $(\cup\{v\})_* \partial\tilde{\tau}_i^S$ by removing all tildes.

The boundary of $\tilde{\tau}_i^S$ will consist of three parts, one that decreases the norm of S, a second that decreases the length of S, and a third that moves points from the interior of f_i onto the boundary. In preparation for stating the result we define each separately. As before we write $\partial_a(S)$ for the partition obtained by decreasing the ath part of S by one, and we recall that $\mu_a(S)$ is the partition obtained by merging the ath and $(a+1)$th parts of S, in other words

$$\mu_a(S) = (s_1, \ldots, s_a + s_{a+1}, \ldots, s_\ell).$$

Since $\partial_a(S)$ has norm $|S| - 1$ and length $\ell(S)$ the cell $\tilde{\tau}_i^{\partial_a(S)}$ has dimension one less than $\tilde{\tau}_i^S$, and the same is true of $\tilde{\tau}_i^{\mu_a(S)}$ since $|\mu_a(S)| = |S|$ and $\ell(\mu_a(S)) = \ell(S) - 1$. Let

$$\begin{aligned}
\partial^\nu \tau_i^S &= -\sum_{a=1}^{\ell(S)} \frac{1 + (-1)^{s_a}}{2} (-1)^{\left|S|_{[a-1]}\right|} \tau_i^{\partial_a(s)}, \\
\partial^\lambda \tau_i^S &= \sum_{a=1}^{\ell(S)-1} (-1)^{(a-1)} \begin{bmatrix} s_a + s_{a+1} \\ s_a \end{bmatrix}_{-1} \tau_i^{\mu_a(S)},
\end{aligned}$$

and extend these maps to $\tilde{\tau}_i^S$ by

$$\begin{aligned}
\partial^\nu \tilde{\tau}_i^S &= 2\partial^\nu \tau_i^S - \widetilde{\partial^\nu \tau_i^S}, \\
\partial^\lambda \tilde{\tau}_i^S &= \widetilde{\partial^\lambda \tau_i^S}.
\end{aligned}$$

The Greek letters ν and λ are intended as mnemonics for "norm" and "length" respectively, and as with graphs a tilde over a chain τ means each cell τ_i^S in τ should be replaced with $\tilde{\tau}_i^S$. The linear combinations $\partial^\nu \tau_i^S$, $\partial^\nu \tilde{\tau}_i^S$ can be recognised as $\partial \sigma^S$, $\partial \tilde{\sigma}^S$ with each σ replaced by τ_i, and it follows that ∂^ν is a boundary operator. It is a consequence of the boundary calculation below with X specialised to S^2 that ∂^λ is a boundary operator as well, and that these two operators commute.

For the third contribution to the boundary of $\tilde{\tau}_i^S$ we identify ∂D^2 with Γ_1, sending v to -1 and giving ∂D^2 the anti-clockwise orientation. Writing $w_i\colon \Gamma_1 \to \Gamma_n$ for the attaching map of f_i, there are chain maps $(\exp_j w_i)_\sharp$ and we define

$$\partial^\gamma \tau_i^S = \tau_i^{S|_{[\ell-1]}} \cup (\exp_{s_\ell} w_i)_\sharp \sigma^{s_\ell},$$
$$\partial^\gamma \tilde{\tau}_i^S = \widetilde{\partial^\gamma \tau_i^S}.$$

Then:

Theorem 4.7. *The boundary of $\tilde{\tau}_i^S$ is given by*

$$\partial \tilde{\tau}_i^S = \partial^\nu \tilde{\tau}_i^S + (-1)^{|S|} \partial^\lambda \tilde{\tau}_i^S + (-1)^{|S|+\ell-1} \partial^\gamma \tilde{\tau}_i^S.$$

Proof. The cell $\tilde{\tau}_i^S$ is a map from the ball $\tilde{\Delta}_{s_1} \times \cdots \times \tilde{\Delta}_{s_\ell} \times \tilde{\Delta}_\ell$ and as before we consider the effect of replacing an inequality with an equality in a simplex in this product. There are two main cases, the simplices $\tilde{\Delta}_{s_a}$ and $\tilde{\Delta}_\ell$, and each breaks into further cases according to whether the equality occurs in the first, last, or an inner position. Four of the possibilities are illustrated in figure 4.3.

Replacing the first or last inequality in $\tilde{\Delta}_{s_a}$ sends a point in the interior of I^2 onto the top or bottom edge of the square, as shown in figure 4.3(i). Since both of these edges map to v in X each case gives a point in $\tau_i^{\partial_a(S)}$, dropping dimension by one, unless $s_a = 1$ in which case it gives a point in $\tau_i^{S|_{[\ell]\setminus\{a\}}}$, dropping dimension by two. A generic point in $\tau_i^{\partial_a(S)}$ is hit once by each face, and as was the case with graphs these contributions come with opposite signs if s_a is odd and matching signs if s_a is even, the sign negative if $a = 1$.

Replacing an inner inequality in $\tilde{\Delta}_{s_a}$ merges two points with the same x co-ordinate, giving a point in $\tilde{\tau}_i^{\partial_a(S)}$ as shown in figure 4.3(ii). A generic point in this cell is hit $s_a - 1$ times, once for each inequality, and as was the case with graphs these contributions alternate in sign. They therefore cancel if s_a is odd and leave one over if s_a is even, the leftover sign being positive if $a = 1$. Putting these together with the contributions to $\tau_i^{\partial_a(S)}$ from the previous paragraph we get the $\partial^\nu \tilde{\tau}_i^S$ term in $\partial \tilde{\tau}_i^S$.

We now look at the contributions to the boundary from $\tilde{\Delta}_\ell$. Replacing the first inequality with an equality moves the entire first column of points onto the left edge of the square, which maps to v in X. Thus this face maps onto $\tau_i^{S|_{[\ell]\setminus\{1\}}}$, dropping dimension by at least two and so contributing nothing to $\partial \tilde{\tau}_i^S$.

Replacing the ath inner inequality merges the ath and $(a+1)$th columns of points, giving a point in $\tilde{\tau}_i^{\mu_a(S)}$ as shown in figure 4.3(iii). Generic points in this cell are each hit

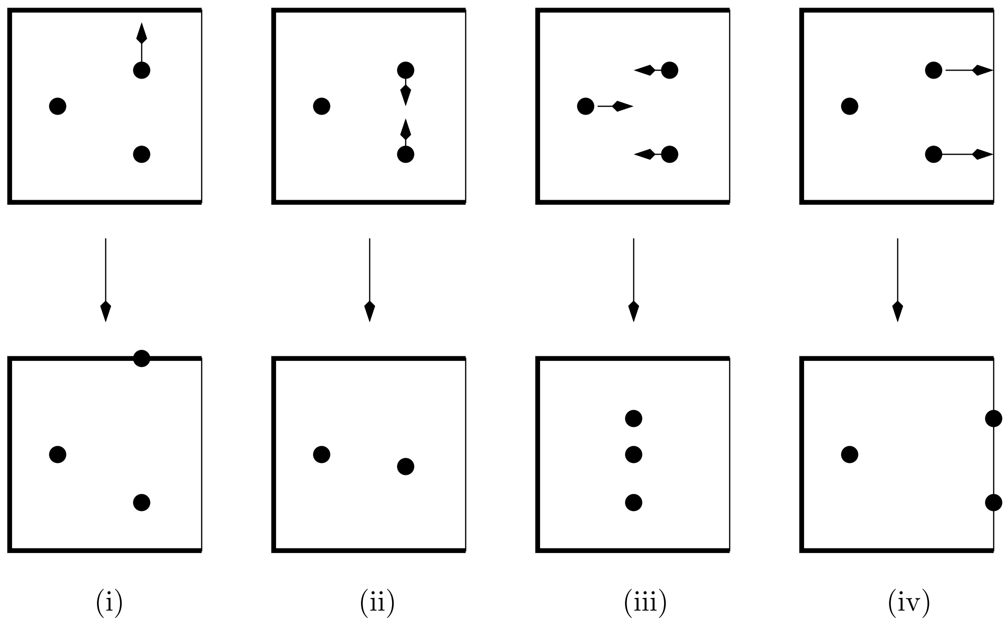

Figure 4.3: Some cells in the boundary of $\tilde{\tau}^{(1,2)}$. (i) Moving a point onto the top or bottom edge gives a set lying in $\tau^{(1,1)}$ (illustrated) or $\tau^{(2)}$ (not shown). (ii) Moving two points with the same x co-ordinate into co-incidence gives a point in $\tilde{\tau}^{(1,1)}$. (iii) Equating distinct x co-ordinates merges two columns, giving a point in $\tilde{\tau}^{(3)}$, and (iv) moving the rightmost column onto the boundary gives a point in $\tilde{\tau}^{(1)} \cup \tilde{\sigma}^2$.

$\binom{s_a+s_{a+1}}{s_a}$ times, once for each choice of s_a points to come from the left, and counting these with signs gives the (-1)–binomial co-efficient $\begin{bmatrix} s_a+s_{a+1} \\ s_a \end{bmatrix}_{-1}$. Collecting these contributions together gives the $\partial^\lambda \tilde{\tau}_i^S$ term in $\partial \tilde{\tau}_i^S$.

Finally, we look at the contribution to the boundary from the last face of $\tilde{\Delta}_\ell$, which moves the last column of points onto the right edge of the square, as shown in figure 4.3(iv). The points left in the interior of the square lie in the cell $\tilde{\tau}_i^{S|_{[\ell-1]}}$, which has dimension $|S| + \ell - s_\ell - 1$, and the points on the boundary lie in some cell σ^J or $\tilde{\sigma}^J$ of $\exp_{s_\ell}\Gamma_n$, which has dimension s_ℓ. Thus this face maps onto cells of smaller dimensions also. The signed sum of the dimension s_ℓ cells hit in $\exp_{s_\ell}\Gamma_n$ is given by $(\exp_{s_\ell} w_i)_\sharp \tilde{\sigma}^{s_\ell}$, and we get the $\partial^\gamma \tilde{\tau}_i^S$ term of $\partial \tilde{\tau}_i^S$. □

The boundary map ∂^λ can be simplified by choosing a suitable basis for the chain groups over $\mathbf{Q}$, at the expense of making ∂^ν mildly more complicated. Recalling from section 3.3 that the (-1)–binomial co-efficient $\begin{bmatrix} m \\ r \end{bmatrix}_{-1}$ is given by

$$\begin{bmatrix} m \\ r \end{bmatrix}_{-1} = \frac{1 + (-1)^{r(m-r)}}{2} \binom{\lfloor m/2 \rfloor}{\lfloor r/2 \rfloor}$$

we let

$$\tau_{\mathbf{Q}}^S = (\lfloor s_1/2 \rfloor! \cdots \lfloor s_\ell/2 \rfloor!)\tau^S.$$

Then

$$\begin{bmatrix} s_a + s_{a+1} \\ s_a \end{bmatrix}_{-1} \tau_{\mathbf{Q}}^{\mu_a(S)} = \frac{1+(-1)^{s_a s_{a+1}}}{2} \frac{\lfloor (s_a+s_{a+1})/2 \rfloor !}{\lfloor s_a/2 \rfloor ! \lfloor s_{a+1}/2 \rfloor !} (\lfloor s_1/2 \rfloor ! \cdots \lfloor s_\ell/2 \rfloor !) \tau^{\mu_a(S)}$$
$$= \frac{1+(-1)^{s_a s_{a+1}}}{2} \tau_{\mathbf{Q}}^{\mu_a(S)},$$

so that with respect to this basis we have

$$\partial^\lambda \tau_{\mathbf{Q}}^S = \sum_{a=1}^{\ell(S)-1} \frac{1+(-1)^{s_a s_{a+1}}}{2} (-1)^{(a-1)} \tau_{\mathbf{Q}}^{\mu_a(S)}. \tag{4.2.4}$$

This simplification comes at the small price of adding a factor of $\lfloor s_a/2 \rfloor$ to the ath term of ∂^ν when s_a is even, giving

$$\partial^\nu \tau_{\mathbf{Q}}^S = -\sum_{a=1}^{\ell(S)} \frac{1+(-1)^{s_a}}{4} (-1)^{\left|S|_{[a-1]}\right|} s_a \tau_{\mathbf{Q}}^{\partial_a(s)}.$$

This mild complication in ∂^ν is of no concern to us, since our main application of (4.2.4) will be in calculating the rational homology of $\exp_k(S^2, *)/\exp_{k-1}(S^2, *)$, where the boundary map consists only of ∂^λ. We note further that $\tau_{\mathbf{Q}}^S = \tau^S$ if each entry of S is at most three.

4.2.4 Higher dimensions

We make a brief digression on constructing lexicographic cell structures for the finite subset spaces of higher dimensional complexes. As was the case with 2–complexes, the lexicographic ordering on I^n may be used to construct an open cell decomposition of $\exp_j(\operatorname{int} I^n)$, and we might hope to use this to build a cell structure for $\exp_k X$ by taking products over cells of X as before. However, ensuring that boundaries decrease dimension under this scheme appears to require compatibility between the ordering on the interior of a cell and the orderings on cells in its boundary. This condition comes for free in the case of 2–complexes or wedges of spheres but appears to require orchestration in general.

To each lexicographically ordered sequence $p_1, \dots, p_j$ of j points in the interior of I^n we associate a $(j-1)$–tuple of integers by setting $j_i = m-1$ if p_i and p_{i+1} are distinguished by their mth co-ordinate but not their $(m-1)$th. This $(j-1)$–tuple describes the dependencies among the co-ordinates of the p_i and as before we consider the collection of lexicographically ordered subsets corresponding to a fixed tuple J. This is easily seen to be parameterised by an open ball of dimension $nj - |J|$, a product of open simplices of the form $\operatorname{int} \tilde{\Delta}_a$, and this gives an open cell decomposition of $\exp_j(\operatorname{int} I^n)$. We again transfer this to $\exp_j(\operatorname{int} B^n)$ by collapsing the entire boundary to a point, with the exception of the sole face $x = 1$; the purpose of this is to avoid constraints between points in the interior and points on the boundary which would otherwise arise along faces of the form shown in figure 4.3(i).

To illustrate the compatibility requirement let $n = 3$ and give the face $x = 1$ the reverse lexicographic ordering

$$(1, y_1, z_1) \prec (1, y_2, z_2) \qquad \text{if } z_1 < z_2, \text{ or if } z_1 = z_2 \text{ and } y_1 < y_2.$$

Three element subsets of $\operatorname{int} I^3$ corresponding to the 2–tuple $(2,2)$ satisfy $x_1 = x_2 = x_3$, $y_1 = y_2 = y_3$ and $z_1 < z_2 < z_3$, and are parameterised by the open 5–ball $\operatorname{int}(I \times I \times \tilde{\Delta}_3)$. Pushing them onto the boundary we obtain subsets corresponding to the partition $(1,1,1)$, the 2–tuple $(0,0)$ in the labeling used here. This is parameterised by the open 6–ball $\operatorname{int}(I^3 \times \tilde{\Delta}_3)$, showing that dimensions can jump if the ordering on the boundary does not agree with that coming from the interior.

4.3 The two-sphere

4.3.1 Introduction

We now use the lexicographic cell structures developed in the previous section to study the finite subset spaces of the two-sphere. We use the standard cell structure for S^2 with a single two-cell, and to avoid clutter we will simply write S and $\tilde{S}$ for τ^S and $\tilde{\tau}^S$ respectively. Where the partition is written out explicitly we will use round brackets for τ^S and square brackets for $\tilde{\tau}^S$.

We begin in section 4.3.2 by describing the chain complexes of $\exp_k(S^2,*)$ and $\exp_k S^2$ and justifying the assertion of section 4.2.3 that ∂^λ and ∂^ν are commuting boundary operators. We look at the finite subset spaces of S^2 for several small values of k in section 4.3.3, and then prove Theorems 4.1 and 4.2 in section 4.3.4. The arguments bear a striking resemblance to those used to calculate the homology of $\exp_k \Gamma_n$. The based space $\exp_k(S^2,*)$ again plays a prominent role, being easier to understand and having cleaner results, and we make use of the exact sequences of the pairs $(\exp_k(S^2,*), \exp_{k-1}(S^2,*))$ and $(\exp_k S^2, \exp_k(S^2,*))$. The main step is the calculation of $H_*(\exp_k(S^2,*)/\exp_{k-1}(S^2,*); \mathbf{Q})$. This involves the study of a combinatorially defined finite complex which may be recognised as the $(k-2)$–cube complex with some signs changed and certain edges "clipped".

4.3.2 The chain complexes

By Theorem 4.6 $\exp_k(S^2,*)$ has a cell structure with a single vertex in which the remaining cells are in one-to-one correspondence with the ordered partitions of the positive integers $j \leq k-1$, and $\exp_k S^2$ has a cell structure obtained by adding additional cells corresponding to the ordered partitions of $j \leq k$. Let $\mathcal{S}_{\ell,j}$ and $\tilde{\mathcal{S}}_{\ell,j}$ be two copies of the free abelian group of rank $\binom{j-1}{\ell-1}$ generated by the ordered partitions of j of length ℓ. Each generator corresponds to a cell of dimension $j+\ell$ and we note that ∂^ν and ∂^λ map $\mathcal{S}_{\ell,j}$, $\tilde{\mathcal{S}}_{\ell,j}$ to $\mathcal{S}_{\ell,j-1}$, $\mathcal{S}_{\ell,j-1} \oplus \tilde{\mathcal{S}}_{\ell,j-1}$ and $\mathcal{S}_{\ell-1,j}$, $\mathcal{S}_{\ell-1,j} \oplus \tilde{\mathcal{S}}_{\ell-1,j}$ respectively. Since the boundary map is given by $\partial = \partial^\nu + (-1)^j \partial^\lambda$ it follows that the cellular chain groups of $\exp_k(S^2,*)$ and $\exp_k S^2$ may be arranged into double complexes with cell counts as shown in figure 4.4, and that $\partial^\nu, \partial^\lambda$ are commuting boundary operators as claimed. Moreover, we see immediately that for $k \geq 2$ we have $\chi(\exp_k(S^2,*)) = 2$ and $\chi(\exp_k S^2) = 3$.

In working with these complexes we will focus mainly on the chain complexes $(\mathcal{S}_{*,j}, \partial^\lambda)$ consisting of a single row and arising from the spaces $\exp_{j+1}(S^2,*)/\exp_j(S^2,*)$. The (-1)–binomial co-efficients appearing in ∂^λ will be extraneous to our purpose so for clarity we will use the simplified boundary map (4.2.4), which we recall comes from using

$j \backslash \ell$	0	1	2	3	4
4		1	3	3	1
3		1	2	1	
2		1	1		
1		1			
0	1				

$j \backslash \ell$	0	1	2	3	4	5
5		1	4	6	4	1
4		2	6	6	2	
3		2	4	2		
2		2	2			
1		2				
0	1					

Figure 4.4: Cell counts for $\exp_5(S^2,*)$ and $\exp_5 S^2$. Left: Cells of $\exp_k(S^2,*)$ may be arranged into a double complex with $\binom{j-1}{\ell-1}$ cells in position (ℓ, j), $1 \leq \ell \leq j \leq k-1$, and one in position $(0,0)$. Since the alternating sum along a row of Pascal's triangle is zero we see immediately that $\chi(\exp_k(S^2,*)) = 2$ for $k \geq 2$. Right: Adding cells to get $\exp_k S^2$ doubles all rows other than the bottom one and adds an extra row of Pascal's triangle on top, giving $\chi(\exp_k S^2) = 3$ for $k \geq 2$.

bases for $\mathcal{S}_{\ell,j}$ obtained by individually scaling each cell. Abusing notation we write (4.2.4) as

$$\partial^{\lambda}_{\mathbf{Q}} S = \sum_{a=1}^{\ell} \frac{1+(-1)^{s_a s_{a+1}}}{2} (-1)^{(a-1)} \mu_a(S).$$

By analogy with the cube complex of section 3.2.3 we call the complex $(\mathcal{S}_{*,j}, \partial^{\lambda}_{\mathbf{Q}})$ the "clipped cube complex", as the lattice of partitions of j, graded by length and partially ordered by refinement, forms a $(j-1)$–dimensional cube, and the boundary of S is again a linear combination of its neighbours of smaller degree. The adjective comes from the fact that $\partial^{\lambda}_{\mathbf{Q}} S$ omits the partitions obtained from S by amalgamating adjacent parts of odd size, so that these edges may be regarded as removed or "clipped". This is illustrated in figure 4.5, which should be compared with figure 3.3 on page 35. We note that ∂^{λ} and $\partial^{\lambda}_{\mathbf{Q}}$ co-incide if each entry of S and $\mu_a(S)$ have size at most three, which holds for the top two chain groups of the complex. We will use this fact to calculate the top integral homology groups of $\exp_k(S^2,*)$ and $\exp_k S^2$. The distinction between ∂^{λ} and $\partial^{\lambda}_{\mathbf{Q}}$ occurs for the first time in the three dimensional clipped cube complex and can be seen in figure 4.5.

An understanding of the clipped cube complex allows us to calculate the rational homology of $\exp_k(S^2,*)$ inductively, and we pass to an understanding of $\exp_k S^2$ using the long exact sequence of the pair $(\exp_k S^2, \exp_k(S^2,*))$. Our tool in doing so is the observation that the natural correspondence $\tilde{S} \leftrightarrow S$ between the tilded cells of $\exp_k S^2$ and the cells of $\exp_{k+1}(S^2,*)$ has the following algebraic consequence:

Lemma 4.1. *The spaces* $\exp_{k+1}(S^2,*)$ *and* $\exp_k S^2 / \exp_k(S^2,*)$ *have the same homology.*

Proof. Comparing $\exp_{k+1}(S^2,*)$ with the quotient space $\exp_k S^2 / \exp_k(S^2,*)$ we see that one has a cell structure consisting of a single vertex, cells S satisfying $|S| \leq k$, and boundary map

$$\partial S = \partial^{\nu} S + (-1)^{|S|} \partial^{\lambda} S,$$

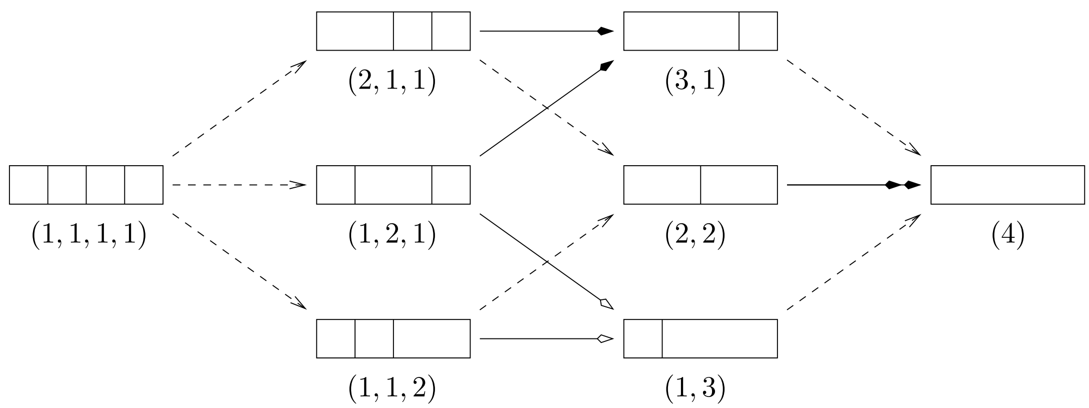

Figure 4.5: The clipped cube complex; compare with figure 3.3, regarding the vertical dividing bars as the set $\{1, 2, 3\}$. The lattice of partitions of 4 forms a 3–dimensional cube, and the boundary of S is a signed sum of its neighbours with fewer parts, omitting those obtained by amalgamating adjacent parts of odd size. As in figure 3.3 positive terms are indicated by solid arrowheads and negative terms by empty arrowheads, and the omitted terms (the "clipped" edges) are shown by dotted arrows. The double-headed arrow from $(2, 2)$ to (4) shows where $\partial^\lambda_{\mathbf{Q}}$ differs from ∂^λ, as $\partial^\lambda(2, 2) = 2(4)$ but $\partial^\lambda_{\mathbf{Q}}(2, 2) = (4)$. We see that the homology of the clipped cube complex is 0 in dimensions 1 and 2 and $\mathbf{Z}$ in dimensions 3 and 4, generated by $(2, 1, 1) - (1, 2, 1) + (1, 1, 2)$ and $(1, 1, 1, 1)$ respectively, and that $\exp_5(S^2, *)/\exp_4(S^2, *)$ has an additional $\mathbf{Z}/2\mathbf{Z}$ summand generated by (4).

and the second has a cell structure consisting of a single vertex, cells $\tilde{S}$ satisfying $|\tilde{S}| \le k$, and boundary map

$$\partial\tilde{S} = -\widetilde{\partial^\nu S} + (-1)^{|S|}\widetilde{\partial^\lambda S}.$$

To account for the minus sign in the first term of the second map we twist the natural correspondence $\tilde{S} \leftrightarrow S$ by $(-1)^{|S|}$, obtaining an (algebraically defined) map $S \mapsto (-1)^{|S|}\tilde{S}$ inducing an isomorphism of chain complexes. □

We emphasise the fact that we have proved this result algebraically, not topologically. The set map

$$\exp_{k+1}(S^2, *) \setminus \{\{*\}\} \to \exp_k S^2/\exp_k(S^2, *) : \Lambda \mapsto \Lambda \setminus \{*\}$$

is discontinuous at each Λ of size k or less, and the map

$$\exp_k S^2 \to \exp_{k+1}(S^2, *) : \Lambda \mapsto \Lambda \cup \{*\}$$

does not descend to a continuous map on the quotient $\exp_k S^2/\exp_k(S^2, *)$.

4.3.3 Small values of k

In this section we calculate the homology of $\exp_k(S^2, *)$ and $\exp_k S^2$ for several small values of k. Our aim is both to build familiarity with the chain complexes and to show by example that Theorem 4.2 does not give the full story on the integral homology of $\exp_k S^2$.

Since $\exp_1 S^2$ and $\exp_2(S^2, *)$ are both simply S^2 with its standard cell structure we begin with $\exp_2 S^2$ and $\exp_3(S^2, *)$. The lexicographic cell structure for $\exp_2 S^2$ has one cell $[1,1]$ in dimension four, one cell $[2]$ in dimension three, two cells $[1]$ and (1) in dimension two, no cells in dimension one and a single vertex. The chain complex is

$$0 \longrightarrow \mathbf{Z} \xrightarrow{0} \mathbf{Z} \xrightarrow{\left[\begin{smallmatrix}1\\-2\end{smallmatrix}\right]} \mathbf{Z} \oplus \mathbf{Z} \longrightarrow 0 \longrightarrow \mathbf{Z} \longrightarrow 0,$$

and the homology is clearly

$$H_i(\exp_2 S^2) = \begin{cases} \mathbf{Z} & i = 0, 2, 4, \\ 0 & \text{else.} \end{cases}$$

Mapping $\exp_2 S^2$ to $\exp_3(S^2, *)$ by adding the vertex $*$ to each set rounds the brackets on the cells $[1,1]$, $[2]$ and $[1]$, giving the chain complex

$$0 \longrightarrow \mathbf{Z} \xrightarrow{0} \mathbf{Z} \xrightarrow{-1} \mathbf{Z} \longrightarrow 0 \longrightarrow \mathbf{Z} \longrightarrow 0$$

with homology

$$H_i(\exp_3(S^2, *)) = \begin{cases} \mathbf{Z} & i = 0, 4, \\ 0 & \text{else.} \end{cases} \tag{4.3.1}$$

Geometrically, $\exp_2 S^2 = \mathrm{Sym}^2 S^2 = \mathrm{Sym}^2 \mathbf{C}P^1$ may be identified with $\mathbf{C}P^2$ via the map

$$\big\{[z_0, w_0], [z_1, w_1]\big\} \mapsto [z_0 z_1, -(z_0 w_1 + z_1 w_0), w_0 w_1],$$

where the co-ordinates of the righthand side are the co-efficients $[a, b, c]$ of the homogeneous quadratic $(z_0 W - w_0 Z)(z_1 W - w_1 Z)$ vanishing at $[z_0, w_0]$ and $[z_1, w_1]$. In this picture the quotient map $\exp_2 S^2 \xrightarrow{\cup\{*\}} \exp_3(S^2, *)$ induces the equivalence relation $[z^2, -2zw, w^2] \sim [z, -w, 0]$, identifying the degree two curve $b^2 - 4ac = 0$ with the degree one curve $a + b = 0$. As seen in (4.3.1) this kills the second homology and the resulting space $\exp_3(S^2, *)$ is homotopy equivalent to S^4.

To calculate the homology of $\exp_4(S^2, *)$ and $\exp_3 S^2$ we start with the clipped cube complex

$$\begin{array}{ccc} (1,1,1) & \xrightarrow{\quad 0 \quad} & (2,1) \\ \big\downarrow{\scriptstyle 0} & & \big\downarrow{\scriptstyle 1} \\ (1,2) & \xrightarrow{\quad 1 \quad} & (3) \end{array} .$$

This has homology groups $\mathbf{Z}$ in the top and middle dimensions, generated by $(1,1,1)$ and $(2,1) - (1,2)$ respectively, so

$$\tilde{H}_i(\exp_4(S^2, *)/\exp_3(S^2, *)) = \begin{cases} \mathbf{Z} & i = 5, 6, \\ 0 & \text{else.} \end{cases}$$

The long exact sequence of the pair $(\exp_4(S^2, *), \exp_3(S^2, *))$ then gives

$$0 \longrightarrow \tilde{H}_6(\exp_4(S^2, *)) \longrightarrow \tilde{H}_6(\exp_4(S^2, *)/\exp_3(S^2, *)) \longrightarrow 0$$

and

$$0 \longrightarrow \tilde{H}_5(\exp_4(S^2,*)) \longrightarrow \mathbf{Z} \xrightarrow{\partial} \mathbf{Z} \longrightarrow \tilde{H}_4(\exp_4(S^2,*)) \longrightarrow 0, \tag{4.3.2}$$

the remaining segments having the form $0 \longrightarrow \tilde{H}_i(\exp_4(S^2,*)) \longrightarrow 0$. The boundary map $\partial\colon \tilde{H}_5(\exp_4(S^2,*)/\exp_3(S^2,*)) \to \tilde{H}_4(\exp_3(S^2,*))$ is ∂^ν which sends $(2,1)-(1,2)$ to $-2(1,1)$, so the middle map in (4.3.2) is multiplication by -2. Hence

$$\tilde{H}_i(\exp_4(S^2,*)) = \begin{cases} \mathbf{Z} & i=6, \\ \mathbf{Z}/2\mathbf{Z} & i=4, \\ 0 & \text{else,} \end{cases}$$

in which the nontrivial groups are generated by $(1,1,1)$ and $(1,1)$ respectively.

We now use Lemma 4.1 and the exact sequence of the pair $(\exp_3 S^2, \exp_3(S^2,*))$ to calculate the homology of $\exp_3 S^2$. The segments where $\tilde{H}(\exp_3 S^2)$ is not bracketed by zeroes are

$$0 \longrightarrow \tilde{H}_6(\exp_3 S^2) \longrightarrow \tilde{H}_6(\exp_3 S^2/\exp_3(S^2,*)) \longrightarrow 0,$$

giving $\tilde{H}_6(\exp_3 S^2) \cong \mathbf{Z}$ generated by $[1,1,1]$, and

$$0 \longrightarrow \mathbf{Z} \longrightarrow \tilde{H}_4(\exp_3 S^2) \longrightarrow \mathbf{Z}/2\mathbf{Z} \longrightarrow 0.$$

To see that this second sequence splits consider the cycle $[1,1]-2(1,1)$. Under the right arrow this maps to the generator $[1,1]$ of $\tilde{H}_4(\exp_3 S^2/\exp_3(S^2,*))$, and the fact that the boundary of $[2,1]-[1,2]$ is $2([1,1]-2(1,1))$ shows it has order two. Hence

$$\tilde{H}_i(\exp_3 S^2) = \begin{cases} \mathbf{Z} & i=6, \\ \mathbf{Z}\oplus\mathbf{Z}/2\mathbf{Z} & i=4, \\ 0 & \text{else,} \end{cases}$$

with generators $[1,1,1]$ in dimension six and $[1,1]$ and $(1,1)$ in dimension four. Using the universal co-efficient theorem we see that this result agrees with the $g=0$ case of Theorem 4.5.

From figure 4.5 the homology of $\exp_5(S^2,*)/\exp_4(S^2,*)$ is $\mathbf{Z}$ in dimensions seven and eight and $\mathbf{Z}/2\mathbf{Z}$ in dimension five. The long exact sequence of $(\exp_5(S^2,*), \exp_4(S^2,*))$ has two nontrivial segments

$$0 \longrightarrow \tilde{H}_8(\exp_5(S^2,*)) \longrightarrow \tilde{H}_8(\exp_5(S^2,*)/\exp_4(S^2,*)) \longrightarrow 0$$

and

$$0 \longrightarrow \tilde{H}_7(\exp_5(S^2,*)) \longrightarrow \mathbf{Z} \xrightarrow{\partial} \mathbf{Z} \longrightarrow \tilde{H}_6(\exp_5(S^2,*)) \longrightarrow 0$$

as above, and an additional nontrivial segment

$$0 \longrightarrow \tilde{H}_5(\exp_5(S^2,*)) \longrightarrow \mathbf{Z}/2\mathbf{Z} \xrightarrow{\partial} \mathbf{Z}/2\mathbf{Z} \longrightarrow \tilde{H}_4(\exp_5(S^2,*)) \longrightarrow 0.$$

The first boundary map sends the generator $(2,1,1)-(1,2,1)+(1,1,2)$ to $-3(1,1,1)$, inducing multiplication by -3, and the second sends the generator (4) to $-(3)$. Since

$$\begin{array}{ccccc} & & (3,1,1) & & \\ & (2,1,1,1) & (1,3,1) & (4,1) & \\ & (1,2,1,1) & (1,1,3) & (1,4) & \\ (1,1,1,1,1) & (1,1,2,1) & (2,2,1) & (3,2) & (5) \\ & (1,1,1,2) & (1,2,2) & (2,3) & \\ & & (2,1,2) & & \end{array}$$

Figure 4.6: Generators of the four dimensional clipped cube complex.

$\partial(2,1) = -(1,1) - (3)$ the second map is an isomorphism and

$$\tilde{H}_i(\exp_5(S^2,*)) = \begin{cases} \mathbf{Z} & i = 8, \\ \mathbf{Z}/3\mathbf{Z} & i = 6, \\ 0 & \text{else.} \end{cases}$$

Again using Lemma 4.1 and the exact sequence of $(\exp_4 S^2, \exp_4(S^2,*))$ we get

$$\begin{gathered} 0 \longrightarrow \tilde{H}_8(\exp_4 S^2) \longrightarrow \tilde{H}_8(\exp_4 S^2/\exp_4(S^2,*)) \longrightarrow 0, \\ 0 \longrightarrow \mathbf{Z} \longrightarrow \tilde{H}_6(\exp_4 S^2) \longrightarrow \mathbf{Z}/3\mathbf{Z} \longrightarrow 0, \end{gathered} \tag{4.3.3}$$

and

$$0 \longrightarrow \mathbf{Z}/2\mathbf{Z} \longrightarrow \tilde{H}_4(\exp_4 S^2) \longrightarrow 0.$$

The 6–cycle $[1,1,1] - 2(1,1,1)$ maps to the generator of the $\mathbf{Z}/3\mathbf{Z}$ term and three times it is the boundary of $[2,1,1] - [1,2,1] + [1,1,2]$, so the second sequence splits and

$$\tilde{H}_i(\exp_4 S^2) = \begin{cases} \mathbf{Z} & i = 8, \\ \mathbf{Z} \oplus \mathbf{Z}/3\mathbf{Z} & i = 6, \\ \mathbf{Z}/2\mathbf{Z} & i = 4, \\ 0 & \text{else.} \end{cases}$$

We calculate one more example to show that the torsion becomes increasingly complicated as k increases. The example will require understanding the four dimensional clipped cube complex, shown in figure 4.6, and will further illustrate the ideas used in the general case.

As always, the boundary of a generator with all entries odd is zero, so we may consider the restriction of the boundary ∂^λ to the span of the generators with one or more even entries. Moreover, the boundaries of $(2,1,1,1)$ and its permutations lie in the span of

$(3,1,1)$ and its permutations, so we may regard ∂_4^λ as a map to this subspace. With these conventions and the bases ordered as shown the matrices of the boundary maps are

$$\partial_4^\lambda = \begin{bmatrix} 1 & 1 & 0 & 0 \\ 0 & -1 & -1 & 0 \\ 0 & 0 & 1 & 1 \end{bmatrix}, \qquad \partial_3^\lambda = \begin{bmatrix} 2 & 0 & 0 \\ 0 & -2 & 0 \\ 0 & 1 & 1 \\ -1 & 0 & -1 \end{bmatrix}, \qquad \partial_2^\lambda = \begin{bmatrix} 1 \\ 1 \\ 2 \\ 2 \end{bmatrix}.$$

Clearly, both ∂_4^λ and ∂_2^λ are surjective and ∂_3^λ is injective. The kernel of ∂_2^λ is equal to $\{2x+2y+z+w=0\}$ and by choosing a suitable basis for this subspace it can be seen that the image of ∂_3^λ has index two. In the now familiar pattern the long exact sequence of the pair $(\exp_6(S^2,*), \exp_5(S^2,*))$ gives

$$0 \longrightarrow \tilde{H}_{10}(\exp_6(S^2,*)) \longrightarrow \tilde{H}_{10}(\exp_6(S^2,*)/\exp_5(S^2,*)) \longrightarrow 0,$$
$$0 \longrightarrow \tilde{H}_9(\exp_6(S^2,*)) \longrightarrow \mathbf{Z} \xrightarrow{\partial} \mathbf{Z} \longrightarrow \tilde{H}_8(\exp_6(S^2,*)) \longrightarrow 0,$$

and an additional segment

$$0 \longrightarrow \tilde{H}_7(\exp_6(S^2,*)) \longrightarrow \mathbf{Z}/2\mathbf{Z} \xrightarrow{\partial} \mathbf{Z}/3\mathbf{Z} \longrightarrow \tilde{H}_6(\exp_6(S^2,*)) \longrightarrow 0.$$

The boundary map in the third sequence is necessarily zero and the boundary map in the second sequence takes the generator $(2,1,1,1)-(1,2,1,1)+(1,1,2,1)-(1,1,1,2)$ to $-4(1,1,1,1)$. Hence

$$\tilde{H}_i(\exp_6(S^2,*)) = \begin{cases} \mathbf{Z} & i=10, \\ \mathbf{Z}/4\mathbf{Z} & i=8, \\ \mathbf{Z}/2\mathbf{Z} & i=7, \\ \mathbf{Z}/3\mathbf{Z} & i=6, \\ 0 & \text{else.} \end{cases}$$

Finally, from the long exact sequence of the pair $(\exp_5 S^2, \exp_5(S^2,*))$ we extract $\tilde{H}_{10}(\exp_5 S^2) \cong \mathbf{Z}$, $\tilde{H}_7(\exp_5 S^2) \cong \mathbf{Z}/2\mathbf{Z}$, and two short exact sequences

$$0 \longrightarrow \mathbf{Z} \longrightarrow \tilde{H}_8(\exp_5 S^2) \longrightarrow \mathbf{Z}/4\mathbf{Z} \longrightarrow 0,$$
$$0 \longrightarrow \mathbf{Z}/3\mathbf{Z} \longrightarrow \tilde{H}_6(\exp_5 S^2) \longrightarrow \mathbf{Z}/3\mathbf{Z} \longrightarrow 0.$$

As usual the first is split by $[1,1,1,1]-2(1,1,1,1)$, and as in (4.3.3) the second is split by $[1,1,1]-2(1,1,1)$. Hence

$$\tilde{H}_i(\exp_5 S^2) = \begin{cases} \mathbf{Z} & i=10, \\ \mathbf{Z} \oplus \mathbf{Z}/4\mathbf{Z} & i=8, \\ \mathbf{Z}/2\mathbf{Z} & i=7, \\ \mathbf{Z}/3\mathbf{Z} \oplus \mathbf{Z}/3\mathbf{Z} & i=6, \\ 0 & \text{else.} \end{cases}$$

4.3.4 The general case

We now turn to the general case. As we have seen, the integral homology of $\exp_k S^2$ becomes increasingly complicated, with more and more torsion arising as k increases. We therefore give a full answer only with respect to rational co-efficients, where the situation is much cleaner, and limit ourselves to calculating only the top three integral groups. Not only are these groups computationally tractable but they also exhibit great regularity.

We begin by calculating the homology of the clipped cube complex. We will be working mainly with the top end, where the partitions consist mostly of ones, and for compactness of notation we write $\mathsf{1}(k)$ for the partition $(1,\dots,1)$ of k as a sum of k ones, or just $\mathsf{1}$ if k is understood. We write $\mathsf{2}_i(k)$ for the partition $(1,\dots,2,\dots,1)$ with a single 2 occurring in the ith place, and write $\mathsf{3}_i$, $\mathsf{4}_i$ for the analogous partition with a single 3 or 4. By extension, we write $\mathsf{2}_i\mathsf{3}_j$ for the partition with a 2 in the ith place, a 3 in the jth place, and the remaining entries ones. With these conventions, the top four chain groups of the clipped cube complex may be written

$$\begin{aligned}
\mathcal{S}_{k,k} &= \operatorname{span}\{\mathsf{1}\},\\
\mathcal{S}_{k-1,k} &= \operatorname{span}\{\mathsf{2}_i | 1 \le i \le k-1\},\\
\mathcal{S}_{k-2,k} &= \operatorname{span}\{\mathsf{3}_i | 1 \le i \le k-2\} \oplus \operatorname{span}\{\mathsf{2}_i\mathsf{2}_j | 1 \le i < j \le k-2\},\\
\mathcal{S}_{k-3,k} &= \operatorname{span}\{\mathsf{4}_i | 1 \le i \le k-3\} \oplus \operatorname{span}\{\mathsf{2}_i\mathsf{3}_j | i \ne j, 1 \le i,j \le k-3\}\\
&\qquad \oplus \operatorname{span}\{\mathsf{2}_i\mathsf{2}_j\mathsf{2}_m | 1 \le i < j < m \le k-3\}.
\end{aligned}$$

Fortunately, there will be no need to count beyond four or work with juxtapositions of more than two characters.

Since the boundary of $\mathsf{1}$ is zero we see immediately that the kth homology of the clipped cube complex is $\mathbf{Z}$. The group H_{k-1} is calculated almost as easily: the boundary of $\mathsf{2}_i$ is given by

$$\partial \mathsf{2}_i = \begin{cases} \mathsf{3}_1 & i = 1,\\ (-1)^i(\mathsf{3}_{i-1} - \mathsf{3}_i) & 2 \le i \le k-2,\\ \mathsf{3}_{k-2} & i = k-1, \end{cases}$$

and taking alternating sums gives

$$\partial \sum_{i=1}^{j} (-1)^{i-1}\mathsf{2}_i = \begin{cases} \mathsf{3}_j & 1 \le j \le k-2,\\ 0 & j = k-1. \end{cases} \tag{4.3.4}$$

This shows that H_{k-1} is isomorphic to $\mathbf{Z}$ also, with generator $\sum_{i=1}^{k-1}(-1)^{i-1}\mathsf{2}_i$. The remaining homology groups are rather more difficult to calculate and are the subject of the following lemma:

Lemma 4.2. *The clipped cube complex $(\mathcal{S}_{*,k}, \partial^{\lambda}_{\mathbf{Q}})$ is exact over $\mathbf{Q}$ at each $\mathcal{S}_{\ell,k}$, $1 \le \ell \le k-2$, and exact over $\mathbf{Z}$ at $\mathcal{S}_{k-2,k}$.*

Proof. The proof is in two parts: we first prove exactness over $\mathbf{Z}$ at $\mathcal{S}_{k-2,k}$ directly, and then prove exactness at the remaining groups by induction over k, using the result for the clipped cube complexes $(\mathcal{S}_{*,k-1}, \partial^\lambda_{\mathbf{Q}})$ and $(\mathcal{S}_{*,k-2}, \partial^\lambda_{\mathbf{Q}})$. The direct proof of exactness at $\mathcal{S}_{k-2,k}$ is also required to complete the induction step. For simplicity, in what follows we write ∂ for $\partial^\lambda_{\mathbf{Q}}$.

By (4.3.4) the image of ∂_{k-1} is the span of $\{3_i | 1 \le i \le k-2\}$, so to prove exactness at $\mathcal{S}_{k-2,k}$ over $\mathbf{Z}$ it suffices to show that ∂_{k-2} restricted to the span of $\{2_i 2_j | 1 \le i < j \le k-2\}$ is injective. Let U be this span and write $\mathcal{S}_{k-3,k} = V \oplus W$, where

$$\begin{aligned} V &= \operatorname{span}\{4_i | 1 \le i \le k-3\} \oplus \operatorname{span}\{3_i 2_j | 1 \le i < j \le k-3\}, \\ W &= \operatorname{span}\{2_i 3_j | 1 \le i < j \le k-3\} \oplus \operatorname{span}\{2_i 2_j 2_m | 1 \le i < j < m \le k-3\}. \end{aligned}$$

Let $\bar V = (V \oplus W)/W$, and observe that $\operatorname{rank} U = \operatorname{rank} \bar V = \binom{k-2}{2}$. The boundary induces a map $\bar\partial \colon U \to \bar V$, and we claim that with respect to suitable orderings of the bases $\{2_i 2_j | i < j\}$ and $\{4_i\} \cup \{3_i 2_j | i < j\}$ the matrix of $\bar\partial$ is upper triangular.

To see this, lexicographically order each basis according to $(j-i, i)$, where for this purpose we regard 4_i as $3_i 2_i$ and place it in the order as $(0, i)$. The boundary of $2_i 2_j$ is given by

$$\partial 2_i 2_j = \begin{cases} (-1)^i (3_{i-1} 2_i - 4_i + 2_i 3_{i+1}) & j = i+1, \\ (-1)^i (3_{i-1} 2_{j-1} - 3_i 2_{j-1}) + (-1)^j (2_i 3_{j-1} - 2_i 3_j) & j - 1 \ge 2, \end{cases}$$

in which the terms containing 3_{i-1} should be omitted if $i = 1$, and the terms containing 3_j should be omitted if $j = k-2$. Passing to the quotient $\bar V$ we have

$$\bar\partial 2_i 2_j = \begin{cases} (-1)^i (3_{i-1} 2_i - 4_i) & j = i+1, \\ (-1)^i (3_{i-1} 2_{j-1} - 3_i 2_{j-1}) & j - 1 \ge 2, \end{cases}$$

and in each case we see that the least element occurring in $\bar\partial 2_i 2_j$ is the one ordered by $(j-i-1, i)$. This implies that the matrix of $\bar\partial$ is lower triangular with each diagonal entry equal to ± 1, and we conclude that $\bar\partial$ is an isomorphism.

We now show by induction on k that the boundary map has rank $\binom{k-2}{\ell-2}$ at $\mathcal{S}_{\ell,k}$ for each $1 \le \ell \le k-2$. This is easily verified for the cases $k = 3$ and $k = 4$ considered in section 4.3.3 and we use these as the base for the induction. The case $\ell = k-2$ is the one just proved and is required for the inductive step. For $1 \le \ell \le k-3$ we relate $\mathcal{S}_{\ell,k}$ to $\mathcal{S}_{*,k-1}$ and $\mathcal{S}_{*,k-2}$ by examining the size of the last element of each partition. Let

$$\mathcal{S}^i_{\ell,k} = \operatorname{span}\{S | s_\ell = i\}$$

for $i = 1, 2$,

$$\mathcal{S}^3_{\ell,k} = \operatorname{span}\{S | s_\ell \ge 3\},$$

and consider the "append" and "plus" operators

$$A_i(S) = (s_1, \ldots, s_\ell, i)$$

for $i = 1, 2$, and

$$P_2(S) = (s_1, \ldots, s_\ell + 2).$$

We have

$$A_i\colon\ \mathcal{S}_{\ell-1,k-i} \xrightarrow{\cong} \mathcal{S}^i_{\ell,k},$$
$$P_2\colon\ \mathcal{S}_{\ell,k-2} \xrightarrow{\cong} \mathcal{S}^3_{\ell,k},$$

and moreover

$$\partial A_i S \in A_i \partial S + \mathcal{S}^3_{\ell,k}$$

for $i = 1, 2$, and

$$\partial P_2 S = P_2 \partial S \tag{4.3.5}$$

since P_2 does not change the parity of the last entry of S. We note also that (4.3.5) depends on the fact we are using the boundary map $\partial^\lambda_{\mathbf{Q}}$ instead of ∂^λ.

Since $\mathcal{S}_{\ell,k} = \mathcal{S}^1_{\ell,k} \oplus \mathcal{S}^2_{\ell,k} \oplus \mathcal{S}^3_{\ell,k}$ it follows that the matrix of ∂_ℓ can be written in the block form

$$D_{\ell,k} = \begin{bmatrix} D_{\ell-1,k-1} & 0 & 0 \\ 0 & D_{\ell-1,k-2} & 0 \\ E & F & D_{\ell,k-2} \end{bmatrix},$$

in which $D_{i,j}$ is the matrix of ∂ acting on $\mathcal{S}_{i,j}$. Hence

$$\begin{aligned} \operatorname{rank} \partial_\ell &= \operatorname{rank} D_{\ell-1,k-1} + \operatorname{rank} D_{\ell-1,k-2} + \operatorname{rank} D_{\ell,k-2} \\ &= \binom{k-3}{\ell-3} + \binom{k-4}{\ell-3} + \binom{k-4}{\ell-2} \\ &= \binom{k-2}{\ell-2} \end{aligned}$$

as desired.

We complete the proof using a rank argument. We have

$$\begin{aligned} \operatorname{rank} \ker \partial_\ell &= \operatorname{rank} \mathcal{S}_{\ell,k} - \operatorname{rank} \partial_\ell \\ &= \binom{k-1}{\ell-1} - \binom{k-2}{\ell-2} \\ &= \binom{k-2}{\ell-1} \\ &= \operatorname{rank} \partial_{\ell+1}, \end{aligned}$$

from which the result follows. □

Since $\partial^\lambda_{\mathbf{Q}}$ and ∂^λ co-incide on $\mathcal{S}_{k,k}$ and $\mathcal{S}_{k-1,k}$ we may restate this lemma and the calculations preceding it in the following form:

Lemma 4.3. *The rational homology of the space $\exp_k(S^2,*)/\exp_{k-1}(S^2,*)$ vanishes except in dimensions $2k-2$ and $2k-3$. With respect to integer co-efficients the top three groups are $\mathbf{Z}$ in dimension $2k-2$, generated by $1(k-1)$, $\mathbf{Z}$ in dimension $2k-3$, generated by $\sum_{i=1}^{k-2}(-1)^{i-1}2_i(k-1)$, and 0 in dimension $2k-4$.*

We are now in a position to prove Theorems 4.1 and 4.2. The argument should be very familiar from the cases considered in section 4.3.3.

Proof of Theorems 4.1 and 4.2. We first prove both results for $\exp_k(S^2,*)$, using induction on k. The top end of the long exact sequence of the pair $(\exp_k(S^2,*), \exp_{k-1}(S^2,*))$ gives

$$0 \longrightarrow \tilde{H}_{2k-2}(\exp_k(S^2,*)) \longrightarrow \tilde{H}_{2k-2}(\exp_k(S^2,*)/\exp_{k-1}(S^2,*)) \longrightarrow 0,$$

implying $\tilde{H}_{2k-2}(\exp_k(S^2,*)) \cong \mathbf{Z}$ with generator $1(k-1)$. The next segment is

$$0 \longrightarrow \tilde{H}_{2k-3}(\exp_k(S^2,*)) \longrightarrow \mathbf{Z} \xrightarrow{\partial} \mathbf{Z} \longrightarrow \tilde{H}_{2k-4}(\exp_k(S^2,*)) \longrightarrow 0,$$

in which the boundary map $\tilde{H}_{2k-3}(\exp_k(S^2,*)/\exp_{k-1}(S^2,*)) \to \tilde{H}_{2k-4}(\exp_{k-1}(S^2,*))$ is given by ∂^ν. Since $\partial^\nu 2_i(k-1) = (-1)^i 1(k-2)$ this sends the generator $\sum_{i=1}^{k-2}(-1)^{i-1}2_i(k-1)$ to $(2-k)(1(k-2))$, inducing multiplication by $2-k$. It follows that $\tilde{H}_{2k-3}(\exp_k(S^2,*))$ is zero and that $\tilde{H}_{2k-4}(\exp_k(S^2,*))$ is isomorphic to $\mathbf{Z}/(k-2)\mathbf{Z}$, generated by the top homology class of $\exp_{k-1}(S^2,*)$. We show that the remaining groups vanish over $\mathbf{Q}$ using the induction hypothesis and the exact sequence

$$\tilde{H}_i(\exp_{k-1}(S^2,*);\mathbf{Q}) \longrightarrow \tilde{H}_i(\exp_k(S^2,*);\mathbf{Q}) \longrightarrow \tilde{H}_i(\exp_k(S^2,*)/\exp_{k-1}(S^2,*);\mathbf{Q}).$$

Since the outer groups are zero for $i \leq 2k-5$ the middle group is too.

We now prove the results for $\exp_k S^2$, using the results just proved, Lemma 4.1, and the long exact sequence of the pair $(\exp_k S^2, \exp_k(S^2,*))$. At the top end we have

$$0 \longrightarrow \tilde{H}_{2k}(\exp_k S^2) \longrightarrow \tilde{H}_{2k}(\exp_k S^2/\exp_k(S^2,*)) \longrightarrow 0 \longrightarrow \tilde{H}_{2k-1}(\exp_k S^2) \longrightarrow 0$$

giving $\tilde{H}_{2k}(\exp_k S^2) \cong \mathbf{Z}$ generated by $\tilde{1}(k)$ and $\tilde{H}_{2k-1}(\exp_k S^2) \cong \{0\}$. The next segment is

$$0 \longrightarrow \mathbf{Z} \longrightarrow \tilde{H}_{2k-2}(\exp_k S^2) \longrightarrow \mathbf{Z}/(k-1)\mathbf{Z} \longrightarrow 0$$

in which the subgroup $\mathbf{Z}$ is generated by $1(k-1)$ and the quotient $\mathbf{Z}/(k-1)\mathbf{Z}$ is generated by $\tilde{1}(k-1)$. This short exact sequence splits: the cycle $\tilde{1}(k-1) - 21(k-1)$ maps to $\tilde{1}(k-1)$ in the quotient and

$$\partial \sum_{i=1}^{k-1}(-1)^{i-1}\tilde{2}_i(k) = (k-1)(\tilde{1}(k-1) - 21(k-1)),$$

showing that this class has order $k-1$. This completes the proof of Theorem 4.2, and the exact sequence

$$\tilde{H}_i(\exp_k(S^2,*);\mathbf{Q}) \longrightarrow \tilde{H}_i(\exp_k S^2;\mathbf{Q}) \longrightarrow \tilde{H}_i(\exp_k S^2/\exp_k(S^2,*);\mathbf{Q})$$

yields $0 \longrightarrow \tilde{H}_i(\exp_k S^2;\mathbf{Q}) \longrightarrow 0$ for $i \leq 2k-3$, completing the proof of Theorem 4.1. □

4.4 Higher genus surfaces

In this section we prove Theorem 4.3 on the top homology of the finite subset spaces of a closed surface, and Theorem 4.4 on the degree of a map $\exp_k f\colon\ \exp_k\Sigma \to \exp_k\Sigma'$ induced by a map $f\colon\ \Sigma \to \Sigma'$ between closed oriented surfaces.

We give Σ the standard cell structure consisting of a single vertex, $b_1(\Sigma)$ edges, and a single two-cell attached along the word $w_+ = [e_1, e_{1+g}]\cdots[e_g, e_{2g}]$ if Σ is orientable, $w_- = e_1^2 \cdots e_g^2$ if Σ is non-orientable. With respect to this cell structure the $2k$– and $(2k-1)$–cells of the lexicographic cell structure for $\exp_k\Sigma$ are the single cell $\tilde{1}(k)$ in dimension $2k$ and the cells

$$\left\{\tilde{2}_i(k)|1 \le i \le k-1\right\} \cup \left\{(\tilde{1}(k-1)) \cup \tilde{\sigma}_i^1 | 1 \le i \le b_1(\Sigma)\right\}$$

in dimension $2k-1$. In order to calculate boundaries we need to know the chain maps $(\exp w_+)_\sharp$ and $(\exp w_-)_\sharp$. By the discussion at the end of section 3.3.3 it suffices to calculate the images of the generators $\tilde{\sigma}^1$ and $\tilde{\sigma}^2$ of the chain ring, and moreover these are given by

$$(\exp w_+)_\sharp \tilde{\sigma}^1 = 0, \qquad (\exp w_-)_\sharp \tilde{\sigma}^1 = 2\sum_{i=1}^{g} \tilde{\sigma}_i^1,$$

$$(\exp w_+)_\sharp \tilde{\sigma}^2 = 2\sum_{i=1}^{g} \tilde{\sigma}_i^1 \cup \tilde{\sigma}_{i+g}^1, \qquad (\exp w_-)_\sharp \tilde{\sigma}^2 = 2\sum_{i=1}^{g} \tilde{\sigma}_i^2 + 4\sum_{i<j} \tilde{\sigma}_i^1 \cup \tilde{\sigma}_j^1.$$

This gives us all the ingredients we need and we now proceed to the proofs.

Proof of Theorem 4.3. Since $\partial^\nu \tilde{1} = \partial^\lambda \tilde{1} = 0$ the boundary of the cell $\tilde{1}(k)$ is equal to $\pm\partial^\gamma \tilde{1}(k)$. We have

$$\partial^\gamma \tilde{1}(k) = \begin{cases} 0 & \Sigma \text{ orientable}, \\ 2\sum_{i=1}^{g} \tilde{1}(k-1) \cup \tilde{\sigma}_i^1 & \Sigma \text{ non-orientable}, \end{cases} \tag{4.4.1}$$

and we see immediately that

$$H_{2k}(\exp_k\Sigma) = \begin{cases} \mathbf{Z} & \text{if } \Sigma \text{ is orientable}, \\ 0 & \text{if } \Sigma \text{ is non-orientable}. \end{cases}$$

To calculate the kernel of ∂_{2k-1} we make the following observation. Let F_d be the span of the d–cells of the form τ^S, $\tilde{\tau}^S$, and let E_d be the span of the d–cells with a σ^J or $\tilde{\sigma}^J$ factor with $|J| > 0$. With respect to the decompositions $C_d = F_d \oplus E_d$ the matrix of ∂ has the block form

$$D_d = \begin{bmatrix} A_d & 0 \\ B_d & C_d \end{bmatrix},$$

and if A_d is injective then $\ker\partial = \ker C_d$. Applying this with $d = 2k-1$ we have

$$F_{2k-1} = \operatorname{span}\{\tilde{2}_i(k)|1 \le i \le k-1\},$$
$$E_{2k-1} = \operatorname{span}\{\tilde{1}(k-1) \cup \tilde{\sigma}_i^1 | 1 \le i \le b_1(\Sigma)\},$$

and A_{2k-1} is injective since $A_{2k-1}\tilde{2}_i$ is equal to the boundary of this cell as a cell in $\exp_k S^2$. It follows that the $(2k-1)$–cycles are contained in the span of $\{\tilde{1}(k-1)\cup\tilde{\sigma}_i^1 | 1 \le i \le b_1(\Sigma)\}$. By equation (4.4.1) we have

$$\partial\big(\tilde{1}(k-1)\cup\tilde{\sigma}_i^1\big) = \begin{cases} 0 & \Sigma \text{ orientable,} \\ \pm 2\sum_{j\neq i} \tilde{1}(k-2)\cup\tilde{\sigma}_j^1\cup\tilde{\sigma}_i^1 & \Sigma \text{ non-orientable.} \end{cases}$$

If Σ is non-orientable then

$$\partial \sum_{i=1}^{g} a_i \tilde{1}(k-1)\cup\tilde{\sigma}_i^1 = \pm 2 \sum_{i<j} (a_i - a_j)\tilde{1}(k-2)\cup\tilde{\sigma}_i^1\cup\tilde{\sigma}_j^1,$$

implying

$$\ker\partial_{2k-1} = \begin{cases} \operatorname{span}\big\{\tilde{1}(k-1)\cup\tilde{\sigma}_i^1 | 1\le i\le 2g\big\} & \Sigma \text{ orientable,} \\ \operatorname{span}\Big\{\sum_{i=1}^{g}\tilde{1}(k-1)\cup\tilde{\sigma}_i^1\Big\} & \Sigma \text{ non-orientable.} \end{cases}$$

It now follows that

$$H_{2k-1}(\exp_k\Sigma) = \begin{cases} \mathbf{Z}^{2g} & \text{if } \Sigma \text{ is orientable,} \\ \mathbf{Z}/2\mathbf{Z} & \text{if } \Sigma \text{ is non-orientable,} \end{cases}$$

completing the proof of Theorem 4.3. □

Next we prove Theorem 4.4, which we recall states that

$$\deg \exp_k f = (\deg f)^k$$

if $f\colon\ \Sigma \to \Sigma'$ is a map between closed oriented surfaces. The result is an almost immediate consequence of the fact that $\exp_k\Sigma \setminus \exp_{k-1}\Sigma$ may be consistently oriented by (4.1.1). We caution that this orientation disagrees with the orientation on $\tilde{1}(k)$ for some k.

Proof of Theorem 4.4. Given a map $f\colon\ \Sigma\to\Sigma'$ let $p_1,\dots,p_k$ be distinct points in Σ' and perturb f to be transverse to each p_i. Each point p_i then has finitely many preimages which we label $q_{i,1},\dots,q_{i,r_i}$. Let $\Lambda = \{p_1,\dots,p_k\}\in\exp_k\Sigma'$. Under $\exp_k f$ the preimage of Λ consists of the $r_1\cdots r_k$ points

$$\Lambda_{s_1\cdots s_k} = \{q_{1,s_i},\dots,q_{k,s_k}\},$$

and perturbing the characteristic maps of the 2–cells of Σ, Σ' if necessary we may assume that all points in question lie in the top dimensional cells $\tilde{1}(k)$. With respect to the canonical orientation on $\exp_k\Sigma\setminus\exp_{k-1}\Sigma$ the sign of $\Lambda_{s_1\cdots s_k}$ is the product $\prod_i \operatorname{sign} q_{i,s_i}$, and we have immediately

$$\deg\exp_k f = \prod_{i=1}^{k}\sum_{j=1}^{r_i}\operatorname{sign} q_{i,j} = (\deg f)^k.$$

□

4.5 A homotopy model for the third finite subset space

We now pursue our second direction in the study of the finite subset spaces of closed surfaces. We begin by constructing a homotopy model for the third finite subset space of a closed orientable surface, and then we use this in section 4.6 to calculate the cohomology of $\exp_3\Sigma$.

4.5.1 The model

To construct a homotopy model for $\exp_3\Sigma$ we begin with the intermediate quotient $\mathrm{Sym}^3\Sigma = \Sigma^3/S_3$. Inside $\mathrm{Sym}^3\Sigma$ we have the preimage of $\exp_2\Sigma$, namely the branch locus $\mathcal{D}$ consisting of the quotient of the diagonals of $\Sigma\times\Sigma\times\Sigma$. Instead of quotienting $\mathcal{D}$ further to get $\exp_3\Sigma$ we attach the mapping cylinder of $\mathcal{D}\to\exp_2\Sigma$ to obtain a homotopy equivalent space $E_3\Sigma$. Fortunately $\mathcal{D}$ is simply a copy of $\Sigma\times\Sigma$ and $\mathcal{D}\to\exp_2\Sigma$ is the quotient map $\Sigma\times\Sigma\to\mathrm{Sym}^2\Sigma$, so the construction is all in terms of known spaces and maps.

Concretely, let $q_k\colon \Sigma^k\to\mathrm{Sym}^k\Sigma$ be the quotient map and $\Delta\colon\Sigma\to\Sigma\times\Sigma$ the diagonal map. Then $\mathcal{D}$ is the image of $\Sigma\times\Sigma$ under the map $\iota = q_3\circ\mathrm{id}\times\Delta$, and is homeomorphic to $\Sigma\times\Sigma$ since ι is injective, $\Sigma\times\Sigma$ is compact, and $\mathrm{Sym}^3\Sigma$ is Hausdorff. Further, $\exp_3\Sigma$ is obtained from $\mathrm{Sym}^3\Sigma$ by identifying $\iota(a,b) = q_3(a,b,b)$ with $\iota(b,a) = q_3(b,a,a)$. Let

$$M_{q_2} = \frac{(\Sigma\times\Sigma\times I)\amalg\mathrm{Sym}^2\Sigma}{(x,1)\sim q_2(x)}$$

be the mapping cylinder of q_2, and note that we adopt the convention that mapping cylinders are attached to the target at $1\in I$ rather than 0. We obtain our model for $\exp_3\Sigma$ by attaching M_{q_2} to $\mathrm{Sym}^3\Sigma$ along $\mathcal{D}$ and $\Sigma\times\Sigma\times\{0\}$, namely

$$\begin{aligned} E_3\Sigma &= \mathrm{Sym}^3\Sigma\cup_{\Sigma\times\Sigma} M_{q_2} \\ &= \frac{\mathrm{Sym}^3\Sigma\amalg M_{q_2}}{\iota(x)\sim(x,0)}. \end{aligned}$$

The space $E_3\Sigma$ is shown schematically in figure 4.7. The subscript 3 reflects the hope that a similar construction may apply for $k\geq 4$, perhaps using several mapping cylinders to successively quotient $\mathrm{Sym}^k\Sigma$ to $\exp_k\Sigma$ in several stages. However, such a generalisation is complicated by the increasing complexity of the branch locus: for example, when $k=4$ it is $\Sigma\times\mathrm{Sym}^2\Sigma$ with an embedded copy of $\Sigma\times\Sigma$ quotiented to $\mathrm{Sym}^2\Sigma$.

The cornerstone of the next section is the following lemma:

Lemma 4.4. *The spaces $E_3\Sigma$ and $\exp_3\Sigma$ are homotopy equivalent.*

We prove the lemma after a brief digression on known facts about symmetric products of surfaces. Not all of what follows is central to our argument, but it nonetheless serves to give a fuller picture of the construction.

4.5.2 Symmetric products of surfaces

We recall that the symmetric product of an orientable surface is a manifold, and moreover that a complex structure on Σ leads to a complex structure on $\mathrm{Sym}^k\Sigma$. Local co-ordinates

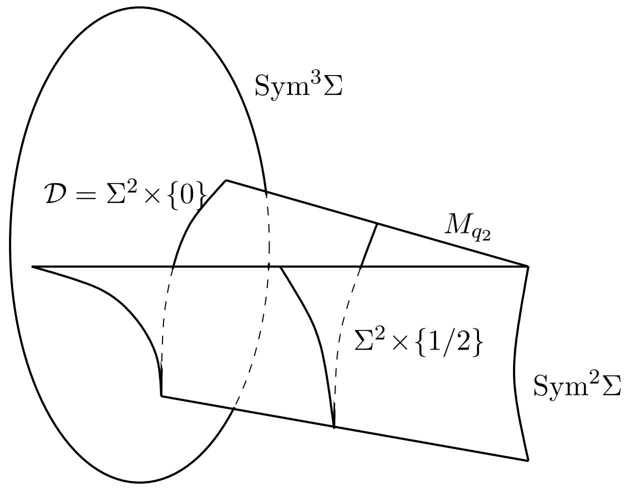

Figure 4.7: A schematic picture of the space $E_3\Sigma$. As we shall see in section 4.5.2, $\mathrm{Sym}^3\Sigma$ is a complex 3–manifold with the branch locus $\mathcal{D} \cong \Sigma^2$ embedded with a cusp along the diagonal. Σ^2 maps two-to-one to $\mathrm{Sym}^2\Sigma$ via q_2, and we form $E_3\Sigma$ by attaching the mapping cylinder M_{q_2} to $\mathcal{D}$ along $\Sigma^2 \times \{0\}$.

about $\{p_1, \ldots, p_k\}$ are given by the elementary symmetric functions in the local complex co-ordinates about the p_i, and are obtained by regarding the points as the zeroes of a polynomial (see Griffiths and Harris [16, p. 326]). In particular $\mathrm{Sym}^n\mathbf{C}P^1$ may be identified with the non-vanishing homogeneous polynomials of degree n in two variables, modulo scaling, and as such is equal to $\mathbf{C}P^n$.

A polynomial p has repeated roots if and only if its discriminant is zero. The discriminant is a polynomial in the co-efficients of p (see Lang [23, pp. 192–194]) and it follows that the branch locus, the image of the diagonals of Σ^k, is locally given by the vanishing of a polynomial and is therefore an algebraic variety. Specialising to $k = 3$, for a suitable choice of complex co-ordinates (a, b, c) the branch locus $\mathcal{D}$ is locally the set $b^2 = c^3$. We see that $\mathcal{D}$ has a cusp along $b = c = 0$, which is precisely the image of the main diagonal in $\Sigma \times \Sigma \times \Sigma$.

4.5.3 The proof of homotopy equivalence

Consider the mapping cylinder of $q\colon\ \mathrm{Sym}^3\Sigma \to \exp_3\Sigma$. This deformation retracts to $\exp_3\Sigma$ and contains $E_3\Sigma$ as a subspace, and our aim is to show that it also deformation retracts to $E_3\Sigma$. To do this it suffices to show that $\mathrm{Sym}^3\Sigma \times I$ deformation retracts to $\mathrm{Sym}^3\Sigma \times \{0\} \cup \mathcal{D} \times I$, as such a homotopy will descend setwise to the quotient M_q and be continuous there.

The existence of a deformation retraction from $\mathrm{Sym}^3\Sigma \times I$ to $\mathrm{Sym}^3\Sigma \times \{0\} \cup \mathcal{D} \times I$ follows from results in Bredon [10, pp. 431–432] and Dugundji [14, pp. 327–328] and the existence of a neighbourhood $U \supseteq \mathcal{D}$ that strongly deforms to $\mathcal{D}$ in $\mathrm{Sym}^3\Sigma$. We will prove it in this way, using the fact that $\mathrm{Sym}^3\Sigma$ and $\mathcal{D}$ are both compact manifolds to construct U. However, an approach of perhaps greater generality might be to realise $\mathcal{D}$ as a subcomplex of $\mathrm{Sym}^3\Sigma$ and appeal to Hatcher [20, Prop. 0.16]. Hatcher [20, pp. 482–483] gives a construction of an S_k–equivariant simplicial structure on X^k for simplicial X, and Lemma 4.4 would follow from checking whether this contains the diagonals as a subcomplex.

Although $\mathrm{Sym}^3\Sigma$ and $\mathcal{D}$ are both manifolds the existence of the desired neighbourhood U does not simply follow from the tubular neighbourhood theorem, since $\mathcal{D}$ is not smoothly embedded. We therefore resort to more hands-on means, and use the fact that manifolds are Euclidean neighbourhood retracts. Embed $M = \mathrm{Sym}^3\Sigma$ in some $\mathbf{R}^n$. Then there are neighbourhoods V of M, W of $\mathcal{D}$, and retractions $r_M\colon V \to M$, $r_W\colon W \to \mathcal{D}$. The neighbourhood W may be taken sufficiently small that the linear homotopy from $W \hookrightarrow \mathbf{R}^n$ to r_W remains in V, and we post-compose this with r_M and intersect W with M to get the desired neighbourhood and deformation.

4.6 The calculation of $H^*(\exp_3\Sigma)$

4.6.1 Introduction

To calculate the cohomology of $E_3\Sigma$ we use the Mayer-Vietoris sequence and the obvious decomposition

$$E_3\Sigma = (E_3\Sigma \setminus \mathrm{Sym}^2\Sigma) \cup (E_3\Sigma \setminus \mathrm{Sym}^3\Sigma).$$

The pieces are homotopy equivalent to $\mathrm{Sym}^3\Sigma$ and $\mathrm{Sym}^2\Sigma$ respectively, and intersect in $\Sigma \times \Sigma \times (0,1) \simeq \Sigma \times \Sigma$, leading to a long exact sequence

$$\cdots \to H^i(E_3\Sigma) \to H^i(\mathrm{Sym}^3\Sigma) \oplus H^i(\mathrm{Sym}^2\Sigma) \to H^i(\Sigma^2) \to H^{i+1}(E_3\Sigma) \to \cdots .$$

Before proceeding we describe the rings $H^*(\Sigma^k)$ and $H^*(\mathrm{Sym}^k\Sigma)$. Recall that integer coefficients are to be assumed except where specified otherwise.

4.6.2 The rings $H^*(\Sigma^k)$ and $H^*(\mathrm{Sym}^k\Sigma)$

Let $\alpha_1, \ldots, \alpha_{2g}$ be generators for $H^1(\Sigma)$ such that

$$\alpha_i\alpha_j = \begin{cases} 0 & |i-j| \neq g, \\ \beta & j = i+g, \end{cases}$$

where β is a generator of $H^2(\Sigma)$. Since $H^*(\Sigma)$ is finitely generated and free the Künneth formula applies and

$$H^*(\Sigma^k) \cong H^*(\Sigma)^{\otimes k}.$$

The cohomology ring of $\mathrm{Sym}^k\Sigma$ is given by Macdonald [24] and Seroul [31]. In addition Seroul's paper [32] gives a sketch of his argument. Macdonald uses methods from algebraic geometry to give generators and relations for $H^*(\mathrm{Sym}^k\Sigma; K)$ over a field K of characteristic zero, and to show that $H^*(\mathrm{Sym}^k\Sigma)$ is torsion free. He then states incorrectly that this implies the same elements generate over the integers. Seroul confirms Macdonald's answer, using purely algebraic-topological techniques to find $H^*(\mathrm{Sym}^k\Sigma; \mathbf{Z})$ directly. In part the result may be stated as follows; we omit the statement of the relations as we will do all ring multiplication in $H^*(\mathrm{Sym}^k\Sigma)$.

Theorem 4.8 (Macdonald [24] and Seroul [31, 32]). *The map*

$$q_k^*\colon\ H^*(\mathrm{Sym}^k\Sigma; R) \to H^*(\Sigma^k; R)$$

is an isomorphism of $H^*(\mathrm{Sym}^k\Sigma; R)$ onto $H^*(\Sigma^k; R)^{S_k}$, the subring of cohomology fixed by S_k, for R a field of characteristic zero, and is injective for $R = \mathbf{Z}$. $H^*(\mathrm{Sym}^k\Sigma; \mathbf{Z})$ is generated by elements $\xi_1, \ldots, \xi_{2g}$ in degree 1 and η in degree 2 such that

$$q_k^*\xi_i = \sum_{j=1}^{k} \pi_j^*\alpha_i, \qquad\qquad q_k^*\eta = \sum_{j=1}^{k} \pi_j^*\beta,$$

where $\pi_j\colon\ \Sigma^k \to \Sigma$ is projection on the jth factor. A basis for $H^r(\mathrm{Sym}^k\Sigma; \mathbf{Z})$ is given by the monomials $\xi_{i_1}\cdots\xi_{i_m}\eta^n$ for which $m + 2n = r$, $i_1 < \cdots < i_m$, and $m \le \min\{r, 2k - r\}$.

We remark that q_k is a degree $k!$ map, so q_k^* is certainly not onto $H^*(\Sigma^k)^{S_k}$ with integer co-efficients.

To avoid confusion we give different names to the generators of $H^*(\mathrm{Sym}^2\Sigma)$ and $H^*(\mathrm{Sym}^3\Sigma)$. Let

$$\begin{aligned}
\zeta_i &= \alpha_i \otimes 1 + 1 \otimes \alpha_i,\\
\theta &= \beta \otimes 1 + 1 \otimes \beta,\\
\xi_i &= \alpha_i \otimes 1 \otimes 1 + 1 \otimes \alpha_i \otimes 1 + 1 \otimes 1 \otimes \alpha_i,\\
\eta &= \beta \otimes 1 \otimes 1 + 1 \otimes \beta \otimes 1 + 1 \otimes 1 \otimes \beta.
\end{aligned}$$

Since q_k^* is injective we shall abuse notation and not take care to distinguish between elements of $H^*(\mathrm{Sym}^k\Sigma)$ and their images in $H^*(\Sigma^k)$, and will regard the ζ_i and θ as generators of $H^*(\mathrm{Sym}^2\Sigma)$, and the ξ_i and η as generators of $H^*(\mathrm{Sym}^3\Sigma)$.

4.6.3 The cohomology calculation

Returning to the Mayer-Vietoris sequence, letting

$$\Phi_i\colon\ H^i(\mathrm{Sym}^3\Sigma) \oplus H^i(\mathrm{Sym}^2\Sigma) \to H^i(\Sigma \times \Sigma)$$

be the map $\iota^* \oplus q_2^* = (q_3 \circ \mathrm{id} \times \Delta)^* \oplus q_2^*$ we have the short exact sequence

$$0 \to \operatorname{coker}\Phi_{i-1} \to H^i(E_3\Sigma) \to \ker\Phi_i \to 0.$$

Since $H^i(\mathrm{Sym}^3\Sigma) \oplus H^i(\mathrm{Sym}^2\Sigma)$ is free the kernel of Φ_i is too, so the sequence splits and we get

$$H^i(E_3\Sigma) \cong \operatorname{coker}\Phi_{i-1} \oplus \ker\Phi_i. \tag{4.6.1}$$

In what follows we calculate the kernel and cokernel of each Φ_i.

Dimension one

Both $H^1(\mathrm{Sym}^3\Sigma) \oplus H^1(\mathrm{Sym}^2\Sigma)$ and $H^1(\Sigma \times \Sigma)$ have rank $4g$, with bases $\{\xi_i\} \cup \{\zeta_i\}$ and $\{\alpha_i \otimes 1\} \cup \{1 \otimes \alpha_i\}$ respectively. For $\alpha \in H^j(\Sigma)$ we have

$$\begin{aligned}(\mathrm{id} \times \Delta)^*(1 \otimes 1 \otimes \alpha) &= (\mathrm{id} \times \Delta)^* \pi_3^* \alpha \\ &= (\pi_3 \circ \mathrm{id} \times \Delta)^* \alpha \\ &= \pi_2^* \alpha = 1 \otimes \alpha,\end{aligned}$$

and similarly $(\mathrm{id} \times \Delta)^*(1 \otimes \alpha \otimes 1) = 1 \otimes \alpha$, $(\mathrm{id} \times \Delta)^*(\alpha \otimes 1 \otimes 1) = \alpha \otimes 1$. Consequently

$$\begin{aligned}\Phi_1(\xi_i) &= (\mathrm{id} \times \Delta)^*(\alpha_i \otimes 1 \otimes 1 + 1 \otimes \alpha_i \otimes 1 + 1 \otimes 1 \otimes \alpha_i) \\ &= \alpha_i \otimes 1 + 2 \otimes \alpha_i.\end{aligned}$$

Since $\Phi_1(\zeta_i) = q_2^* \zeta_i = \alpha_i \otimes 1 + 1 \otimes \alpha_i$ and $\det \begin{bmatrix} 1 & 1 \\ 2 & 1 \end{bmatrix} = -1$, Φ_1 maps $\mathrm{span}\{\xi_i, \zeta_i\}$ isomorphically onto $\mathrm{span}\{\alpha_i \otimes 1, 1 \otimes \alpha_i\}$. Thus

$$\ker \Phi_1 \cong \operatorname{coker} \Phi_1 \cong \{0\}.$$

Dimension two

$H^2(\mathrm{Sym}^3\Sigma) \oplus H^2(\mathrm{Sym}^2\Sigma)$ has basis

$$\{\xi_i \xi_j | i < j\} \cup \{\zeta_i \zeta_j | i < j\} \cup \{\eta, \theta\}$$

and rank $2\binom{2g}{2} + 2$, while $H^2(\Sigma \times \Sigma)$ has basis

$$\{\alpha_i \otimes \alpha_j\} \cup \{\beta \otimes 1, 1 \otimes \beta\}$$

and rank $4g^2 + 2$. Under Φ_2 we have

$$\begin{aligned}\xi_i \xi_j &\mapsto (\alpha_i \otimes 1 + 2 \otimes \alpha_i)(\alpha_j \otimes 1 + 2 \otimes \alpha_j) \\ &= \begin{cases} 2(\alpha_i \otimes \alpha_j - \alpha_j \otimes \alpha_i) & |i - j| \neq g, \\ 2(\alpha_i \otimes \alpha_j - \alpha_j \otimes \alpha_i) + \beta \otimes 1 + 4 \otimes \beta & j = i + g, \end{cases} \\ \zeta_i \zeta_j &\mapsto (\alpha_i \otimes 1 + 1 \otimes \alpha_i)(\alpha_j \otimes 1 + 1 \otimes \alpha_j) \\ &= \begin{cases} \alpha_i \otimes \alpha_j - \alpha_j \otimes \alpha_i & |i - j| \neq g, \\ \alpha_i \otimes \alpha_j - \alpha_j \otimes \alpha_i + \beta \otimes 1 + 1 \otimes \beta & j = i + g, \end{cases} \\ \eta &\mapsto \beta \otimes 1 + 2 \otimes \beta, \\ \theta &\mapsto \beta \otimes 1 + 1 \otimes \beta.\end{aligned}$$

Clearly the image of Φ_2 is the span of

$$\{\beta \otimes 1, 1 \otimes \beta\} \cup \{\alpha_i \otimes \alpha_j - \alpha_j \otimes \alpha_i | i < j\}, \tag{4.6.2}$$

a subspace of rank $\binom{2g}{2} + 2$. Thus the kernel of Φ_2 has rank $\binom{2g}{2}$. The set in (4.6.2) may be augmented to a basis for $H^2(\Sigma \times \Sigma)$, so the cokernel of Φ_2 is free of rank $4g^2 + 2 - \binom{2g}{2} - 2 = \binom{2g}{2} + 2g$. Hence

$$\ker \Phi_2 \cong \mathbf{Z}^{\binom{2g}{2}}, \qquad \operatorname{coker} \Phi_2 \cong \mathbf{Z}^{\binom{2g}{2} + 2g}.$$

Dimension three

A basis for $H^3(\mathrm{Sym}^3\Sigma) \oplus H^3(\mathrm{Sym}^2\Sigma)$ is given by

$$\{\xi_i\xi_j\xi_k | i < j < k\} \cup \{\xi_i\eta\} \cup \{\zeta_i\theta\}.$$

If the genus of Σ is greater than one the rank is $\binom{2g}{3} + 4g$, but in genus equal to one there are only two distinct ξ_i, so the leftmost set in this union is empty and the rank of $H^3(\mathrm{Sym}^3\Sigma) \oplus H^3(\mathrm{Sym}^2\Sigma)$ is $4g = 4$. In either case $H^3(\Sigma \times \Sigma)$ has basis

$$\{\alpha_i \otimes \beta\} \cup \{\beta \otimes \alpha_i\}$$

and rank $4g$. We have

$$\begin{aligned}
\zeta_i\theta &\mapsto (\alpha_i \otimes 1 + 1 \otimes \alpha_i)(\beta \otimes 1 + 1 \otimes \beta) \\
&= \alpha_i \otimes \beta + \beta \otimes \alpha_i, \\
\xi_i\eta &\mapsto (\alpha_i \otimes 1 + 2 \otimes \alpha_i)(\beta \otimes 1 + 2 \otimes \beta) \\
&= 2(\alpha_i \otimes \beta + \beta \otimes \alpha_i),
\end{aligned}$$

and in genus one it follows that the kernel and cokernel of Φ_3 both have rank two. When $g \geq 2$ the triple product $\xi_i\xi_j\xi_k$ maps to 0 if i, j, k are distinct mod g, while

$$\begin{aligned}
\xi_i\xi_{i+g}\xi_j &\mapsto (2(\alpha_i \otimes \alpha_{i+g} - \alpha_{i+g} \otimes \alpha_i) + \beta \otimes 1 + 4 \otimes \beta)(\alpha_j \otimes 1 + 2 \otimes \alpha_j) \\
&= 2\beta \otimes \alpha_j + 4\alpha_j \otimes \beta
\end{aligned}$$

for $i \neq j \neq i + g$. Considering the images of $\zeta_i\theta$ and $\xi_i\xi_{i+g}\xi_j$ we see that the image of Φ_3 has rank $4g$ and that

$$\operatorname{coker} \Phi_3 \cong \frac{\mathrm{span}\{\beta \otimes \alpha_j + 2\alpha_j \otimes \beta\}}{\mathrm{span}\{2(\beta \otimes \alpha_j + 2\alpha_j \otimes \beta)\}} \cong [\mathbf{Z}/2\mathbf{Z}]^{2g},$$

so that

$$\ker \Phi_3 \cong \begin{cases} \mathbf{Z}^2 & g = 1, \\ \mathbf{Z}^{\binom{2g}{3}} & g \neq 1, \end{cases} \qquad \operatorname{coker} \Phi_3 \cong \begin{cases} \mathbf{Z}^2 & g = 1, \\ [\mathbf{Z}/2\mathbf{Z}]^{2g} & g \neq 1. \end{cases}$$

Dimension four

$H^4(\mathrm{Sym}^3\Sigma) \oplus H^4(\mathrm{Sym}^2\Sigma)$ has rank $\binom{2g}{2} + 2$ and basis

$$\{\xi_i\xi_j\eta | i < j\} \cup \{\eta^2, \theta^2\},$$

while $H^4(\Sigma \times \Sigma)$ has rank one and basis $\{\beta \otimes \beta\}$. Under Φ_4 we have

$$\begin{aligned}
\theta^2 &\mapsto (\beta \otimes 1 + 1 \otimes \beta)^2 \\
&= 2\beta \otimes \beta, \\
\eta^2 &\mapsto (\beta \otimes 1 + 2 \otimes \beta)^2 \\
&= 4\beta \otimes \beta, \\
\xi_i\xi_j\eta &\mapsto 2(\alpha_i \otimes \beta + \beta \otimes \alpha_i)(\alpha_j \otimes 1 + 2 \otimes \alpha_j) \\
&= \begin{cases} 0 & |j - i| \neq g, \\ 6\beta \otimes \beta & j = i + g. \end{cases}
\end{aligned}$$

Clearly

$$\ker \Phi_4 \cong \mathbf{Z}^{\binom{2g}{2}+1}, \qquad \operatorname{coker} \Phi_4 \cong \mathbf{Z}/2\mathbf{Z}.$$

Dimensions five and six

$\Sigma \times \Sigma$ and $\mathrm{Sym}^2\Sigma$ have no cohomology in dimensions five and six so the cokernel of Φ_i is trivial and the kernel is $H^i(\mathrm{Sym}^3\Sigma)$ for $i = 5, 6$. $H^5(\mathrm{Sym}^3\Sigma) = \mathrm{span}\{\xi_i\eta^2\}$ has rank $2g$ and $H^6(\mathrm{Sym}^3\Sigma) = \mathrm{span}\{\eta^3\}$ has rank one, so

$$\begin{aligned} \ker \Phi_5 &\cong \mathbf{Z}^{2g}, & \operatorname{coker} \Phi_5 &\cong \{0\}, \\ \ker \Phi_6 &\cong \mathbf{Z}, & \operatorname{coker} \Phi_6 &\cong \{0\}. \end{aligned}$$

Completing the proof of Theorem 4.5

Putting the kernels and cokernels calculated above together using equation (4.6.1) gives the table in Theorem 4.5. Taking alternating sums of Betti numbers gives

$$\begin{aligned} \chi(\exp_3\Sigma) &= 3 - 4g + \binom{2g}{2} - \binom{2g}{3} \\ &= \frac{-4g^3 + 12g^2 - 17g + 9}{3} \end{aligned} \tag{4.6.3}$$

for $g \geq 2$, and direct substitution shows it holds for $g \geq 0$ also. As a check we calculate the Euler characteristic using

$$\chi(E_3\Sigma) = \chi(\mathrm{Sym}^3\Sigma) + \chi(\mathrm{Sym}^2\Sigma) - \chi(\Sigma \times \Sigma).$$

Macdonald gives $\chi(\mathrm{Sym}^n\Sigma) = (-1)^n\binom{2g-2}{n}$, so

$$\begin{aligned} \chi(E_3\Sigma) &= -\binom{2g-2}{3} + \binom{2g-2}{2} - (2-2g)^2 \\ &= \frac{-4g^3 + 12g^2 - 17g + 9}{3}, \end{aligned}$$

in agreement with (4.6.3).

Chapter 5

An application to cell complexes

5.1 Introduction

Handel [18] has shown that for path-connected Hausdorff X the map on π_i induced by the inclusion $\exp_k X \hookrightarrow \exp_{2k+1} X$ is zero. Using the results of Chapter 3 we complement this result, proving the following vanishing theorem for the homotopy groups of the finite subset spaces of a connected cell complex.

Theorem 5.1. *If X is a connected cell complex then the homotopy group $\pi_i(\exp_k X)$ vanishes for $i \leq k-2$.*

Equivalently, this result states that the kth finite subset space of a connected cell complex is $(k-2)$–connected. As noted after the statement of Theorem 4.6, $\exp_k X$ is $(k-1)$–connected if X is a simply connected finite 2–complex, and this may be used to prove that the same result holds without the dimension or finiteness restrictions. More generally, the discussion of section 4.2.4 suggests that we can expect $\exp_k X$ to be $(k+m-2)$-connected if X is an m–connected cell complex. We discuss this further in section 5.3.

By an almost identical argument to the proof of Theorem 5.1 we show that, from the standpoint of homology, the dimension of $\exp_k X$ behaves as expected:

Theorem 5.2. *If X is a connected n–complex then the homology group $H_i(\exp_k X)$ vanishes for $i > nk$.*

This result is of course wholly unsurprising: although we have only constructed cell structures for the finite subset spaces of connected 1– and 2–complexes we expect that they should exist in general, and in fact Jacob Mostovoy (private communication) has indicated that they may be built using the machinery of simplicial sets. It is nevertheless interesting that this bound can be proved using only the corresponding result for 1–complexes, and we include the proof as a second example of the inductive technique of Theorem 5.1.

We prove the results in section 5.2, and discuss them further in section 5.3.

5.2 Proof of the vanishing theorems

The two theorems are proved almost identically, so we will prove Theorem 5.1 and then indicate how to adapt the argument to obtain Theorem 5.2. In each case we first prove the theorem for finite complexes and then pass to the infinite case via a compactness argument.

We note that Theorem 5.1 is immediate for $k = 2$, since the finite subset spaces of a path-connected space are again path-connected, so in proving it we assume $k \geq 3$. In this case the conclusion is equivalent to the statement that $\exp_k X$ is simply connected with vanishing reduced homology in dimensions less than $k - 1$, by the Hurewicz theorem, and we shall freely use this formulation.

Proof of Theorem 5.1 for finite X. The proof is by induction on the dimension of X, with the base case $\dim X = 1$ given by Theorems 3.1 and 3.3. The keys to the inductive step are the following two observations:

1. If $P_1, \ldots, P_{k+1}$ are disjoint subsets of X then a k element subset of X must lie in $X \setminus P_\ell$ for some ℓ.

2. If X is a connected finite $(n+1)$–complex, $n \geq 1$, and $P \subseteq X$ is a subset of the open $(n+1)$–cells intersecting each in a non-empty finite set, then $X \setminus P$ has the homotopy type of a connected finite n–complex.

We use these in conjunction with the following lemma, itself proved inductively using the Mayer-Vietoris sequence.

Lemma 5.1. *Let Y be a union of open sets $U_1, \ldots, U_r$ such that $U_1 \cap \cdots \cap U_r$ is non-empty and each $U_{i_1} \cap \cdots \cap U_{i_s}$ has vanishing reduced homology in dimensions less than j. Then Y itself has vanishing reduced homology in dimensions less than j.*

Suppose the theorem holds for connected finite n–complexes, some $n \geq 1$, and let X be a connected finite $(n+1)$–complex. Let v be a vertex of X and let $P_1, \ldots, P_{k+1}$ be disjoint subsets of X each consisting of exactly one point from each open $(n+1)$–cell. By observation (1) the sets

$$\mathcal{U}_\ell = \exp_k(X \setminus P_\ell)$$

cover $\exp_k X$, and each $\mathcal{U}_\ell$ is open since $(X \setminus P_\ell)^k$ is open in X^k. Moreover the intersection $\mathcal{U}_1 \cap \cdots \cap \mathcal{U}_{k+1}$ contains $\{v\}$ and is therefore non-empty.

Consider

$$\mathcal{U}_{\ell_1} \cap \cdots \cap \mathcal{U}_{\ell_s} = \exp_k(X \setminus (P_{\ell_1} \cup \cdots \cup P_{\ell_s})).$$

By observation (2) the space $X \setminus (P_{\ell_1} \cup \cdots \cup P_{\ell_s})$ has the homotopy type of a connected finite n–complex, so by the inductive hypothesis $\mathcal{U}_{\ell_1} \cap \cdots \cap \mathcal{U}_{\ell_s}$ has vanishing reduced homology in dimensions less than $k-1$. It follows that the hypotheses of Lemma 5.1 are satisfied by the cover $\{\mathcal{U}_\ell\}$ with $j = k - 1$, and we conclude that $\exp_k X$ has vanishing reduced homology in dimensions less than $k - 1$.

To complete the inductive step it remains to show that $\exp_k X$ is simply connected. This follows immediately from the van Kampen theorem applied to the cover $\{\mathcal{U}_\ell\}$ with basepoint $\{v\}$. By the inductive hypothesis $\pi_1(\mathcal{U}_\ell, \{v\}) \cong \{1\}$ for all ℓ, and since each $\mathcal{U}_j \cap \mathcal{U}_\ell$ is path-connected we have immediately that $\pi_1(\exp_k X, \{v\}) \cong \{1\}$ also. □

To pass to the infinite dimensional case we use the following lemma, which we prove with no assumptions on X.

Lemma 5.2. *If $C \subseteq \exp_k X$ is compact in $\exp_k X$ then $\bigcup C = \bigcup_{\alpha \in C} \alpha$ is compact in X.*

Proof. Given an open cover $\mathcal{O}$ of $\bigcup C$ the set

$$\mathcal{O}' = \left\{\exp_k \bigcup O \middle| O \subseteq \mathcal{O} \text{ finite}\right\}$$

is an open cover of C. Extracting a finite subcover $\left\{\exp_k \bigcup O_1, \dots, \exp_k \bigcup O_m\right\}$ from $\mathcal{O}'$ we obtain a finite subcover $O_1 \cup \cdots \cup O_m$ of $\mathcal{O}$. □

Since compact subspaces of cell complexes lie in finite subcomplexes we have immediately:

Corollary 5.1. *If X is a cell complex and $C \subseteq \exp_k X$ is compact, then $C \subseteq \exp_k A$ for some finite subcomplex A of X.*

Proof of Theorem 5.1 for X infinite. Let $[\phi] \in \pi_i(\exp_k X, \{v\})$ for some vertex v of X and $i \leq k-2$. By Corollary 5.1 $\phi(S^i)$ lies in $\exp_k A$ for some finite subcomplex A of X, and we may take A to be connected since X is. By the finite case of the theorem $[\phi]$ is trivial in $\pi_i(\exp_k A, \{v\})$, and so in $\pi_i(\exp_k X, \{v\})$ also. □

We now indicate how to adapt the proof of Theorem 5.1 to prove Theorem 5.2.

Proof of Theorem 5.2. For finite X the base case $\dim X = 1$ is again given by Theorem 3.1, and for the inductive step we simply replace Lemma 5.1 with Lemma 5.3 below. Lemma 5.3 is almost exercise 2.2.33 of Hatcher [20, p. 158], and is again proved inductively using the Mayer-Vietoris sequence.

Lemma 5.3. *Let Y be a union of open sets $U_1, \dots, U_r$ such that the homology of each $U_{i_1} \cap \cdots \cap U_{i_s}$ vanishes in dimensions greater than j. Then Y has vanishing homology in dimensions greater than $j + r - 1$.*

To pass to the infinite case note that the image of a singular i–cycle is again a compact set, and so lies in $\exp_k A$ for a connected finite subcomplex A of X. □

5.3 Discussion

Theorem 5.1 is consistent with the following conjecture on finite subset spaces of cell complexes, as the theorem follows from the conjecture together with Handel's inclusion result. We restrict our attention to complexes with a single vertex in each component, with no loss of generality up to homotopy.

Conjecture. *Let X be a finite n–complex with m components, each containing a single vertex. Then $\exp_k X$ has a cell structure obtained from $\exp_{k-1} X$ by adding cells of dimensions $k - m \leq i \leq nk$.*

The conjecture is true in the connected case for $n = 1$ by Lemma 3.1, and for $n = 2$ by Theorem 4.6. To see that it implies Theorem 5.1 note that it implies that the homotopy groups of $\exp_k X$ stabilise as k increases. By Handel's result the stable groups must be zero when X is connected, and careful attention to the point at which the stabilisation occurs gives the bound in the theorem.

Jacob Mostovoy (private communication) has indicated that finite subset spaces of cell complexes *do* have cell structures, which we proved here only for connected finite 1– and 2–complexes. The cell structures are built using the machinery of simplicial sets, described in May's book [26] or Curtis's article [13]. Given a simplicial set K we let $\exp_j K$ be the simplicial set whose n–simplices are subsets of size at most j of the n–simplices of K, and whose face and degeneracy operators are the face and degeneracy operators of K acting elementwise. Then if X is the geometric realisation of K, $\exp_j X$ will be the geometric realisation of $\exp_j K$, showing that triangulated spaces have triangulated finite subset spaces. The power of this method comes at the expense of difficulties with concrete calculations: for example, the triangulations produced for $\exp_3 S^2$ and $\exp_4 S^2$ have 77 and 1039 cells,[1] in contrast with our lexicographic cell structures which have 11 and 23.

The triangulations obtained using simplicial sets prove Theorem 5.2, but apparently do not satisfy the lower bound $k - m$ needed to prove Theorem 5.1. The bound comes from the following heuristic, motivated by the form of our lexicographic cell structures. We suppose that $\exp_k X$ has a cell structure such that for each open cell e of X the set map

$$\exp_k X \to \mathbf{N} : \Lambda \mapsto |\Lambda \cap e|$$

is constant on each open cell σ of $\exp_k X$, and moreover that the dimension of σ is at least the common number of points in X less the 0–skeleton for $\Lambda \in \sigma$. In particular we suppose that the vertices of $\exp_k X$ can be chosen to be subsets of the vertices of X, without adding more through subdivision. If X has a single vertex in each component then an open cell of $\exp_k X \setminus \exp_{k-1} X$ in such a cell structure would have dimension at least $k - m$.

Theorem 5.1 can be strengthened for simply connected complexes, and we expect that it can be strengthened further for m–connected cell complexes. With this in mind we prove the following lemma, showing it suffices to prove the strengthened result for wedges of spheres.

Lemma 5.4. *Suppose that finite wedges of $(m+1)$–spheres have r–connected kth finite subset spaces. Then m–connected cell complexes have r–connected kth finite subset spaces also.*

Proof. We simply adapt the inductive step of the proof of Theorem 5.1, replacing observation (2) with the following observation (2′):

2′. If X is an m–connected finite $(n+1)$–complex, $n \geq m+1$, and $P \subseteq X$ is a subset of the open $(n+1)$–cells intersecting each in a non-empty finite set, then $X \setminus P$ has the homotopy type of an m–connected finite n–complex.

If X is an m–connected finite cell complex then up to homotopy we may assume that the $(m+1)$–skeleton of X is a finite wedge of $(m+1)$–spheres. The base for the induction is then given by hypothesis and the argument goes through exactly as before. □

[1] These numbers are derived from cell counts sent by Jacob Mostovoy.

Since Theorem 4.6 implies that $\exp_k \bigvee_n S^2$ is $(k-1)$–connected we conclude that simply connected cell complexes have $(k-1)$–connected kth finite subset spaces. More generally, the construction outlined in section 4.2.4 should yield cell structures for the finite subset spaces of wedges of spheres in which $\exp_k \bigvee_n S^{m+1}$ is obtained from $\exp_{k-1} \bigvee_n S^{m+1}$ by adding cells in dimensions $k+m-1$ and higher. Verifying the details of this construction would show that m–connected cell complexes have $(k+m-2)$–connected kth finite subset spaces.

We conclude with an example showing the necessity of the connectedness hypothesis in Theorem 5.1. Consider the third finite subset space of a pair of circles, $\exp_3(S^1 \amalg S^1)$. This has three connected components, two "pure" components consisting of subsets contained entirely in one or the other component circle, and a "mixed" component consisting of subsets meeting both. The two pure components are each homeomorphic to S^3, but the mixed component is formed by gluing two copies of $\exp_2 S^1 \times \exp_1 S^1 \cong \text{Möb} \times S^1$ along their boundary. The gluing interchanges the roles of the boundary of the Möbius strip and the S^1 direction, and π_1 of the resulting three manifold has presentation $\langle a, b | [a, b^2] = [a^2, b] = 1 \rangle$.

Bibliography

[1] J. Baez. This week's finds in mathematical physics. http://math.ucr.edu/home/baez/TWF.html.

[2] A. Beilinson and V. Drinfeld. Chiral algebras. Online at http://www.math.uchicago.edu/~benzvi/BD/CHA.ps.gz. Version of Sept. 2000.

[3] M. G. Bell. Hyperspaces of finite subsets. In *Topological Structures II*, volume 115 of *Mathematical Centre Tracts*, pages 15–28, 1979.

[4] S. Bigelow. Braid groups are linear. *J. Amer. Math. Soc.*, 14(2):471–486, 2001.

[5] J. Birman. *Braids, Links, and Mapping Class Groups*. Number 82 in Annals of Mathematics Studies. Princeton University Press, 1974.

[6] K. Borsuk. On the third symmetric potency of the circumference. *Fund. Math.*, 36:236–244, 1949.

[7] K. Borsuk and S. Ulam. On symmetric products of topological spaces. *Bull. Amer. Math. Soc.*, 37:875–882, 1931.

[8] R. Bott. On the third symmetric potency of S_1. *Fund. Math.*, 39:264–268, 1952.

[9] R. Bott and C. Taubes. On the self-linking of knots. *J. Math. Physics*, 35(10):5247–5287, 1994.

[10] G. Bredon. *Topology and Geometry*. Number 139 in Graduate Texts in Mathematics. Springer-Verlag, 1993.

[11] D. Curtis. Hyperspaces of finite subsets as boundary sets. *Topology and its Applications*, 22(1):97–107, 1986.

[12] D. Curtis and N. To Nhu. Hyperspaces of finite subsets which are homeomorphic to $\aleph_0$–dimensional linear metric spaces. *Topology and its Applications*, 19(3):251–260, 1985.

[13] E. B. Curtis. Simplicial homotopy theory. *Advances in Mathematics*, 6:107–209, 1971.

[14] J. Dugundji. *Topology*. Allyn and Bacon Series in Advanced Mathematics. Allyn and Bacon, 1966.

[15] W. Fulton and R. MacPherson. A compactification of configuration spaces. *Annals of Math.*, 139(1):183–225, 1994.

[16] P. Griffiths and J. Harris. *Principles of Algebraic Geometry.* John Wiley & Sons, 1978.

[17] D. Handel. On the configuration spaces of non-empty subsets of the circle of bounded finite cardinality. Unpublished work.

[18] D. Handel. Some homotopy properties of spaces of finite subsets of topological spaces. *Houston J. of Math.*, 26(4):747–764, 2000.

[19] A. Hatcher. Notes on basic 3–manifold topology. In preparation. Available on the web at `http://www.math.cornell.edu/~hatcher/`.

[20] A. Hatcher. *Algebraic Topology.* Cambridge University Press, 2001. Also available on the web at `http://www.math.cornell.edu/~hatcher/`.

[21] A. Illanes. Multicoherence of symmetric products. *An. Inst. Mat. Univ. Nac. Autónoma México*, 25:11–24, 1985.

[22] V. Kac and P. Cheung. *Quantum Calculus.* Universitext. Springer-Verlag, 2002.

[23] S. Lang. *Algebra.* Addison-Wesley, 3rd edition, 1993.

[24] I. G. Macdonald. Symmetric products of an algebraic curve. *Topology*, 1:391–343, 1962.

[25] S. Macías. On symmetric products of continua. *Topology and its Applications*, 92:173–182, 1999.

[26] J. P. May. *Simplicial objects in algebraic topology.* Number 11 in Van Nostrand Mathematical Studies. D. Van Nostrand Co., Inc., 1967. Reprinted in 1992 by University of Chicago Press in the series Chicago Lectures in Mathematics.

[27] J. Milnor. *Introduction to Algebraic K-Theory.* Princeton University Press, 1971.

[28] R. Molski. On symmetric products. *Fund. Math.*, 44:165–170, 1957.

[29] J. Mostovoy. Lattices in $\mathbf{R}^2$ and finite subsets of a circle. arXiv:math.GT/9911224, 1999.

[30] Z. Ran. Derivatives of moduli. *Internat. Math. Res. Notices*, 1993(4):93–106, 1993.

[31] R. Seroul. Anneau de cohomologie entière et KU^*–théorie d'un produit symétrique d'une surface de Riemann. *Publ. Dép. Math. (Lyon)*, 9(4):27–66, 1972.

[32] R. Seroul. Cohomologie entière et KU^*–théorie d'un produit symétrique d'une surface de Riemann. *C. R. Acad. Sci. Paris Sr. A-B*, 274:A1536–A1538, 1972.

[33] R. Stanley. *Enumerative Combinatorics, Volume I.* Number 49 in Cambridge Studies in Advanced Mathematics. Cambridge University Press, 1986.

[34] W. Thurston. *Three-Dimensional Geometry and Topology*, volume 1. Princeton University Press, 1997.

[35] C. Tuffley. Finite subset spaces of graphs and punctured surfaces. arXiv:math.GT/0210315, 2002. Submitted.

[36] C. Tuffley. Finite subset spaces of S^1. *Alg. Geom. Topology*, 2:1119–1145, 2002. arXiv:math.GT/0209077.

[37] C. Tuffley. Two vanishing theorems for finite subset spaces of cell complexes. arXiv:math.GT/0304086, 2003.

Appendix A

Table of Betti numbers of finite subset spaces of graphs

Table A.1 lists the Betti numbers

$$
\begin{aligned}
b_k(\exp_k\Gamma_n) &= \sum_{j=1}^{k}(-1)^{j-k}\binom{n+j-1}{n-1} \\
&= \begin{cases} \sum_{j=1}^{\ell}\binom{n+2j-2}{n-2} & \text{if } k=2\ell \text{ is even,} \\ n+\sum_{j=1}^{\ell}\binom{n+2j-1}{n-2} & \text{if } k=2\ell+1 \text{ is odd,} \end{cases}
\end{aligned}
$$

for $1 \leq k \leq 20$, $1 \leq n \leq 10$. To find the other non-vanishing Betti numbers recall that $b_{k-1}(\exp_k\Gamma_n) = b_{k-1}(\exp_k(\Gamma_n, v)) = b_{k-1}(\exp_{k-1}\Gamma_n)$ for $k \geq 2$.

		n									
		1	2	3	4	5	6	7	8	9	10
	1	1	2	3	4	5	6	7	8	9	10
	2	0	1	3	6	10	15	21	28	36	45
	3	1	3	7	14	25	41	63	92	129	175
	4	0	2	8	21	45	85	147	238	366	540
	5	1	4	13	35	81	167	315	554	921	1462
	6	0	3	15	49	129	295	609	1162	2082	3543
	7	1	5	21	71	201	497	1107	2270	4353	7897
	8	0	4	24	94	294	790	1896	4165	8517	16413
	9	1	6	31	126	421	1212	3109	7275	15793	32207
k	10	0	5	35	160	580	1791	4899	12173	27965	60171
	11	1	7	43	204	785	2577	7477	19651	47617	107789
	12	0	6	48	251	1035	3611	11087	30737	78353	186141
	13	1	8	57	309	1345	4957	16045	46783	125137	311279
	14	0	7	63	371	1715	6671	22715	69497	194633	505911
	15	1	9	73	445	2161	8833	31549	101047	295681	801593
	16	0	8	80	524	2684	11516	43064	144110	439790	1241382
	17	1	10	91	616	3301	14818	57883	201994	641785	1883168
	18	0	9	99	714	4014	18831	76713	278706	920490	2803657
	19	1	11	111	826	4841	23673	100387	379094	1299585	4103243
	20	0	10	120	945	5785	29457	129843	508936	1808520	5911762

Table A.1: Betti numbers $b_k(\exp_k \Gamma_n)$ for $1 \leq k \leq 20$ and $1 \leq n \leq 10$.